



**HAL**  
open science

# Environmental challenges related to methane hydrate decomposition from climate change scenario and anthropic activities: State of the art, potential consequences and monitoring solutions

Livio Ruffine, Anh Minh Tang, Nick O'Neill, Laurent M.A.A. Toffin, Jean Daniel Paris, Jinhai Yang, Valentin Georgiev, Peer Fietzek, Michela Giustiniani, Umberta Tinivella

## ► To cite this version:

Livio Ruffine, Anh Minh Tang, Nick O'Neill, Laurent M.A.A. Toffin, Jean Daniel Paris, et al.. Environmental challenges related to methane hydrate decomposition from climate change scenario and anthropic activities: State of the art, potential consequences and monitoring solutions. *Earth-Science Reviews*, 2023, 246, 10.1016/j.earscirev.2023.104578 . hal-04294670

**HAL Id: hal-04294670**

**<https://hal.science/hal-04294670>**

Submitted on 10 Jan 2024

**HAL** is a multi-disciplinary open access archive for the deposit and dissemination of scientific research documents, whether they are published or not. The documents may come from teaching and research institutions in France or abroad, or from public or private research centers.

L'archive ouverte pluridisciplinaire **HAL**, est destinée au dépôt et à la diffusion de documents scientifiques de niveau recherche, publiés ou non, émanant des établissements d'enseignement et de recherche français ou étrangers, des laboratoires publics ou privés.

Copyright

# Environmental challenges related to methane hydrate decomposition from climate change scenario and anthropic activities: State of the art, potential consequences and monitoring solutions

Livio Ruffine<sup>1</sup>, Anh Minh Tang<sup>2</sup>, Nick O'Neill<sup>3</sup>, Laurent Toffin<sup>4</sup>, Jean-Daniel Paris<sup>5</sup>, Jinhai Yang<sup>6</sup>, Valentin Georgiev<sup>7</sup>, Peer Fietzek<sup>8</sup>, Michela Giustiniani<sup>9</sup>, Umberta Tinivella<sup>9</sup>

<sup>1</sup>Ifremer, Univ Brest, CNRS, UMR Geo-Ocean, F-29280 Plouzané, France

<sup>2</sup>Ecole Ponts ParisTech, Lab Navier, F-77455 Marne La Vallee, France

<sup>3</sup>PIP Secretariat, ISPSG, 7 Dundrum Business Pk, Dublin 14 N2Y7, Ireland

<sup>4</sup>Ifremer, Univ Brest, CNRS, UMR BEEP, F-29280 Plouzané, France

<sup>5</sup>Laboratoire des Sciences du Climat et de l'Environnement (CEA-CNRS-UVSQ), Gif sur Yvette, France

<sup>6</sup>Heriot-Watt University, Institute of GeoEnergy Engineering, Edinburgh, Scotland

<sup>7</sup>GeoMarine Ltd, Bulgaria

<sup>8</sup>Kongsberg Maritime Germany GmbH, Hamburg, Germany

<sup>9</sup>Istituto Nazionale di Oceanografia e di Geofisica Sperimentale - OGS, Borgo Grotta Gigante 42C, I-34010 Trieste, Italy

Corresponding author: Email: [livio.ruffine@ifremer.fr](mailto:livio.ruffine@ifremer.fr) ; Tél : + 33 2 98 22 48 88

## Abstract

Natural gas hydrate deposits (NGHD) have been investigated for decades and represent one of the major methane reservoirs on Earth. They are encountered in sediment of both the continental margins and the permafrost region; areas considered to host amongst the most climate-sensitive ecosystems on Earth. With worldwide temperature increases affecting continental margins and the permafrost, it is important to raise concern about the fate of the NGHD in the coming centuries. Thus, this review presents an overview of the potential consequences of hydrate decomposition on its surrounding areas. It compiles and discusses hydrate-derived methane fluxes measured or inferred from *in situ* data at several sites by considering both dissociation and dissolution. Depending on the magnitude and the duration of hydrate decomposition, the amounts of methane released can affect to varying degrees the seafloor and the microbial communities that sustain the methane cycle and regulate its transfer from the sediment to the water column; and that aspect is addressed in this review. Here, we also considered the transfer of methane from NGHDs and more broadly from marine emissions to the atmosphere, as it is assumed that such transfer will likely increase in the future. Finally, multi-scale monitoring in space and time is a key element to evaluate the impacts of natural and anthropic perturbations

39 on NGHDs. We thus propose potential engineering solutions for the monitoring of  
40 NGHD, mainly based on the long-term deployment of sensor systems.

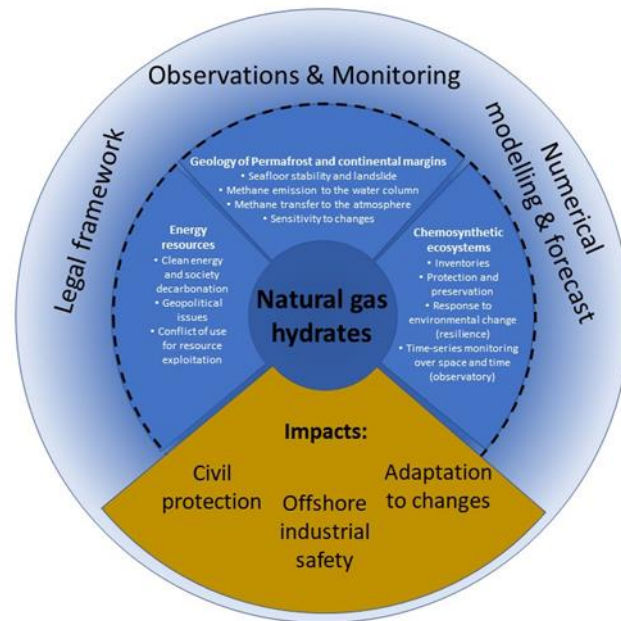
41 **Keywords:** Continental margins, gas emissions, methane flux into the atmosphere,  
42 natural gas hydrate deposits, permafrost and slope stability

43

## 44 **1. Introduction**

45 Natural gas hydrate deposits (NGHD), one of the major methane (CH<sub>4</sub>) reservoirs  
46 on Earth, are mainly located on continental margins, generally at water depth beyond  
47 ~500 m (Max, 2003; Max and Lowrie, 1996; Mienert et al., 2022; Milkov, 2004; Paull  
48 and Dillon, 2001; Ruppel, 2011). They are found in the upper sedimentary interval where  
49 the temperature is rather low (below 4 °C at the sediment-water interface for open seas)  
50 to meet their stability requirements. On continental margins, NGHD are generally  
51 encountered within the sediment at cold seep areas, which are specific ecosystem areas  
52 characterized by natural gas emissions at the seafloor (Sassen et al., 1993; Suess, 2014;  
53 Villar-Muñoz et al., 2021). Outcropping hydrates are less common but can also be  
54 observed at sites characterized by intense gas venting (MacDonald et al., 1994; Olu et al.,  
55 2009; Sassen et al., 1999). The amount of methane stored within the marine hydrate-  
56 bearing sediments ranges between 3-1469 GtC (Burwicz et al., 2011; Lee et al., 2022;  
57 Pinero et al., 2013; Wallmann et al., 2012). Methane released from hydrates promotes the  
58 development of chemosynthetic communities. At the higher latitude, in Polar Regions  
59 where the temperature is almost permanently below freezing point, natural gas hydrates  
60 are found in the permafrost at shallower water depth. The mind map in Figure 1 illustrates  
61 the large variety of disciplines the studies of the dynamics of NGHDs can collate: from  
62 field work including observations, sampling and monitoring, to laboratory study with  
63 analyses, modeling and forecast. Such studies are also relevant for societal issues such as  
64 civil protection and offshore industrial safety when dealing with seafloor stability, gas  
65 emissions, climate change adaptation, meeting energy needs, and preservation of  
66 chemosynthetic ecosystems. Tackling these issues requires the need of legal framework.

67



68 Figure 1: Mind-map representing the principal hydrate-driven scientific researches with  
 69 the societal issues.

70 The hydrate-bound gases either come from deep thermogenic reservoirs that contain  
 71 methane, and usually a significant amount of heavier hydrocarbons (often called C<sub>2+</sub>), or  
 72 are generated by the microbial degradation of organic matter at shallower sedimentary  
 73 depth, that produces mainly methane (Kvenvolden, 1995; Milkov, 2005; Milkov and  
 74 Etiope, 2018; Whiticar, 1994, 1999). The presence of hydrocarbons other than methane  
 75 in the hydrate-bound gases expands the hydrate stability field towards lower pressure and  
 76 higher temperature. For instance, thermogenic hydrates are found in the Sea of Marmara  
 77 at ~660 m water depth and ~15 °C (Bourry et al., 2009), whereas the microbial gas hydrate  
 78 deposit present in the Romanian sector of the Black Sea is located at >700 m water depth  
 79 and 9 °C (Burwicz and Haeckel, 2020; Chazallon et al., 2020; Ker et al., 2019; Riboulot  
 80 et al., 2018; Zander et al., 2017).

81 Most of the NGHD inventoried on Earth contain microbial gases. Thus, they are more  
 82 sensitive to changes in temperature, pressure and fluid chemistry, especially salinity. Any  
 83 changes in one of these physicochemical parameters can trigger their decomposition (also  
 84 called breakdown), leading to the discharge of the hydrate-bound gases into the water  
 85 column, with potential input into the atmosphere (Schmale et al., 2005; Shakhova et al.,  
 86 2010; Solomon et al., 2009; Thatcher et al., 2013; Westbrook et al., 2009). Here, the term  
 87 decomposition refers to either dissolution with release of methane-enriched water, or  
 88 dissociation when the NGHD is brought outside its stability field and the hydrates are  
 89 fully decomposed into water and free gases. Previous studies have shown that other  
 90 natural geological processes such as tides, seismic activity, seawater infiltration, change  
 91 in the Gulf Stream current, or the decrease and cease in gas supply may also trigger  
 92 hydrate decomposition (Lapham et al., 2013; Phrampus and Hornbach, 2012; Riboulot et  
 93 al., 2018; Sultan et al., 2014). Less frequently observed in nature, hydrate-piece  
 94 detachment has been proposed as a possible mechanism for causing the degradation of

95 NGHD and allowing the transfer of significant amounts of methane into the hydrosphere  
96 (Pape et al., 2011a).

97 Furthermore, hydrate decomposition changes the mechanical properties of the subsoil and  
98 affects the seafloor stability (Fig. 1). Such decomposition can enhance the formation of  
99 seafloor structures like pockmarks and carbonate build-up, and/or can also trigger  
100 sediment sliding (Hovland et al., 2002; Maslin et al., 2010; McConnell et al., 2012; Sultan  
101 et al., 2014; Yan et al., 2020). Climate change and/or anthropogenic activities are amongst  
102 the two major processes that may cause NGHD decomposition in the future (Dickens,  
103 2001; Dickens and Quinby-Hunt, 1997; Kennett et al., 2003; Marcelle-De Silva and  
104 Dawe, 2011; Moridis and Collett, 2003; Moridis et al., 2009; Ruppel, 2011; Ruppel and  
105 Kessler, 2017; Schicks et al., 2011; Vargas-Cordero et al., 2020b). Seabed deformation  
106 and prolonged release of methane in the water column are the two main hazards related  
107 to hydrate decomposition (Maslin et al., 2010), and they may have severe consequences  
108 on the dynamics of the surrounding ecosystems (Fig. 1). Thus, NGHD decomposition  
109 may be considered as a threat to the biodiversity of these ecosystems. However, they also  
110 represent a potential energy resource (Fig. 1) and several countries have undertaken  
111 comprehensive programmes for hydrate inventory on continental margins located within  
112 their Exclusive Economic Zone (EEZ), with the aim of estimating the amount of methane  
113 that can be recovered (Boswell et al., 2017; Collett et al., 2014; Collett et al., 2012; Konno  
114 et al., 2017; Li et al., 2018; Ruppel et al., 2008). It is worth noticing that current solutions  
115 for methane production from NGHD are not economically viable, and our increasing  
116 awareness of climate change requires us to advance our researches on the understanding  
117 of natural-gas hydrate dynamics and its relevance in the global carbon cycle. Such  
118 research studies are key to developing sustainable solutions for the aforementioned  
119 societal issues.

120 Furthermore, it is worth emphasizing that the time scale of hydrate decomposition can  
121 extend from a few years to millennia, depending on the nature of the disturbance. Thus,  
122 here we define disturbances leading to short-term decomposition as resulting from  
123 processes that significantly affect the NGHD after few years from their onset; whereas  
124 disturbances leading to long-term decomposition refer to processes for which the impacts  
125 on the NGHD appear after few decades, centuries or millennia. For instance, the influence  
126 of temperature change on hydrate stability is different when considering hydrate  
127 production (short-term human-induced disturbances to recover the methane as quick as  
128 possible) and climate change (long-term human-induced disturbances). Indeed, as an  
129 example of disturbance leading to long-term decomposition, modeling of the West  
130 Svalbard by Thatcher et al. (2013) and Marín-Moreno et al. (2015), respectively,  
131 suggested that the delay between the onset of warming and the inception of gas emissions  
132 due to this warming could amount to ~20-30 years. Such a time lag is not conceivable for  
133 hydrate production induced by thermal stimulation for instance. The magnitude of the  
134 decomposition and its duration also raise the question of the resilience and adaptation of  
135 the ecosystems associated with these deposits.

136 In this paper, an analysis of the environmental challenges associated with the  
137 decomposition of NGHD is proposed. It starts with a detailed description of the possible  
138 hazards related to the decomposition of NGHD and their consequences on the marine  
139 ecosystems considering disturbances leading to both short-term and long-term  
140 decomposition. Finally, it discusses possible monitoring solutions to assess the state of  
141 decomposition of a deposit and quantify the gas discharge over time.  
142

## 143 2. Prerequisites and main factors governing hydrate dynamics

144 The necessary thermodynamic conditions to form and sustain hydrate growth  
145 within sediments are the saturation of pore water with gas in coexistence or not with free  
146 gas, low temperature and high pressure. A failure of one of these three prerequisites will  
147 systematically trigger hydrate decomposition. However, several other factors govern the  
148 formation, distribution and extent of gas hydrates in nature. Amongst them, the  
149 physicochemical properties of the hydrate-forming geofluids and the sediment (*e.g.* gas  
150 generation and transport processes, gas fluxes, pore-water salinity, sediment mineralogy  
151 and permeability) and the geological characteristics of the setting (*e.g.* tectonics and fluid  
152 transport pathway, sedimentation regime and lithology, geothermal gradient and heat flux  
153 pattern) are key points. These factors affect both the formation and the decomposition of  
154 hydrates to varying extents as stressed in previous review papers (Hassanpouryouzband  
155 et al., 2020; Malagar et al., 2019; Ruppel and Waite, 2020; Waite et al., 2009), making  
156 the prediction of the consequences of changing any of them on the surrounding geosphere  
157 as well as on the hydrosphere, and potentially the atmosphere, a challenging task. Such a  
158 prediction becomes even more demanding once we consider that the accumulation of  
159 natural gas hydrates within the sediments is a time and space-evolving process due to the  
160 continuous changes in the deposit permeability and thermal properties that, in turn,  
161 continuously modifies the hydrate growth kinetics, the gas flow regime and pathway, and  
162 thus reroutes their distribution pattern (Schmidt et al., 2022). Such a behavior explains  
163 the wide varieties of hydrate habits encountered in nature, from disseminated through lens  
164 to massive nodules, and its heterogeneous distribution within the sediment from  
165 microscale to kilometer scales (Daigle and Dugan, 2011a, b; Egeberg and Dickens, 1999;  
166 Guo et al., 2020; Kossel et al., 2018; Naudts et al., 2012; Pape et al., 2011b; Paull and  
167 Dillon, 2001; Simonetti et al., 2013; Solomon et al., 2014; Stern and Lorenson, 2014;  
168 Stern et al., 2011; Wang et al., 2020). Thus, the knowledge of how all the aforementioned  
169 properties and factors affect the hydrate dynamics is often site-specific and depends on  
170 the geological history of the setting. Nevertheless, these properties are critical to  
171 predicting and quantifying the macroscale responses of hydrate-bearing sediments to  
172 environmental changes at different time scales. The environmental challenges are  
173 primarily related to gas hydrate decomposition, which also leads to severe and time-  
174 evolving changes in the permeability field of the deposit. The magnitude of the  
175 decomposition and how it happens strongly depend on the nature and magnitude of the  
176 disturbances applied to the NGHD. The following section focuses on the environmental  
177 challenges related to anthropic (human-induced) disturbances and climate change. As

178 explained above, the first corresponds to short-term perturbations with localized  
179 consequences, while the second induces disturbances spanning over a larger timescale  
180 and with broader impacts.

181

### 182 **3. Environmental challenges related to hydrate decomposition**

#### 183 **i. Impact of hydrate decomposition on the seafloor** 184 **morphology and stability**

185 Methane hydrate formation and decomposition induce the build-up or loss of solid  
186 materials that have a density significantly different from that of pore water or free gas  
187 (Lee et al., 2010; Loreto et al., 2011; Pape et al., 2011a). Density difference is one of the  
188 physical mechanisms that drives seafloor deformation. Several studies have demonstrated  
189 that hydrate formation and decomposition modifies the regime and pathway of free gas  
190 migration through the sediments, and can strongly affect the morphology of the seafloor  
191 by creating or enhancing the formation of pockmarks, mounds or pingos (Andreassen et  
192 al., 2017; de Prunelé, 2015; Gupta et al., 2022; Hovland and Svensen, 2006; Loreto et al.,  
193 2011; Paull et al., 2007; Riboulot et al., 2016; Serié et al., 2012; Sultan et al., 2014; Sultan  
194 et al., 2010; Taleb et al., 2020; Vargas-Cordero et al., 2020a; Waage et al., 2020; Zander  
195 et al., 2020). Besides the formation and decomposition of hydrates, dislodgement of  
196 hydrate pieces has been proposed to explain the rough seafloor topography encountered  
197 in the Eastern Black Sea (Pape et al., 2011a). While the hydrate formation stores methane  
198 within the sediment, the melting of hydrates triggers its release, and this is accompanied  
199 by the development of excess pore pressure that, in turn, reduces the mechanical strength  
200 of the sediment (Le et al., 2020; Nguyen-Sy et al., 2019; Sultan et al., 2007). In the rest  
201 of this section, we will focus on the consequences of hydrate decomposition as this  
202 process can trigger sediment mass flow (Sultan et al., 2004), which can be prodigious in  
203 scale and generate damaging tsunamis on open continental slopes (Talling et al., 2014).

204

205 In nature, hydrate dissolution is more widespread than dissociation because dissolution  
206 does not require the significant amount of energy needed to take the system outside its  
207 stability field (Ruppel and Waite, 2020). It can result from the shutdown or the slowdown  
208 of the gas flux supplying the NGHD, or an increase in either the pore water salinity or the  
209 bottom water temperature. Very few works mention explicitly the consequences of  
210 hydrate dissolution on the seafloor. Sultan et al (2010, 2014) showed that the formation  
211 of pockmarks in the Nigeria deep-water and the evolution of their morphology are  
212 strongly related to hydrate formation and dissolution. The observed pockmarks can be 40  
213 m depth and nearly a kilometer in diameter, making the installation of offshore oil and  
214 gas production facilities in their close vicinity a risky task. The dissociation of natural  
215 hydrates requires severe and more rapid changes in the (T, p) conditions. It can result  
216 from an increase in the bottom water temperature or a decrease in the hydrostatic pressure  
217 (Andreassen et al., 2017; Marin-Moreno et al., 2015). Most of the existing articles on the

218 impact of gas hydrate decomposition on the seafloor mentioned hydrate dissociation  
219 explicitly.

220  
221 The role of gas hydrate dissociation on submarine slope instability has been investigated  
222 over decades but controversy persists (Collett et al., 2014; Hassanpouryouzband et al.,  
223 2020). Dillon and Max (2000) have argued that dissociation of gas hydrates can be  
224 considered as the main cause of submarine slope failure only when the three following  
225 criteria are met: (i) gas hydrates are widespread; (ii) slides are initiated in areas within the  
226 hydrate phase boundaries; and (iii) sediment of low permeability (mainly fine-grained  
227 sediments) is present at the base of the gas hydrate occurrence zones. There are two well-  
228 studied submarine slope failures that happened in interglacial periods that have been  
229 potentially attributed to hydrate dissociation, although debate still remains: Storegga  
230 Slide and Hinlopen Slide. The Storegga Slide is one of the largest submarine slope failures  
231 known to have happened 8000 years ago (Bugge et al., 1988). The slide was most likely  
232 triggered by a strong earthquake and developed as a retrogressive slide, where massive  
233 sediments of about 150-200 m thick and up to 10.30 km wide slid down over ~200 km,  
234 causing huge tsunamis (Bryn et al., 2005). Besides, data presented few years ago (Geissler  
235 et al., 2016) strongly indicates that gas hydrates, free gas and excess pore pressure may  
236 have been the trigger or at least supportive factors for the slope instabilities north of  
237 Svalbard, in the vicinity of the Hinlopen Slide. Considering other locations, Lee argued  
238 that hydrate dissociation might have played a role in the large submarine landslides on  
239 the US Atlantic margin (Lee, 2009). Gas hydrate dissociation during deglaciation phases  
240 was also mentioned as one of the possible climate-driven changes that significantly  
241 affected slope stability in the Mediterranean Sea (Urgeles and Camerlenghi, 2013). In  
242 another recent work, by considering a seafloor temperature increase of 2 or 4 °C,  
243 Alessandrini et al (2019) simulated the impact of future global warming over the next 50  
244 and 100 years on the Gas Hydrate Stability Zone (GHSZ) off the Chilean margin. They  
245 suggested that, despite an increase in hydrostatic pressure due to sea level rise, seafloor  
246 temperature increase would induce the dissociation of the entire NGHD located along the  
247 upper slope in the next century. The dissociation will cause slope instability in some areas,  
248 and could seriously damage coastal cities if this dissociation triggers tsunamis. Using a  
249 large geophysical dataset including bathymetry and 2D/3D P-cable seismic data, Hillman  
250 et al. (2018) investigated the potential relationship between gas migration pathways, gas  
251 vents observed at the seafloor and submarine slope failures near the S2 Canyon in the  
252 Danube fan (Northwestern Black Sea). They found abundant evidence for gas migration  
253 in the area that suggests a connection between slumps and gas migration, although it is  
254 not clear whether gas migration facilitates slope failure through pressure and pre-  
255 conditioning of the sediments, or vice versa. From 2D seismic reflection profiles along  
256 the active margin of northern Colombia in the western Caribbean Sea, Leslie and Mann  
257 defined a series of three giant, previously unidentified, submarine landslides (Leslie and  
258 Mann, 2016). They suggested that an over-pressurized zone of weakness located at the  
259 boundary of the hydrate stability has likely facilitated slope failure.

260



261 Since the early works of McIver (1982), several studies have argued for a causal link  
262 between gas hydrate dissociation and the occurrence of submarine landslides (Bünz et al.,  
263 2005; Dawson et al., 2011; Elger et al., 2018; Grozic, 2010; McIver, 1982; Mienert et al.,  
264 2005). Such a link was supported by theoretical considerations based on the loss of  
265 cementation coupled with the release of free gas, giving rise to the development of excess  
266 pore pressure when changes in environmental conditions are no longer favorable for  
267 stable gas hydrates (Sultan et al., 2004; Tinivella and Giustiniani, 2013). Indeed, the  
268 dissociation of hydrates at the basis of their stability field could liberate free gas and  
269 increase the pore pressure just beneath the Bottom Simulating Reflector (BSR), and  
270 consequently decrease the effective normal stress (Hornbach et al., 2004). Thus, such  
271 focused dissociation weakens the strength of sediments due to loss of hydrate cementation  
272 between grains (Brown et al., 2006; Tinivella and Giustiniani, 2013). In the last two  
273 decades, the role of excess pore pressure (overpressure) on submarine slope instability  
274 has been very often put forward. The overpressure could potentially (i) facilitate or trigger  
275 submarine slides, (ii) form nearly vertical columns of focused fluid flow and gas  
276 migration, and (iii) determine the failure of a permeable layer in presence of low-  
277 permeability zone (Xu and Germanovich, 2006). Recent analyses aiming to assess  
278 quantitatively the role of gas hydrates on submarine slope instability have highlighted the  
279 importance of sediment lithology (Handwerker et al., 2017) and drainage conditions  
280 (Priest and Grozic, 2016), or fracture formation (Yang et al., 2018) on the development  
281 of excess pore pressures during hydrate dissociation. Mountjoy et al. (2014) analyzed  
282 seismic reflection data of the Tuaheni landslide complex (New Zealand East Coast) and  
283 proposed that, gas hydrates can directly destabilize the seafloor via three mechanisms  
284 (Mountjoy et al., 2014): (1) excess pore pressure induced by gas hydrate dissociation; (2)  
285 hydro-fracturing in the gas hydrate zone; (3) and time-dependent plastic deformation of  
286 hydrate-bearing sediment. Recently, unlike previous studies, Gross et al. (2018)  
287 performed a 3D analysis of the distribution of gas and gas hydrate indicators and did not  
288 show evidence of gas hydrates within the upper landslide unit. However, their  
289 observations support the hypotheses of Mountjoy et al. (2014) that argue that build-up of  
290 overpressure below low permeability gas hydrate-bearing sediments could cause hydro-  
291 fracturing in the gas hydrate zone and valving excess pore pressure into the landslide  
292 body. The hypotheses also suggested that gas is migrating into the critical mechanical  
293 zone at the base of the landslide, and thus building up overpressure that can lead to the  
294 reactivation of the landslide. Results obtained by Horozal *et al.* (2017) in the Ulleung  
295 Basin also suggested that excess pore pressure caused by gas hydrate dissociation could  
296 have contributed to slope failures. Such an increase in the interstitial pore pressure  
297 generated by gas hydrate dissociation was equally reported by Ker et al. (2019) in the  
298 Western Black Sea. They suggested that values of excess pore pressure of 1-2 MPa are  
299 probably the result of the low permeability of hydrate-bearing sediments. This excess  
300 pore pressure is expected to drastically reduce sediment stability and could be at the origin  
301 of some of the observed landslides in the area. Such assumptions agree with the study of  
302 Elger et al. (2018) who used reflection seismic data from the Arctic Ocean and numerical  
303 modeling to show a direct link between hydrates and slope instability. Their study showed  
304 that hydrates reduce the sediment permeability and causes the build-up of overpressure at

305 the base of the GHSZ. This overpressure reaches the shallow permeable beds, through  
306 hydro-fracturing forms like pipe structures, and then it is transferred laterally within the  
307 sedimentary column, weakening the slope sediment and leading to its destabilization.

308  
309 Hovland and Gudmestad discussed the engineering significance of gas hydrates and the  
310 possible engineering consequences on seabed installations (Hovland and Gudmestad,  
311 2001). Offshore petroleum exploration and production involves operations that alter  
312 ambient subsurface conditions (changes in stress, temperature and compositions of pore  
313 fluids), which in turn, may induce gas hydrate dissociation. For this reason, gas hydrates  
314 may be considered as a geohazard for this sector of activity. The consequences of gas  
315 hydrate-related seafloor instability to engineering structures would be very damaging  
316 such as causing hydrocarbon release from producing wells, or seafloor slumping  
317 obliterating subsea oil and gas production facilities. The following activities would also  
318 trigger gas hydrate dissociation in the sediment:

- 319 - Drilling into the sea bottom produces heat that could dissociate gas hydrates in the  
320 sediment and release gas. If the free gas released during drilling forms gas  
321 hydrates around the wellhead, it could cause a loss of mud density, resulting in  
322 wellbore instability and even mechanical system failure. More important gas  
323 releases could have consequences on the stability of the drilling rig. In addition,  
324 excess local pressure caused by gas hydrate dissociation in the sediment can  
325 induce casing collapse.
- 326 - Heat from a warm pipeline will propagate in the surrounding sediments. This  
327 could cause gas hydrate dissociation, inducing sediment instability and slumping.  
328 Under such conditions, the pipeline may rupture.
- 329 - Suction anchors usually used in deep water to keep floating structures anchored  
330 to the seafloor would reduce pressure and cause local gas hydrate dissociation,  
331 disturbing the friction forces along the walls of the anchor and thus threatening  
332 the safety of the operation.

333 McConnell et al. reviewed the history of gas hydrate shallow hazard assessment and  
334 found that low-saturation, mud-hosted hydrate layers can be safely drilled using existing  
335 industry protocols (McConnell et al., 2012). For highly saturated hydrate-bearing sand  
336 reservoirs, they will likely continue to be avoided, unless they are the specific targets of  
337 the well for methane production.

338  
339 Mining of hydrates may also cause submarine landslides. Song et al. (2019) applied a  
340 thermal-fluid-solid-stress coupling model to NGHD to investigate the failure process of  
341 submarine landslides induced by hydrate decomposition. Their results show that hydrate  
342 mining may cause settlement of the seafloor and slippage of submarine sedimentary  
343 layers to the mining center, and thus can potentially trigger submarine landslides. Based  
344 on geophysical and geotechnical data, Zander et al. (2017) investigated the potential  
345 impacts of gas hydrate exploitation on slope stability in the Danube deep-sea fan in  
346 northwestern Black Sea. Their 2D slope stability model applied to a hypothetical gas  
347 hydrate reservoir suggests that the area is relatively safe against slope failure under static

348 conditions, but probably not sufficiently safe to allow the implementation of  
349 infrastructure for hydrate production at the seabed without taking specific mitigation  
350 measures into account (*e.g.* relocation options, design criteria).

## 351 **ii. Impact of hydrate decomposition on permafrost**

352 It has been generally accepted that global warming tends to destabilize gas hydrates  
353 present in permafrost through different mechanisms, such as directly melting top layers  
354 of gas hydrates (Mienert et al., 2005), thermal shock led by sea level rise (Maslin and  
355 Thomas, 2003), and reduction in lithostatic pressure hence hydrostatic pressure due to  
356 shrinking of subsea permafrost (Paull and Dillon, 2001; Tinivella and Giustiniani, 2016;  
357 Tinivella et al., 2019; Waage et al., 2020; Wallmann et al., 2018). However, the  
358 environment in which hydrates are found is different from that encountered on continental  
359 margins. In permafrost regions, gas hydrates and ice may coexist with salts, water, and  
360 free gas in the offshore sediments, which leads to unique characteristics of the ice-  
361 hydrate-bearing sediments compared to those of the other marine sediments. However,  
362 little work has been done to understand such properties of permafrost sediments  
363 containing gas hydrates, although the mechanical properties of frozen soil and rock in the  
364 absence of gas hydrates and unfrozen gas hydrate-bearing sediments were extensively  
365 investigated (*e.g.* (Arenson et al., 2007; Tsyтович, 1975; Waite et al., 2009)). The  
366 mechanical properties of frozen sand, silt and clay containing tetrahydrofuran (THF)  
367 hydrate were determined at -10 °C (Yun et al., 2007), and they found that shearing results  
368 in particle rotation, slippage, and rearrangement in the absence of THF hydrates. In  
369 contrast, shear force leads hydrates to detach from the mineral surface in the presence of  
370 low saturation (<40%) of THF hydrates, or to debond from the sediment grains in the  
371 presence of high saturation (>40%) of THF hydrates. The mechanical properties of kaolin  
372 clay-ice powder mixtures were investigated in the presence of carbon-dioxide (Liu et al.,  
373 2013) and methane hydrates (Li et al., 2016; Li et al., 2019; Luo et al., 2018; Yun et al.,  
374 2007). The determined shear strength was unexpectedly low compared to the sediments  
375 containing gas hydrates only, and this was mainly explained by the lack of cementation  
376 between hydrate crystals, ice powders and clay grains. Recently, Yang et al. (2019)  
377 reported a set of comprehensive experiments for methane hydrate-bearing frozen  
378 sediments. Their results showed that gas hydrates can form micro frames or network  
379 structures, resulting in distinctive effects on the mechanical properties (higher shear  
380 strength and less brittle under compressional loading) of the simulated hydrate-bearing  
381 permafrost sediments compared to frozen sediments in the absence of gas hydrates (Yang  
382 et al., 2019).

383 Old estimation provided huge volumes (up 9.2 to 22.3x10<sup>3</sup> Pg (1 Pg = 10<sup>15</sup> g)) of methane  
384 trapped as hydrates in permafrost of the Arctic regions (Max and Lowrie, 1996).  
385 However, more recent studies provided most lower estimates ranging from 27 (~1% of  
386 global hydrate estimate) to 800 Pg of methane (Knoblauch et al., 2018; Miesner et al.,  
387 2023; Ruppel, 2015). Gas hydrate-bearing permafrost sediments (GHBPS) are sensitive  
388 to temperature changes that could be induced by global warming, seasonal changes,  
389 geothermal fluxes, and human activities. Particularly, global warming is causing the

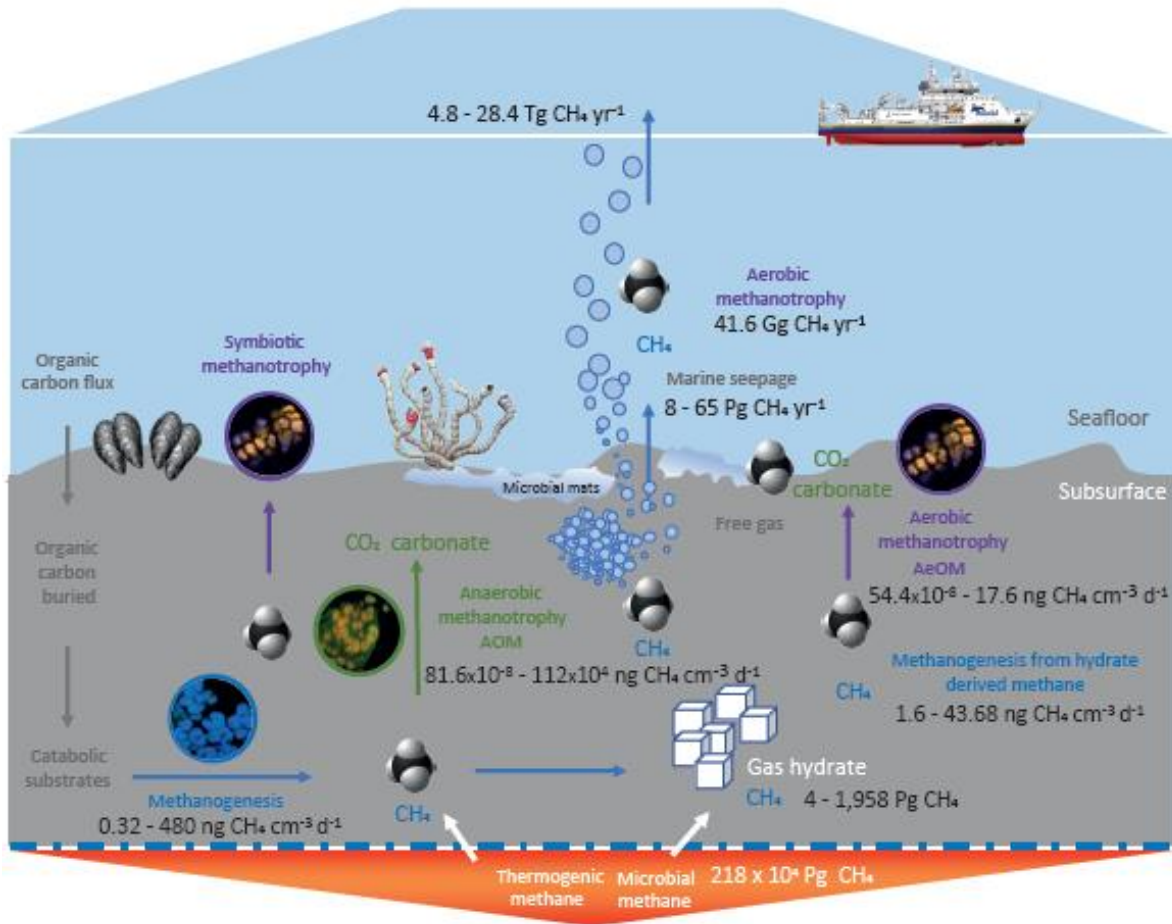
390 shrinking of both terrestrial and subsea permafrost, leading to a reduction in lithostatic  
391 pressure and hence hydrate decomposition (Maslin et al., 2010). Scientific research has  
392 revealed that global warming has accelerated the rate of ice thawing and gas hydrate  
393 decomposition in permafrost regions, and, consequently, led to the release of methane  
394 and carbon dioxide into the atmosphere, exacerbating global warming (Andreassen et al.,  
395 2017; Portnov et al., 2016). A more detailed review on gas release follows in the next  
396 section. This adverse effect of greenhouse gases reaching the atmosphere becomes even  
397 more severe in the Arctic regions due to the effect of polar amplification. In other words,  
398 the atmosphere or an extensive ocean circulation can lead to heat transport toward the  
399 poles. Consequently, climate warming would affect the areas adjacent to the Earth poles  
400 at relatively greater magnitude compared to the rest of the Earth surface (Polyakov et al.,  
401 2002), accelerating decomposition of gas hydrates in permafrost regions such as the  
402 Arctic. Observations of natural catastrophic events have demonstrated that this increasing  
403 negative feedback could tip over the mechanical stability of GHBPS, and trigger a chain  
404 of large-scale land and/or seafloor failures, and subsequently induce an abrupt greenhouse  
405 gas venting from subsea permafrost in the East Siberian Arctic Shelf (Ruppel and Kessler,  
406 2017) and life-threatening events such as tsunamis that could reach the shore of the UK  
407 based on evidence of historic events (Long et al., 2016; Tinivella et al., 2019). The  
408 instability of GHBPS has been attributed to landslides in Yukon Territory in Canada  
409 (Maslin et al., 2010), the permafrost lava observed on the Tien Shan Mountains in China  
410 (Marchenko et al., 2007), the formation of massive gas blow-out craters in the northern  
411 Barents Sea (Andreassen et al., 2017) and in the Yamal and Gydan Peninsulas in northern  
412 Siberia in Russia (Bogoyavlensky et al., 2020). These destructive consequences in recent  
413 years are also attributed to the global warming of anthropogenic activities. Based on  
414 numerical modeling, Andreassen et al. (2017) developed an understanding of how the  
415 craters and mounds were formed in the northern Barents Sea and postulated that climate  
416 warming leads to the ice sheet retreating, and this is accompanied with catastrophic  
417 reduction of the sediment pore pressure. Consequently, gas hydrates initially in  
418 permafrost or sediments dissociate. The dissociation of gas hydrates at depth, particularly  
419 those underlying impermeable layers, results in building up of overpressure in pores.  
420 Finally, when the overpressure reaches a certain threshold, gas hydrate pingos could be  
421 formed, and their collapse creates craters in permafrost regions. Furthermore,  
422 composition analysis of the gas from such craters showed particularly high concentration  
423 of methane (Kvenvolden and Field, 1981). Such high concentration of methane only  
424 allows formation of structure I hydrate which makes the gas hydrate-bearing permafrost  
425 more vulnerable to global warming. Furthermore, the occurrence of methane hydrates in  
426 permafrost layers gives GHBPS more complex characteristics than the sediments  
427 containing either ice (*e.g.* hydrate-free frozen soils) or gas hydrates (*e.g.* unfrozen  
428 hydrate-bearing sediments). Such characteristics include fluid distribution in pores,  
429 unfrozen water content, and ice/hydrate morphologies such as pore filling or grain  
430 cementing, load bearing or micro frame structures. At present, there is little knowledge  
431 about the physical properties of permafrost sediments that are saturated with variable ice,  
432 hydrate, gas, and saline water (Farahani et al., 2021a, b; Hassanpouryouzband et al., 2020;  
433 Yang et al., 2019).

434

#### 435 4. Gas release from hydrate decomposition

436 Figure 2 illustrates the functioning of cold seep areas where the main methane-involving  
437 biogeochemical processes are presented. It provides some numbers related to methane  
438 transport from one compartment to another, storage, and transformations (genesis and  
439 degradation) that will be discussed throughout this paragraph.

440



441

442

443

444

445 Fig.2: Conception scheme of biogeochemical processes taking place at hydrate-bearing  
446 setting on continental margins with estimated fluxes and stocks. Ranges of microbial  
447 methane fluxes (methanogenesis, AOM and AeOM) were converted in mole-to-mass  
448 from microbial rates reported and estimated from cited references in Table 2.

449

450 Methane venting at the seafloor widely occurs on shelves and continental margins. There,  
451 methane and hydrogen sulfide are generated, transported and transformed within the  
452 sediment, and part of the former is discharged into the water column (Suess, 2014). At  
453 hydrate-bearing settings, the amount of methane that can potentially be released from

454 hydrate decomposition processes is variable and site-specific (Baumberger et al., 2022;  
455 Braga et al., 2020; de la Cruz Vargas-Cordero et al., 2021; Ketzer et al., 2020; Marcon et  
456 al., 2022; Marin-Moreno et al., 2015; Merle et al., 2021; Meurer et al., 2021; Riboulot et  
457 al., 2018; Thatcher et al., 2013). However, judging from the number of articles published  
458 in recent years, methane discharge from hydrate decomposition is not a sporadic event  
459 (Fu et al., 2021; Hautala et al., 2014; Johnson et al., 2015; Phrampus et al., 2014;  
460 Westbrook et al., 2009), and it is likely that this process will further increase in the  
461 decades and centuries to come due to climate change.

462 Once released from the hydrates, methane undergoes several physical and  
463 biogeochemical processes, starting from its dissolution in the pore water followed by its  
464 oxidation (Figure 2). The remaining methane is transferred into the hydrosphere where it  
465 undergoes similar processes. These processes act as efficient barriers preventing methane  
466 transfer to the atmosphere. However, the efficiency of these barriers depends on multiple  
467 factors (*e.g.* water depth, upwelling flowrate, local current, water stratification, *etc.*); and,  
468 at the end, only a small portion of the total amount of methane released from NGHD  
469 decomposition may reach the atmosphere (de Garidel-Thoron et al., 2004; Ruppel, 2011;  
470 Ruppel and Kessler, 2017; Westbrook et al., 2009). Such a transfer occurs particularly in  
471 the case of catastrophic releases.

472 In the following sections, we discuss in detail the variability of the seafloor methane from  
473 hydrate decomposition, followed by the impact of such a leakage on the seafloor  
474 ecosystems, seawater chemistry, and the conditions that lead to its transfer to the  
475 atmosphere.

#### 476 **i. Fluxes of methane discharged at the seafloor**

477 Due to the sensitivity of the NGHD to environmental changes, concerns have been  
478 raised regarding a massive and prolonged release of methane from hydrate decomposition  
479 and its consequences in terms of climate feedback, ocean acidification and ecosystem  
480 vulnerability (Archer, 2007; Biastoch et al., 2011; Garcia-Tigreros et al., 2021). To  
481 provide some answers to these societal issues, it is necessary to consider the fluxes of  
482 methane released from hydrate decomposition. These fluxes are related to the rate of  
483 hydrate decomposition, which depends on multiple factors. For outcropping hydrates, the  
484 main factors are the flow velocity of the contacting methane-free water, the extent of  
485 partial-sediment cover, and the presence of oil film or biofilms and non-methane guest  
486 molecules. Considering hydrate-bearing sediments, the porosity, thickness and thermal  
487 properties of the sediment are key factors affecting build-up and flow of methane-charged  
488 fluids until its release at the seabed; and these flow-driving factors depend on both the  
489 free-gas and hydrate saturation levels that evolve over the course of the decomposition.

490 Although hydrates are widespread on continental margins and in the permafrost,  
491 and were intensively investigated in the former location, there are few natural sites where  
492 hydrate decomposition has been quantified (Tables 1 and 2). The rate of hydrate  
493 dissolution has been determined in the Cascadia Margin (Heeschen et al., 2005; Hester et  
494 al., 2009; Lapham et al., 2010; Linke et al., 1994; Riedel et al., 2010; Römer et al., 2016;  
495 Suess et al., 1999; Torres et al., 2002; Wilson et al., 2015), the Gulf of Mexico (Lapham  
496 et al., 2014; Solomon et al., 2008) and the Monterey Bay (Rehder et al., 2004). The data,  
497 either measured or calculated from other measured parameters, revealed high variabilities

498 not only from one region to another, but also within a given geological setting (Table 1).  
499 Thus, for studies undertaken in the Cascadia Margin the dissolution rate ranges between  
500 29 to  $7.9 \times 10^6$  mmol.m<sup>-2</sup>.yr<sup>-1</sup>. Lowest values were obtained for deposits characterized by  
501 thermogenic hydrates trapping multiple guest molecules, and/ or oil film covering the  
502 outcropping specimens as the presence of such cover significantly mitigates the  
503 dissolution rate. Lapham et al. (2014) showed that the aforementioned range of  
504 dissociation rates is similar to previously reported laboratory measurements (Bigalke et  
505 al., 2009). In the Gulf of Mexico, Lapham et al. (2014) measured a dissolution rate of  
506  $6.6 \times 10^6$  mmol.m<sup>-2</sup>.yr<sup>-1</sup> for thermogenic hydrates. Such a rate for thermogenic hydrates is  
507 in the same order of magnitude than the value of  $4.7 \times 10^6$  mmol.m<sup>-2</sup>.yr<sup>-1</sup> obtained by Hester  
508 et al (2009) at Barkley Canyon, and it is in the same range than the rate range of 8-  $9.5 \times 10^6$   
509 mmol.m<sup>-2</sup>.yr<sup>-1</sup> (141-167 cm.yr<sup>-1</sup>) measured from synthetic methane hydrates brought at  
510 the seafloor for *in situ* decomposition experiments (Rehder et al., 2004). Furthermore,  
511 Bigalke et al. (2009) performed laboratory-based experiments at temperature and pressure  
512 conditions within the hydrate stability field to investigate the dissolution of methane  
513 hydrates in undersaturated seawater. The dissolution rate was found to be strongly  
514 dependent on the friction velocity and the temperature of the seawater turbulent flow,  
515 showing that hydrate dissolution in undersaturated seawater is a diffusion-controlled  
516 process. They suggested that additional experimental work is required to address the  
517 dissolution kinetics of non-pure methane hydrates, as both, the solubility limit and the  
518 understanding of the molecule transfer processes at the phase boundary during  
519 dissolution, are less well constrained. It is also important to note that the measurement  
520 principles, the instruments and the computing approaches used for these aforementioned  
521 studies of *in situ* hydrate-dissolution may differ from one research group to another,  
522 leaving bias in the comparison.

523 Moreover, methane hydrate dissolution rate depends on the thickness of the  
524 diffusion boundary layer and the methane concentration in water, and this second  
525 parameter is in turn controlled by the solubility of methane. Rehder et al. (2004) showed  
526 that gas hydrate dissolution rate depends on the difference between the local solubility in  
527 the presence of gas hydrates and the local dissolved-phase concentration of the hydrate-  
528 forming gas. Lapham et al. (2010 and 2014) measured the methane concentration in  
529 sediments immediately surrounding outcropping deep-sea gas hydrates for two sites in  
530 Barkley Canyon and the Gulf of Mexico, respectively. Their results showed that pore-  
531 fluids are significantly under-saturated with respect to expected values at equilibrium  
532 with methane hydrates, indicating that the hydrates should continue to dissolve. They also  
533 showed that dissolution rates calculated from *in situ* methane concentration gradients are  
534 significantly lower than those predicted for methane-undersaturated pore water in direct  
535 contact with pure methane hydrates if equilibrium methane concentrations exist  
536 immediately adjacent to the hydrate surface. Lapham et al. (2010) suggested that the  
537 factors that retard hydrate decomposition in sediments here could be oil coating or  
538 biofilms. This is supported by Wilson et al. (2015) who investigated how that sediment  
539 cover can affect hydrate dissolution by means of field (at Barkley Canyon) and laboratory  
540 measurements. The dissolution rate of outcropping thermogenic hydrates covered with  
541 sediment was around  $3.4 \times 10^3$  mmol.m<sup>-2</sup>.yr<sup>-1</sup> (<1 cm.yr<sup>-1</sup>), whereas that of synthetic  
542 hydrates exposed directly to bulk water was an order of magnitude higher. Their results

543 are in agreement with dissolution-rate values calculated by Riedel et al (2010) for buried  
1 544 hydrates at sites on the Clayoquot Slope of the Cascadia margin. Thus, as hydrate  
2 545 dissolution is mainly controlled by diffusion, the presence of sediment slows the rate of  
3 546 molecular diffusion via porosity/tortuosity effects.  
4 547

5 548 For its part, hydrate dissociation has been investigated at the high latitude regions such as  
6 549 the Western Svalbard (Ferre et al., 2020; Marin-Moreno et al., 2015; Marin-Moreno et  
7 550 al., 2013; Thatcher et al., 2013; Westbrook et al., 2009), the U.S. Beaufort margin  
8 551 (Phrampus et al., 2014) and the Laptev Sea (Chernykh et al., 2020); as these regions are  
9 552 very sensitive to temperature increase due to climate change (Hassol, 2004; Hassol and  
10 553 Corell, 2006). Investigations on the U.S. Atlantic margins also suggest that multiple  
11 554 methane emission sites are partly related to hydrate dissociation due to the sea-bottom  
12 555 temperature increase (Phrampus and Hornbach, 2012; Skarke et al., 2014; Weinstein et  
13 556 al., 2016). However, as it is relatively usual to observe gas emissions associated with  
14 557 hydrates at cold seeps, this coexistence makes it difficult to accurately assess the  
15 558 contribution of hydrate dissociation in the total gas discharge. The dissociation process  
16 559 requires bringing the pressure and temperature conditions of the deposits to the boundary  
17 560 of the GHSZ to allow the formation of gas bubbles, and the common factor amongst the  
18 561 aforementioned sites is the occurrence of intense gas emissions at the upper limit of the  
19 562 GHSZ. Nevertheless, like for hydrate dissolution, Table 2 shows that the estimated  
20 563 methane fluxes and the potential discharge trajectory are highly heterogeneous. In one of  
21 564 the first estimates, Westbrook et al (2009) estimated that  $\sim 20 \text{ Tg.yr}^{-1}$  of methane can be  
22 565 released from hydrates over an area of  $22,300 \text{ km}^2$  corresponding to a swath within 360-  
23 566 400 m water depth nearly all around the Svalbard archipelago. Marin-Moreno et al (2013  
24 567 and 2015) also investigated the sensitivity to climate change of the hydrate deposit present  
25 568 in the Western Svalbard continental margin by considering a temperature-increase path  
26 569 following either the lower (2.6) or the upper (8.5) cases of the Representative  
27 570 Concentration Pathways (RCP). Their projection indicated that  $0.029\text{-}0.053 \text{ Tg.yr}^{-1}$  of  
28 571 methane can be released from hydrate dissociation over an area of  $\sim 134 \text{ km}^2$  during the  
29 572 next three centuries. Such a projection is also in agreement with the estimates of  $22.4 \text{ Tg.}$   
30 573  $\text{yr}^{-1}$  proposed by Ferré et al (2020) along the 360 m isobaths at the Norwegian-western  
31 574 Svalbard Margin. By extending to the swath width of Svalbard archipelago corresponding  
32 575 to 400-500 m water depth (swath width complementary to the one considered by  
33 576 Westbrook et al., 2009), Marin-Moreno et al. (2013 and 2015) showed that the methane  
34 577 discharge may reach  $1.7\text{-}9 \text{ Tg.yr}^{-1}$  over  $41,400 \text{ km}^2$ . Thus, their estimates of vulnerable  
35 578 hydrates are more than twice smaller than the estimate obtained by Westbrook et al (2009)  
36 579 for a surface area three times larger but located at deeper depth. Their results also showed  
37 580 that hydrates remain stable beyond 500 m water depth. Such studies illustrate the  
38 581 importance of the water depth (hydrostatic pressure) on the stabilization of hydrates. It is  
39 582 very interesting to mention that they found that the choice of the RCP scenario has a small  
40 583 impact on the total discharge. The calculated methane fluxes off Svalbard ranges from an  
41 584 estimated average of  $2 \text{ mmol.m}^{-2}.\text{yr}^{-1}$  (Thatcher et al., 2013) to  $13.5 \text{ mol.m}^{-2}.\text{yr}^{-1}$   
42 585 calculated by Marin-Moreno et al (2013). The fluxes calculated by Phrampus et al. (2014)  
43 586 fall within this range of values for the U.S. Beaufort margin ( $0.88\text{-} 4.4 \text{ mol.m}^{-2}.\text{yr}^{-1}$ ),  
44 587 whereas values up to two and three order of magnitude higher were obtained by Skarke  
45  
46  
47  
48  
49  
50  
51  
52  
53  
54  
55  
56  
57  
58  
59  
60  
61  
62  
63  
64  
65



588 et al (2014) and Chernykh et al (2020) on the U.S. Atlantic margin and in the Laptev Sea,  
 589 respectively.

590 Moreover, it is important to recall that these methane fluxes are not constant over the  
 591 time; and therefore, there is a need to take into account processes and seasonal changes  
 592 that induced short to long-term variations that affect annual fluxes such as tides (Römer  
 593 et al., 2016; Sultan et al., 2020), seismic activities (Fischer et al., 2013; Franek et al.,  
 594 2017; Lapham et al., 2013) and temperature (Berndt et al., 2014; Ferre et al., 2020).

595 Table 1: Dissolved methane fluxes measured from field study of hydrate dissolution

Hydrate dissolution			
Location	Dissolution rate/cm.yr <sup>-1</sup>	Dissolution rate/mm <sup>2</sup> .yr <sup>-1</sup>	Reference
Monterey Bay (Monterey Canyon- MontC)	187 <sup>*</sup> -220 <sup>*</sup>	1.07 – 1.26 x 10 <sup>7</sup>	Rehder et al. (2004)
Gulf of Mexico (Green Canyon- BC and Mississippi Canyon- MC)	15 <sup>#</sup> (GC)	8.57 x 10 <sup>5</sup>	Lapham et al. (2014)
	0.001 <sup>#π</sup> (MC)	63	Lapham et al. (2010)
Northern Cascadia Margin: (Barkley Canyon- BC), South Hydrate ridge, Hydrate ridge (regional average- RA), Clayoquot Slope (CS)	62 <sup>#</sup> and 104 (BC)	4.7 x 10 <sup>6#</sup> and 7.9 x 10 <sup>6</sup>	Hester et al. (2009); Lapham et al. (2014)
	0.0005/ 0.03 <sup>#π</sup> (BC)	29/ 1800	Lapham et al. (2010)
	3.5 <sup>#</sup> (BC)	0.2 x 10 <sup>6</sup>	Lapham et al. (2010)
	0.06- 0.33 (CS)	3.43 x 10 <sup>3</sup> - 1.88 x 10 <sup>4</sup>	Romer et al. (2016) Riedel et al. (2010)
	0.06 <sup>#</sup> (BC)	3.4 x 10 <sup>3</sup>	Wilson et al. (2015)

597 # for complex thermogenic hydrates, \* for synthetic hydrates, <sup>π</sup> for buried hydrates (otherwise it is outcropping hydrates)

598  
 599  
 600 Table 2: Free methane fluxes measured from field study of hydrate dissociation and over a hydrate deposit

Hydrate dissociation		
Location	Methane flux from gas discharged at hydrate sites	Reference
Svalbard Continental margin; West Svalbard	0.027 Tg yr <sup>-1</sup> (30-km-long plume-area) potentially 20 Tg yr <sup>-1</sup> (22300 km <sup>2</sup> )	Westbrook et al. (2009)
	2 mMol.m <sup>-2</sup> .yr <sup>-1</sup>	Thatcher et al (2013)
	0.0053-0.029 Tg yr <sup>-1</sup> over the next 300 years; e.g 2.5–13.5 mol yr <sup>-1</sup> m <sup>-2</sup>	Marín-Moreno et al (2013)

	0.0004–0.0015 Tg yr <sup>-1</sup> and 0.0017-0.0045 Tg yr <sup>-1</sup> over the next 100 years	Marín-Moreno et al (2015)
	22.4 Gg yr <sup>-1</sup> (along the 360 m isobaths at the Norwegian–western Svalbard Margin); e.g 2120 mol m <sup>-1</sup> yr <sup>-1</sup>	Ferré et al (2020)
Hudson Canyon	4.375- 17.5 Mmol yr <sup>-1</sup> for the extended area	Weinstein et al (2016)
From Cape Hatteras to Georges Bank	0,938- 5,625 Mmol yr <sup>-1</sup> e.i. 25-150 mol m <sup>-2</sup> yr <sup>-1</sup>	Skarke et al (2014)
Carolina rise off the east coast of North America	2.5 Gt of methane stored as GH would be destabilized	Phrampus and Hornbach (2012)
U.S. Beaufort margin	0.44-2.2 Gt of methane would be released e.i. 0.88- 4.4 mol m <sup>-2</sup> yr <sup>-1</sup>	Phrampus et al. (2014)
Laptev Sea	9360- 11 170 mol.m <sup>-2</sup> .yr <sup>-1</sup>	Denis Chernykh et al (2020)

## ii. Microbial processes and methane discharge at the seafloor

Currently global methane emissions are about 500-600 Tg per year (Ehhalt et al., 2001; Saunio et al., 2020) (see section 4.iv “Transfer to the atmosphere”), with around 70% (350-400 Tg) of which is due to methanogenesis from a wide variety of habitats including anoxic seafloor ecosystems (Conrad, 2009). Around 40% of the methane produced by methanogenesis escapes to the atmosphere (Lyu et al., 2018). In marine sediments, microbial methanogenesis produces methane through the terminal anaerobic breakdown of organic matter deposited on the seafloor (Parkes et al., 2014; Wellsbury et al., 2000) (Fig.2). Estimations suggest that 3-18% of the buried organic carbon within the seafloor is converted to CH<sub>4</sub> by methanogenesis in continental margin (Egger et al., 2018; Xu et al., 2022). Recent estimates from Xu et al. (2022) indicates that the global methanogenesis budget approximates 13 Tg of methane per year. Methanogenic activities have been observed from surface to deep sub-seafloor sediments (Table 3).

Table 3: Rates of methanogenesis, anaerobic methanotrophy (AOM) and aerobic methanotrophy (AeOM) in various microbial marine habitats.

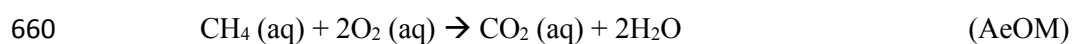
	<b>Methanogenesis</b>	<b>Anaerobic methanotrophic oxidation</b>	<b>Aerobic methanotrophic oxidation</b>
Sediments:	0.02 to 30 nmol cm <sup>-3</sup> d <sup>-1*****</sup>	5.1 x 10 <sup>-8</sup> to 7.0 x 10 <sup>4</sup> nmol cm <sup>-3</sup> d <sup>-1****</sup>	3.4 x 10 <sup>-8</sup> to 1.1 nmol cm <sup>-3</sup> d <sup>-1****</sup>
-with hydrate	0.1-2.73 nmol cm <sup>-3</sup> d <sup>-1***</sup> < 4.25 x 10 <sup>-6</sup> nmol cm <sup>-3</sup> d <sup>-1*</sup>	10 <sup>2</sup> to 5x10 <sup>3</sup> nmol cm <sup>-3</sup> d <sup>-1*****</sup>	0-12 mmol m <sup>-2</sup> d <sup>-1*****</sup>
-without hydrate	0.015-0.62 nmol cm <sup>-3</sup> d <sup>-1**</sup>	0.001 to 10 <sup>4</sup> nmol cm <sup>-3</sup> d <sup>-1*****</sup>	0-289 mmol m <sup>-2</sup> d <sup>-1*****</sup>

\*Estimation of microbial methane production rates in deep marine sediment at hydrate ridge is based on representative species of methanogen *Methanoculleus submarinus* starved in culture with Biomass

621 Recycle Reactor coupled to quantitative PCR of *mcrA* gene abundances (Colwell et al., 2008). \*\*Vigneron  
622 et al., 2015, Cold seeps at Guaymas Basin in Sonora margin; \*\*\*Wellsbury et al., 2000, Blake Ridge; \*\*\*\*(Gao  
623 et al., 2022). \*\*\*\*\*(Parkes et al., 2007) and (Newberry et al., 2004) \*\*\*\*\*Boetius and Wenzhöfer, 2013. The  
624 < sign indicate underlying uncertainties.

625 The formation of methane involves a group of strictly anaerobic archaea called  
626 methanogens. However, smaller amounts of methane are produced from  
627 methylphosphonates in oxic waters by both phytoplanktons with mainly Cyanobacteria  
628 and Thaumarchaea (Bižić et al., 2020; Klintzsch et al., 2019; Metcalf et al., 2012).  
629 Methanogens use various low-molecular-weight catabolic substrates for biosynthesis of  
630 methane, and thus the rate of methanogenesis can be difficult to estimate. The Redox  
631 reaction of dihydrogen (H<sub>2</sub>) with carbon dioxide (CO<sub>2</sub>) and/or with formate are  
632 considered as the main substrates for methanogenesis in marine sediments (Newberry et  
633 al., 2004; Parkes et al., 2007). However, it has been shown that acetate can become the  
634 dominant substrate in deeper sediments (Reeburgh, 2007). Methanogens also performed  
635 methanogenesis with methylated compounds. Methylophilic methanogenesis may be an  
636 important methane source in coastal shallow sediment (Conrad, 2020). Acetate and other  
637 potential substrates for microbial methanogenesis could derive from either thermal  
638 alteration or biological degradation of organic matter. Recent developments in high  
639 throughput sequencing techniques have revealed an unexpected larger diversity within  
640 the methanogens and suggest that this metabolic pathway is one of the most ancient on  
641 Earth (Vanwonterghem et al., 2016; Wang et al., 2021). Metagenome assembled genomes  
642 (MAGs) of potential methanogens suggest the acquisition of both novel functions in  
643 activation of alternative catabolic substrates such as short and medium chain of alkanes  
644 and volatile fatty acids (Laso-Pérez et al., 2019; Wang et al., 2021), and in derivation of  
645 cellular energy from methoxylated aromatic compounds from lignin occurring in coal bed  
646 (Inagaki et al., 2015; Kurth et al., 2021). The overall rates of methanogenesis in marine  
647 sediments range from 0.02 to 30 nmol cm<sup>-3</sup> d<sup>-1</sup> (Table 3) (mole-to-mass conversion is 0.32  
648 to 480 ng cm<sup>-3</sup> d<sup>-1</sup> reported in Figure 2). However, microbial rates are limited and  
649 restricted to discrete habitats and mostly obtained in incubation with radiotracers in  
650 laboratory conditions and ambient pressure. Thus, the extrapolation to estimates of global  
651 microbial methane production and consumption per year may be subjected to high  
652 uncertainties. All the methanogenesis pathways lead to the production rate of 5-33 Tg of  
653 methane yr<sup>-1</sup> in continental marine sediment at global scale (Wallmann et al., 2012).  
654 However, the transfer of this amount of methane generated from the seabed along  
655 continental margins to the atmosphere is efficiently buffered and controlled by both  
656 aerobic (AeOM) and anaerobic oxidation of methane (AOM), respectively at and below  
657 the oxic-anoxic interface of the sediment and water columns (Reeburgh, 2007) (Fig.2).  
658 These two oxidation processes can be expressed as follows:

659



662 AeOM occurs into the geosphere at cold seeps and hydrothermal fields from a symbiotic  
663 association between specific methane-oxidizing bacteria with marine animals (Petersen  
664 and Dubilier, 2009). In the water column, AeOM represents the final sink for methane  
665 before reaching the atmosphere. Within the anoxic sediment, AOM is a microbial-  
666 mediated process that occurs within the geochemical horizon commonly called the  
667 sulfate-methane transition zone (SMTZ) where upward diffusion of methane reacts with  
668 downward diffusing seawater sulfate (Borowski et al., 1996, 1999; Gao et al., 2022;  
669 Hinrichs and Boetius, 2002; Pohlman et al., 2008). Laboratory experiments from natural  
670 samples have shown that the overall rates of AOM in marine sediments coupled to sulfate,  
671 metal oxides and nitrite/nitrate as electron acceptors range from  $5.1 \times 10^{-8}$  to  $7.0 \times 10^4$   
672  $\text{nmol cm}^{-3} \text{ d}^{-1}$  (Gao et al., 2022, Table 3) (mole-to-mass conversion is  $81.6 \times 10^{-8}$  to  $112 \times$   
673  $10^4 \text{ ng cm}^{-3} \text{ d}^{-1}$  reported in Figure 2). Predicted global rates of AOM based on the  
674 regression model with diffusive fluxes of  $\text{CH}_4$  suggest that 45-61 Tg of methane are  
675 oxidized annually; corresponding to ~3-4% of the organic debris deposited on the seabed  
676 (Egger et al., 2018). On a global scale, 8 to 65 Tg of methane per year bypasses the two  
677 aforementioned sedimentary biofilters and is released in the water column (Saunois et al.,  
678 2016; Steinle et al., 2015). This estimate is not restricted to hydrate decomposition only  
679 as it is difficult to decipher, but involves several methane pools, including free methane  
680 generated either from thermal cracking at deep depth or shallow methanogenesis.

681 Methane released from hydrate decomposition affects the transport of chemical species  
682 within the sediment overlaying the deposits by generating a continuous carbon flux that  
683 represents an energy supply for the benthic chemosynthetic assemblages (Niemann et al.,  
684 2006). Such an energy supply stimulates the seepage-associated ecosystems located in  
685 the sediment as well as in the water column (Boetius and Suess, 2004; Marcon et al.,  
686 2014; Sahling et al., 2002; Suess, 2014) and gives rise to the following consequences:

- 687 • **Formation of interface horizons shaped by redox processes.** The microbial  
688 processes and the community diversity that characterized them are often  
689 stimulated at discrete subsurface geochemical interfaces (Parkes et al., 2014),  
690 creating a zonation within the sedimentary column. From a biogeochemical  
691 viewpoint, anaerobic methane oxidation, methanogenesis from acetate and  
692 Hydrogen/ Carbon Dioxide, acetate oxidation, sulfate-reduction, and bacterial  
693 productivity were stimulated in both the hydrate and the free-gas sediment  
694 horizons beneath compared to hydrate-free sediments (from 1.5 to 15 times  
695 higher) at the Black Ridge setting in NW Atlantic Ocean (Wellsbury et al., 2000)  
696 and surface sediment of the Cascadia Margin in the North Pacific Ocean (Cragg  
697 et al., 1995); and distinct microbial communities dominated the former  
698 sedimentary environments. Estimations of microbial methane production rate  
699 ranged from  $0.015$  to  $0.62 \text{ nmol cm}^{-3} \text{ d}^{-1}$  in sediments without hydrate to  $0.1$  to  
700  $2.73$  in methane hydrate bearing sediments (Table 2) (mole-to-mass conversion  
701 of methane production rates in hydrate bearing sediments were  $1.6$  to  $43.68 \text{ ng}$   
702  $\text{cm}^{-3} \text{ d}^{-1}$  reported in Figure 2). Thus, the cell numbers as well as the microbial  
703 activities involved in the methane cycle (methanogenesis and anaerobic

704 methanotrophy) strongly increase within the sedimentary geochemical-horizons,  
705 thus increasing the amount of hydrates and associated free gas (Dickens and  
706 Quinby-Hunt, 1997; Wellsbury et al., 2000). At the Black Ridge hydrate-setting,  
707 the total microbial number is significantly higher around the Bottom Simulating  
708 Reflector (BSR), especially beneath it within the free-gas or dissolved-gas  
709 occurrence zone (Wellsbury et al., 2000). Indeed, the potential rates of microbial  
710 activity increase at the interface between the BSR and the free-gas zone beneath,  
711 mainly towards the free-gas zone (Cragg et al., 1996; Cragg et al., 1995;  
712 Wellsbury et al., 2000). Thus, the presence of free gas associated with hydrate  
713 deposits rather than free gas-depleted hydrates, impacts on the microbial activities  
714 including methane and acetate metabolisms. At the SMTZ, pore water methane  
715 and sulfate are consumed through the AOM by syntrophic consortia of anaerobic  
716 methanotroph archaea (ANME) and sulfate reducing bacteria (SRB). The depth  
717 of the SMTZ is strongly affected by the intensity of the methane flux, while its  
718 state (steady or transient) is rather linked to the flux variations over time  
719 (Borowski et al., 1999; de Prunelé et al., 2017; Jørgensen and Kasten, 2006;  
720 Kasten et al., 2003). A recent investigation of site located at the rim of a hydrate-  
721 bearing zone off Svalbard has shown that nonvertical methane transport can  
722 significantly affect the gas migration pathway, leading to the occurrence of double  
723 SMTZs and unusual microbial distribution within the sediment (Treude et al.,  
724 2020). Previous studies have shown that the settlement of the SMTZ starts around  
725 100 to 1000 years after the inception of gas hydrate dissociation (Argentino et al.,  
726 2021; de Prunelé, 2015; de Prunelé et al., 2017; Hong et al., 2016; Pape et al.,  
727 2020; Sultan et al., 2016). The SMTZ depth is controlled by the diffusive fluxes  
728 of methane and sulfate, which depend on continuous decrease in the reactivity of  
729 organic matter with the increasing sediment depth and therefore the age of the  
730 sediment (Borowski et al., 1999). The sedimentation rate and the associated  
731 organic matter burial flux are the key control factors to define the depth of the  
732 SMTZ (Egger et al., 2018). These two factors depend in turn on the water depth,  
733 the distance from land and surface biological productivity in the overlying water  
734 column. Human alteration of nutrient loading and oceanographic regimes due to  
735 global warming can also impact on the SMTZ distribution in sediment (Egger et  
736 al., 2018).

- 737 • **Ecosystems-hosted methanotrophy.** Microbial consortia of anaerobic  
738 methanotroph archaea and sulfate-reducing bacteria are not restricted to gas  
739 hydrate-bearing sediments (Boetius et al., 2000), but are widely distributed in  
740 other marine environments including cold seeps (Hinrichs et al., 1999; Vigneron  
741 et al., 2013), mud volcano (Lazar et al., 2011), deep hypersaline sediments (La  
742 Cono et al., 2011) and hydrothermally impacted sediments (Holler et al., 2011;  
743 Teske et al., 2002). The major controlling factors for the ANME population  
744 distribution are the availability of methane and sulfate, or known alternative  
745 electron acceptors such as nitrate, iron or manganese (Wallenius et al., 2021).  
746 ANME is believed to use a process of “reverse methanogenesis” biochemical  
747 pathway and are phylogenetically related to methanogenic lineages. The doubling

748 time of ANME/SRB consortia, estimated to approximately seven months under  
749 controlled *in vitro* conditions (Nauhaus et al., 2007), suggests that the set-up of an  
750 efficient AOM microbial filter in sediments would be on the order of decades  
751 (James et al., 2016). The coupled process of AOM and sulfate-reduction increases  
752 alkalinity, promoting the precipitation of authigenic carbonate by reacting with  
753 the seawater calcium (Luff and Wallmann, 2003). This authigenic carbonate  
754 precipitation results in a decreasing of the sediment porosity that changes the fluid  
755 flow pattern, and in turn affects the supply of methane at the SMTZ (Steeb et al.,  
756 2014). At Hydrate Ridge in the Cascadia margin subduction zone, carbon volume  
757 estimations suggest that 14% of the oxidized methane is sequestered into this  
758 seafloor mineral. Thus, carbonate mounds may represent a significant methane  
759 sink in deep-sea (Marlow et al., 2021; Marlow et al., 2014). Natural and  
760 anthropogenic methane seepages into an oxygenated water column stimulate the  
761 distribution, abundance and activity of aerobic methanotrophic bacterial  
762 populations (Rogener et al., 2018; Steinle et al., 2015). The AeOM reaction  
763 hinders the methane transfer to the atmosphere by converting it into biomass or  
764 dissolved inorganic carbon; which in turn could affect the pH in the ocean  
765 (Biaostoch et al., 2011). Estimations of aerobic methanotrophic oxidation rates in  
766 oxygenated sediments ranged from  $3.4 \times 10^{-8}$  to  $1.1 \text{ nmol of CH}_4 \text{ cm}^{-3} \text{ d}^{-1}$  (Table  
767 2, Gao et al., 2022) (mole-to-mass conversion is  $54.4 \times 10^{-8}$  to  $17.6 \text{ ng of CH}_4 \text{ cm}^{-3} \text{ d}^{-1}$  reported in Figure 2).

- 769 • **Temporal and spatial dynamics of (micro)-biological communities.** The  
770 methane concentration and flux strongly affect the diversity of the chemosynthetic  
771 communities such as sulfur bacterial mats, tubeworms, and clams that are settled  
772 on the seafloor (Fischer et al., 2012; Pop Ristova et al., 2012). These  
773 chemosynthetic seep fauna are therefore bioindicators of AOM activity and  
774 methane flux. Thus, macrofauna colonies such as vesicomyid clam populating the  
775 *Beggiatoa* mats (filamentous microbes) settled on methane hydrate-bearing  
776 sediments consist nearly exclusively of endemic species and are found in higher  
777 density at seeps and hydrothermal vents compared to non-seep environments  
778 (Sahling et al., 2002). The methane fluxes may vary on very large spatial scales  
779 as a consequence of factors such as the variation of the rate of hydrate  
780 decomposition or carbonate precipitations, or after a submarine mud eruption, a  
781 continental slope sliding, and even an earthquake. Thus, large expulsions of fluids  
782 and mud from active submarine volcanos may strongly affect the distribution of  
783 communities; sometimes causing their extinction. However, long-term  
784 observation after such large expulsions of fluids also indicates a resilience of the  
785 ecosystem to recover the main microbial function. For instance, the re-  
786 colonization of complex pioneer microbial populations composed of aerobic and  
787 anaerobic methanotrophs were observed several years after a subsurface mud  
788 eruption at the active center of the Håkon Mosby mud volcano (Ruff et al., 2019).

790 Predicting how climate change will affect the aforementioned microbial processes  
791 remains elusive. Several studies have claimed that microbial methane production may be

1 792 enhanced by global warming. In fact, methanogens are active in most habitats where  
2 793 temperature ranges from 0 to 122°C (Hoehler et al., 2018). In marine sediments, the  
3 794 methanogenesis process is restricted to either the sediment layer deep below the SMTZ  
4 795 (meter to tens of meters) and used acetate and hydrogen, or in surficial sediment (<1 m)  
5 796 where non-competitive substrates such as methanol and other methylated compounds are  
6 797 available. Interestingly, the coexistence of sulfate-reduction and methanogenesis also  
7 798 occur in shallow sediment when methylotrophic pathway to produce methane takes place  
8 799 (L'Haridon et al., 2014). Methanogen distribution may be limited by competition for  
9 800 acetate and dihydrogen and are rapidly out-competed by sulfate-reducers for these same  
10 801 substrates. In shallow sulfate-rich sediments, methanogens utilizing non-competitive  
11 802 substrates such as methylated amines could meet the substrate requirements of sulfate-  
12 803 reducing bacteria. Thus, variation of *in-situ* temperature in marine sediments can strongly  
13 804 impact methane production pathways via biochemical, bioenergetic and/or ecological  
14 805 mechanisms (Conrad, 2020; Hoehler et al., 2018). Temperature increase positively  
15 806 impacts methanogenesis activity (Maltby et al., 2018), resulting in higher methane  
16 807 production with potential higher emission budget to the hydrosphere. In fact, a warming  
17 808 of bottom water may result in increasing the amount of methane contained within the  
18 809 shallow sediments and eventually lead to the shoaling of the SMTZ in vast areas of the  
19 810 continental shelf. Even if representative isolated microbes grow within a wide range of  
20 811 temperatures in the laboratory, changing global temperatures may also shift the diversity  
21 812 of the microbial community towards more responsive and efficient microbial  
22 813 metabolisms at higher *in situ* temperature.

23 814 Moreover, the lifetime of methane in the water column is longer when it is transferred  
24 815 from the seafloor as bubbles, partly because microbes use dissolved methane. The aerobic  
25 816 oxidation of methane by free-living and symbiont-associated bacteria occurs on the  
26 817 seafloor and within water column at sites where free methane is released (Levin, 2018;  
27 818 Steinle et al., 2015; Sweetman et al., 2017). Accordingly, hydrate dissociation may affect  
28 819 the water column even more than hydrate dissolution. If the methane hydrate dissociation  
29 820 is fast enough and releases large quantities of gas, part of it will escape the function of  
30 821 the microbial filter, as it will not be accessible by the microorganisms. However,  
31 822 additional methane loss prior to reaching the atmosphere occurs as bubble stripping, *i.e.*  
32 823 dissolution in the surrounding water, or replacement by oxygen, nitrogen or other  
33 824 dissolved gases in the water masses. Such a gas exchange may not be complete over a  
34 825 short distance, and thus a significant methane fraction would be transferred to the  
35 826 atmosphere at shallow water depth. The amount of methane bypassing sedimentary  
36 827 benthic biofilters, entering in the water column, and transfer to the atmosphere can vary  
37 828 widely depending on the type of water and specific environmental conditions. For coastal  
38 829 and marine environments, estimation is challenging due to complex interactions between  
39 830 sediments, water column and the atmosphere. Therefore, it is difficult to provide depth  
40 831 threshold from which sedimentary methane is transferred to the atmosphere. McGinnis et  
41 832 al. (2006) studied methane emissions in the Black Sea and showed that significant transfer  
42 833 to the atmosphere occurs at water depth shallower than 100 m. Other studies highlighted  
43 834 the coastal region located in water depth ranging between ~0 and 50/ 75m, where gas

835 hydrates are not stable, as being by far the more important contributor of sedimentary  
836 methane to the atmosphere (Mao et al., 2022; Michel et al., 2021; Römer et al., 2021;  
837 Weber et al., 2019). In a recent study, Joung et al. (2022) investigated the transfer of  
838 methane from the seafloor to the sea surface along the US margins at seep areas including  
839 hydrate-bearing sites, both in the Atlantic and Pacific sides. Their results showed no  
840 occurrence of such a vertical transfer at water depth deeper than 430m, which is shallower  
841 than the upper boundary of the hydrate-stability field (Joung et al., 2020; Joung et al.,  
842 2022). In addition, during the aerobic oxidation of methane in the water column, bacteria  
843 produce biomass and/or carbon dioxide, which latter is dissolved in the seawater. Large  
844 production of carbon dioxide may contribute to the decrease of the water pH, and lead to  
845 local ocean acidification as mentioned in section 4.i. Biastoch et al (2011) estimated that  
846 the oxidation of methane discharged in the Arctic Ocean within the next centuries will  
847 result in a drop of 0.25 pH units and a local decrease of up to 25% of the oxygen  
848 concentration. A bloom of aerobic methanotroph communities in response to the large-  
849 scale methane release may happen, creating a vertical stratification of aerobic  
850 methanotrophs consuming the dissolved oxygen and depleting the amount of oxygen in  
851 the water column. Such a microbial bloom has been observed from the Deep Water  
852 Horizon blowout in the northern Gulf of Mexico, which has increased methane oxidation  
853 rates in the water column compared to natural methane seepage (Rogener et al., 2018).

### 854 **iii. Marine methane transfer to the atmosphere**

855 After CO<sub>2</sub>, atmospheric methane is the second most important climate-forcing trace gas  
856 driven by anthropogenic sources. Its burden in the atmosphere has drastically increased  
857 by 150% since the pre-industrial era and is currently rising at a high rate (Nisbet et al.,  
858 2014; Nisbet et al., 2016; Platt et al., 2018). Our understanding on the respective  
859 contribution from its different natural sources and sinks remains incomplete (Kirschke et  
860 al., 2013; Saunio et al., 2016; Saunio et al., 2017; Saunio et al., 2020). Top-down and  
861 bottom-up studies show that natural processes emit between 218 and 371 Tg CH<sub>4</sub> yr<sup>-1</sup> on  
862 average, respectively (Saunio et al., 2020).

863 Aquatic methane enters the atmosphere either as bubbles rising from the seafloor or by  
864 diffusion from saturated waters across the sea-air interface. Early estimates by Lambert  
865 & Schmidt (1993) provided a marine source to the atmosphere of 3.5 Tg CH<sub>4</sub> yr<sup>-1</sup> and  
866 predicted that the open ocean might become a sink at atmospheric concentrations  
867 equivalent to today's concentrations (Lambert and Schmidt, 1993). That prediction did  
868 not materialize. Survey of the global ocean ΔCH<sub>4</sub> data combined with estimates of  
869 ebullitive fluxes found a range of 6-12 Tg CH<sub>4</sub> yr<sup>-1</sup> (Weber et al., 2019). It is generally  
870 admitted that seafloor emissions reach the atmosphere only at shallow depth (continental  
871 shelf and upper slope), whereas in the open ocean methane flux correlates with net  
872 primary production and would therefore be mainly produced *in situ* by organic matter  
873 cycling (Weber et al., 2019). Rosentreter et al. (2021) further extended the study of  
874 Weber et al (2019) to sources from coastal ecosystems, and estimated a median flux of  
875 8.4 Tg CH<sub>4</sub> yr<sup>-1</sup> (interquartile range 4.8–28.4 Tg CH<sub>4</sub> yr<sup>-1</sup>) (Rosentreter et al., 2021)  
876 (Fig.2). These estimates can separate emissions from seafloor reaching the atmosphere



877 on one side with *in situ* production on the other side. However, atmospheric estimates are  
878 based on measurements that do not discriminate whether sedimentary methane has been  
879 buffered in methane hydrates that eventually decomposed or is a direct emanation of  
880 methane from seeps.

881 Focusing on submarine seeps only, Etiope et al. (2019), compiling the available literature,  
882 estimated the methane transfer from the geosphere to the atmosphere at 3.9 Tg CH<sub>4</sub> yr<sup>-1</sup>  
883 with a maximum potential value of 9 Tg CH<sub>4</sub> yr<sup>-1</sup>. In this synthesis, all sources were  
884 located at depths shallower than 500 m. The main emitting area is the East Siberian Arctic  
885 Shelf with 2 Tg CH<sub>4</sub> yr<sup>-1</sup> (range 0-4 Tg CH<sub>4</sub> yr<sup>-1</sup>, (Berchet et al., 2016)). Etiope et al.'s  
886 estimate is nearly twice lower than a previous geological estimates of 20 Tg CH<sub>4</sub> yr<sup>-1</sup>  
887 (Judd, 2004; Kvenvolden et al., 2001). There, offshore direct sources account for 5-20 Tg  
888 CH<sub>4</sub> yr<sup>-1</sup> and hydrate dissociation around 0-5 Tg CH<sub>4</sub> yr<sup>-1</sup>.

889 Numerous investigations on the consequence of methane release from hydrate  
890 decomposition during past climate change such as the Paleocene-Eocene thermal  
891 maximum argued that these events have contributed to an increased injection of methane  
892 into the atmosphere that moderately accelerated climate change (Dickens et al., 1997;  
893 Kennett et al., 2003; McInerney and Wing, 2011; Norris and Röhl, 1999). Such an impact  
894 involves a huge amount of methane passing through the entire water column to reach the  
895 atmosphere. Several modelling and simulation studies explored the interactions between  
896 hydrate dissociation and climate change (Archer, 2007; Ruppel and Kessler, 2017 and  
897 references therein). Most of these studies found moderate release of methane to the  
898 atmosphere under the worst climate scenario (RCP 8.5) (Biajoch et al., 2011; Hunter et  
899 al., 2013; Kretschmer et al., 2015). Kretschmer et al. (2015) estimated that up to 4.73 Tg  
900 CH<sub>4</sub> yr<sup>-1</sup> could be released on average, ignoring potential oxidation in the water column.  
901 This is comparable to today's global ocean methane sources, a minor term in the global  
902 annual methane budget. They also noted the importance of the uncertainty associated with  
903 the inventory of hydrates in the sediment within the GHSZ. Serov et al. (2017) highlighted  
904 the importance of understanding the post-glacial history of present-day gas hydrate  
905 provinces to better predict the trajectory of their destabilization. It is also important to  
906 assess the role of anthropic activities on the vulnerability of NGHDs. Indeed, although  
907 several studies investigated the monitoring of marine methane emissions from oil and gas  
908 wells (Böttner et al., 2020), there is no study related to human-induced destabilization of  
909 NGHD from seafloor or sub-seafloor resource extraction. To our knowledge there is no  
910 literature dealing with the quantification of methane leaks during production tests from  
911 hydrates and its fate, nor on its impact on the associated ecosystems over time. As  
912 mentioned previously, the water column acts as a relatively efficient but still poorly  
913 characterized oxidative-barrier to prevent seafloor methane from reaching the  
914 atmosphere. Therefore, continuous efforts driven by field-based quantitative approaches  
915 are needed to achieve an in-depth understanding of the transfer and fate of gases in the  
916 different Earth compartments, as well as to identify under which circumstances marine  
917 methane reaches the atmosphere. Thus, the assessment of the physical and  
918 biogeochemical processes related to methane in the water column and its probability to  
919 reach the atmosphere remains timely and challenging.

1 920 Besides, like seafloor methane emissions, methane transfer from the ocean to the  
2 921 atmosphere is influenced by environmental factors such as seasonality. Experiments  
3 922 showed that strong vertical density gradients in the water column developed during the  
4 923 warm season might limit the ascent of methane gas to the sea surface and its release into  
5 924 the atmosphere. During winter, the vertical mixing in the water column is enhanced and  
6 925 consequently more methane is released into the atmosphere (Gentz et al., 2014; von  
7 926 Deimling et al., 2011). Such a seasonal effect could also explain variations in the extent  
8 927 of the gas hydrate stability zone (GHSZ) on the Svalbard margin and the distribution of  
9 928 gas flares in the water column (Ferre et al., 2020; Riedel et al., 2018), but the net methane  
10 929 budget still needs to be estimated. Apart from seasonal shifting, meteorological events  
11 930 such as storms (Shakhova et al., 2014), chemical gradients and geological site-specific  
12 931 parameters (Ryerson et al., 2011; Schmale et al., 2010a; Schmale et al., 2010b; Yvon-  
13 932 Lewis et al., 2011; Zhang, 2003) can also facilitate methane transfer from the sea to the  
14 933 atmosphere.  
15 934 As mentioned in section 4.ii, the methane injected in seawater is then submitted to  
16 935 dissolution, gas exchange within the bubbles and oxidation. Modeling of gas bubble  
17 936 ascent can predict the evolution of bubble sizes and the fractions of methane gas reaching  
18 937 the sea surface, and then transferred to the atmosphere under idealized conditions  
19 938 (McGinnis et al., 2006; Ruppel and Kessler, 2017). For a water depth of 100m, methane  
20 939 from only bubbles with a diameter larger than 2cm at the seafloor can reach the  
21 940 atmosphere (Ruppel and Kessler, 2017). Furthermore, the internal dynamics of large-  
22 941 scale bubble plumes and the interactions with ambient bottom currents and density  
23 942 stratification adds further complexity that is not yet fully resolved by numerical models  
24 943 (Leifer et al., 2015; Schneider von Deimling et al., 2015). Such an achievement  
25 944 necessarily requires a sound knowledge, not only of its micro-biological state of the local  
26 945 water column, but also its the physical properties (*i.e.* currents, temperature). Hence,  
27 946 hydro-acoustic measurements and more additional field data are required to monitor and  
28 947 forecast the fate of methane gas released at the seabed to improve the existing models.  
29 948 Thus, in order to reliably evaluate methane contribution from hydrate decomposition to  
30 949 the global atmospheric budget, it is necessary to (1) develop new bio-geochemical tools  
31 950 to better identify and decipher all oceanic sources and understand the processes that  
32 951 degrade this molecule in the water column, and (2) intensify observations and monitoring  
33 952 of sites by increasing the number of devoted cruises as well as the deployment of  
34 953 autonomous or remotely operated systems to achieve reliable estimates of the methane  
35 954 fluxes across the interfaces sediment (geosphere)/ seawater (hydrosphere)/ atmosphere.  
36 955 Once reaching the uppermost water layer, the diffusive transfer to the atmosphere is  
37 956 strongly affected by ocean state and weather conditions (James et al., 2016; Wanninkhof  
38 957 et al., 2009). Wind speed modifies the exchange velocity across the interface. Wave  
39 958 breaking further enhances gas exchange through bubble formation. Strong winds during  
40 959 storms combine effects of increased water column vertical mixing and gas exchange. At  
41 960 the high latitudes, sea ice acts as a barrier preventing the transfer of methane to the  
42 961 atmosphere (Kort et al., 2012), and accordingly the reduction in sea ice is expected to  
43 962 significantly increase the annual total methane flux to the atmosphere (He et al., 2013).

963 Currently, attempts to accurately measure atmospheric methane inputs from NGHDs,  
964 especially in the Arctic where hydrate-bearing sediments are encountered at shallow  
965 locations, failed due to widely varying numbers of factors that need to be considered.  
966 Using a diffusive model (Wanninkhof, 1992), Thornton et al., (2016) estimated a  
967 maximum flux range of 68-87 mmol.m<sup>-2</sup>.yr<sup>-1</sup> in the Laptev Sea and East Siberian Arctic  
968 Shelf. Comparably, using inverse modelling of atmospheric measurements Myhre et al.  
969 (2016) found a source not higher than 120 mmol.m<sup>-2</sup>.yr<sup>-1</sup> off the coast of Svalbard on a  
970 known methane seep area (Myhre et al., 2016). When including the impact of storm,  
971 Shakhova et al. (2014) proposed higher annual average estimate reaching up to 506  
972 mmol.m<sup>-2</sup>.yr<sup>-1</sup> for the East Siberian Arctic Shelf. For the same area, Berchet et al. (2016)  
973 used an atmospheric inversion method and propose that atmospheric observations in the  
974 Arctic are compatible with a mean source ranging between 0-134 mmol.m<sup>-2</sup>.yr<sup>-1</sup>.  
975 The estimates are different from each other from one site to another as well as from one  
976 method to another for the same site, and such a result indicates that several challenges  
977 still remain for a better quantification of these fluxes at the sea-air interface. Indeed, the  
978 aforementioned studies assumed an atmospheric diffusive flux and estimated it through  
979 the gradient method, which does not represent adequately ebullitive fluxes. Atmospheric  
980 inversions as top-down methods are unable to unambiguously quantify specifically  
981 methane released from hydrate dissociation distinctly from that originating from other  
982 marine sources. They are further limited by model transport error, embedded sources and  
983 atmospheric data coverage. However, top-down methods may provide valuable upper  
984 constraints to marine emissions (Berchet et al., 2016). Estimates from closed chamber  
985 accumulation could be more accurate but is restricted to a very small spatial coverage,  
986 weakening the spatial representativity and therefore remain difficult to operate in open  
987 ocean and large areas. The eddy covariance technique deployed on ships is technically  
988 adequate (Thornton et al., 2020) but challenging in marine environment, especially  
989 because it requires a careful correction of the measured high-frequency, three-  
990 dimensional wind for ship motion and attitude (Edson et al., 1998). Measurements are  
991 also needed to characterize the sub-seafloor origin of methane, and ground-checked on  
992 whether or not it has been buffered in hydrates.

## 993 994 **5. Strategy to tackle environmental challenges related to hydrate** 995 **decomposition**

996 In the previous sections, we have shown the scarcity of methane flux measurements at  
997 hydrate-bearing sites and the need to intensify such measurement campaigns. We also  
998 stressed the need to undertake investigations at different spatial and temporal scales to  
999 gain insights into the impacts of hydrate decomposition on the seafloor stability and the  
1000 fate of the permafrost. The outcomes of such studies will help to clarify the evolution path  
1001 of NGHDs and its impact upon climate change or/ and human activity, and how this  
1002 evolution path affects the ecosystems colonizing the sediment as well as the water  
1003 column. Addressing the aforementioned environmental challenges requires both the  
1004 definition of an environmentally sound monitoring strategy and the assessment of the  
1005 legal framework regulating the release of gases and particles in the water column. The

1006 current legal framework must be adjusted to account for the specific environmental risks  
1007 associated with natural gas hydrate dynamics. Therefore, the following actions should be  
1008 considered:

- 1009 ● Assess how slope stability may be compromised by either global warming or gas  
1010 production from hydrates under different geological boundary conditions;
- 1011 ● Identify suitable precursors/changes for slope failure to be targeted in monitoring  
1012 program;
- 1013 ● Develop a generic strategy for environmental baseline studies and the  
1014 environmental monitoring of hazards related to gas hydrate dynamics;
- 1015 ● Evaluate whether national and international legal frameworks are suitable to  
1016 protect the environment.

1017  
1018 In the previous sections, the hazards related to gas hydrate decomposition have been  
1019 identified and discussed, whereas this section is devoted to the risk analysis related to  
1020 hydrate decomposition. Risk analysis is essential to ensure safety of operations. Although  
1021 the terms “risk” and “hazard” are often used interchangeably, “risk” and “hazard” have  
1022 well defined meanings in risk assessment procedure. Hazard is a potential source of harm  
1023 or damage. Harm or damage is always the consequence of an accident, whereas risk is a  
1024 combination of the likelihood (L) of the harm occurring and the severity of that harm  
1025 (damage D). Thus, risk can be formulated as follows:

$$R = f(D, L) = D \times L$$

1026  
1027 Where R represents the risk matrix.

1028

### 1029 **a. Generic strategy related to gas production from NGHDs**

1030 The production of gas hydrates, whether or not coupled with carbon dioxide  
1031 sequestration, can create environmental hazards by affecting seafloor stability and  
1032 delicate microbial/benthic ecosystems and by releasing methane and particles into the  
1033 water column. Therefore, countries that are considering such resources are committed to  
1034 developing an appropriately focused environmental baseline survey prior to gas hydrate  
1035 production operations to quantify those risks. An environmental risk assessment of gas  
1036 hydrate exploration and production (E&P) operations will be generated from the baseline  
1037 survey and will include proposed mitigation measures to minimize the impacts of the  
1038 E&P operations. During E&P operations, an appropriate monitoring program to assess  
1039 the effectiveness of mitigation measures is necessary. There are precedents for baseline  
1040 and monitoring studies from oil and gas E&P (IOGP, October 2017) and CO<sub>2</sub> storage  
1041 (<https://www.quintessa.org/case-studies/coupled-process-modelling-for-co2-storage>).

1042 A lightweight drillship using coiled tubing drilling over a short period of time may be  
1043 used in NGHD exploration because the NGHD prospect will be at shallow depths in  
1044 unconsolidated marine sediments. Production of NGHD is likely to be carried out by

1045 subsea infrastructure on the seafloor with real-time monitoring and control from a remote  
1 1046 location (Max and Johnson, 2019). Hydrate is stable and effectively inert in its reservoir  
2  
3 1047 host sediment. During depressurization, which seems the most promising method of  
4 1048 production, pressure in the reservoir is lower than normal formation pressure which  
5 1049 means that a blow-out is physically impossible and the likelihood of leakage of gas is  
6  
7 1050 highly reduced. If gas leakage does occur methane gas bubbles are dissolved in ambient  
8 1051 seawater during their ascent through the water column and oxidized by aerobic  
9 1052 microorganisms using dissolved oxygen as terminal electron acceptor (Atlas and Hazen,  
10 1053 2011) with the potential consequences of oxygen depletion in the water column as  
11 1054 detailed in section 4.ii.

1055 Prior to drilling an NGHD exploration borehole, a site survey to establish baseline  
15 1056 environmental conditions and identify drilling hazards at the proposed drill site is needed.  
16 1057 Site surveys are performed to minimize the risk of harm to personnel and equipment, and  
17 1058 to protect the natural environment. Therefore, the site survey must acquire sufficient data  
18 1059 over an appropriate period of time to adequately describe the physical, chemical,  
19 1060 geological and biological environments in the operational area. Initially a desktop study  
20 1061 is carried out to inform the design of the site survey. With respect to the specific hazards  
21 1062 presented by NGHDs the integrated analysis of exploration 3D and/or 2D seismic data,  
22 1063 offset well data (logs, operation reports, industry databases, etc.), geotechnical borehole  
23 1064 information, offset site surveys and relevant public domain data will allow an initial  
24 1065 ground model of the seabed and shallow section to be developed. This geological  
25 1066 characterization will include detailed bathymetry, geochemical, mineralogical and  
26 1067 petrophysical characteristics of the sediment and geological structures. The  
27 1068 biogeochemical characteristics of the seafloor and its surroundings (bottom water, near  
28 1069 seafloor sediment characteristics as well as pore water composition, together with the  
29 1070 dissolved benthic fluxes) must be measured. Further measurements will be required to  
30 1071 establish baseline environmental conditions. These include the physical and chemical  
31 1072 characteristics of the entire water column especially in relation to oxygenation and  
32 1073 acidification, *i.e.* dissolved gases such as O<sub>2</sub>, CO<sub>2</sub>, and CH<sub>4</sub> as well as other parameters  
33 1074 of the carbonate system (pH, DIC, alkalinity), nutrients, SO<sub>4</sub><sup>2-</sup>, H<sub>2</sub>S, Ca<sup>2+</sup>, and total  
34 1075 Hardness. Potential gas emissions from the seafloor into the water column in the target  
35 1076 area should be known, and qualitatively and quantitatively mapped (Bayrakci et al., 2014;  
36 1077 Greinert et al., 2006; Greinert and Nützel, 2004; Jerram et al., 2015; Leblond et al., 2014)  
37 1078 as well by appropriate acoustic devices and sensors (*e.g.* single-, split- and multi-beam  
38 1079 echo sounder systems, dissolved gas sensors). The biological environment must also be  
39 1080 described including the biological community of the seafloor and near seafloor sediments  
40 1081 (biocenosis) with reference to conservation of protected areas, habitats and species.  
41 1082 Economic activity that might be impacted by NGHD production operations should be  
42 1083 described including archaeological heritage.

1084 The desktop study will confirm if the shallow geology and the environmental hazards  
56 1085 generated by the production of gas hydrates is well understood. Invariably supplemental  
57 1086 data acquisition will be required, and a site survey will be designed to fill the data gaps

1087 identified by the desktop study. Because NGHD E&P operations will involve deploying  
1088 a seabed coring tool from a workboat, a seabed clearance survey will be required. An  
1089 indicative site survey area is 200 m below seabed and 500 m radius around the borehole  
1090 site location.

1091 The baseline studies can be carried out by an autonomous underwater vehicles (AUV)  
1092 and a seafloor and water column generic instrument module or lander deployed from a  
1093 site survey vessel with seabed sampling equipment and a towed magnetometer (cf. Klar,  
1094 2019 for information on monitoring technology). The seabed sampling using box cores  
1095 and piston cores deployed from the site survey vessel will acquire geotechnical  
1096 information on the strength of near seabed sediments and biological habitats. The  
1097 magnetometers will provide archaeological information. The AUV and lander should be  
1098 equipped with suitable instruments to monitor the water column, the water-sediment  
1099 interface and partially the sub-seafloor as well (*e.g.* side scan sonar and synthetic aperture  
1100 sonars (SAS), echo sounders, sub-bottom profilers, hydrophones, physical sensors,  
1101 chemical sensors, still camera, sediment traps, benthic chambers, etc.). It may be  
1102 necessary to deploy an autonomous, fully instrumented lander for several months at the  
1103 proposed site to acquire adequate baseline data and capture variabilities related to season,  
1104 tide, storm or other aforementioned environmental and anthropogenic events.

1105 Geological characterization is necessary to assess the risk and likely impacts of seafloor  
1106 deformation caused by NGHD E&P operations. The geological characterization will  
1107 include the aforementioned of surveys and analyses proposed for the site surveys,  
1108 together with data from OBS (Ocean-Bottom Seismometer) or OBC (Ocean-Bottom  
1109 Cable), as well as high-resolution multibeam bathymetry/backscatter mapping of the  
1110 seabed and hydro-acoustic imaging of shallow gas accumulations in the seabed if they are  
1111 not already available from site surveys. A paleo-geological history study will also be  
1112 required. The combination of multibeam backscatter data with the results of the analyses  
1113 of box cores will allow the characterization of the benthic biotopes of the operational area.

1114 Likewise, to assess the likely impacts of methane gas release on the environment, several  
1115 parameters will need to be measured in the baseline site survey. In addition to all  
1116 aforementioned measurements, these include detection and quantification of gas bubbles  
1117 in the water column through acoustic systems; sampling and analyses, including both  
1118 isotopic and molecular composition determination of any ascending gases; video/photo  
1119 imaging of biota at the seabed; biological integrity; oceanographic measurements to  
1120 model the transport of sediments and gases; chemical detection of dissolved gases;  
1121 chemical and isotopic compositions of key pore-water elements and dissolved gases;  
1122 habitat mapping. Several of these measurements can be achieved by deploying an  
1123 autonomous seafloor and water column generic instrument module, water column  
1124 moorings and/ or lander from the site survey vessel to collect the data. However, although  
1125 some gas (*e.g.* methane, carbon dioxide) sensors can be implemented on these platforms,  
1126 most of the geochemical analyses of the gas bubbles and pore water will be performed  
1127 onshore after sampling with appropriate tools such as corer and bubble sampler (Chen et  
1128 al., 2007; Ruffine et al., 2018a; Ruffine et al., 2018b; Wu et al., 2013; Wu et al., 2014).

1129 The environmental impact assessment will also need to assess the impact of NGHD E&P  
1130 operations on human economic activity. Therefore, the site survey will also need to  
1131 acquire information on the physical infrastructures, pipelines, telecommunication cables,  
1132 fishing activity, etc., in the vicinity of the NGHD E&P operation area. A stakeholder  
1133 engagement plan may also be necessary based on the human activity that may be  
1134 impacted.

1135 With respect to the environmental monitoring plan for long-term NGHD production  
1136 operations, it is advisable to deploy an instrumented lander and/ water column moorings  
1137 to monitor essential environmental variables at an undisturbed reference site within a  
1138 suitable distance from production operations where a similar lander/ and or water column  
1139 moorings acquires information on the same essential environmental variables for  
1140 comparison (Klar et al., 2019). The results of the baseline study based on the site survey  
1141 data will form the input for modelling (geotechnical, geochemical, fluid flow, etc.) to  
1142 predict reservoir conditions during production and to compare after decommissioning. In  
1143 addition, the modelling can be used as a tool to plan the monitoring regime and to define  
1144 the area that may be influenced both temporarily and spatially by the NGHD production.  
1145 The modelling can help to understand if an additional dataset is necessary to complete the  
1146 baseline study. Commercial software is only available for partially modelling site  
1147 evolution, so one suggestion would be to evaluate the possibility to develop new software  
1148 to enable complete modelling of site evolution.

#### 1149 **b. Generic strategy to monitor gas seepages from hydrates**

1150 After the baseline study has delivered the comprehensive characterization of the site,  
1151 monitoring is necessary in order to identify any anomalies relative to the anthropic- (*e.g.*  
1152 pre-production state) or the climate change-related impacts (Liu et al., 2019). Indeed, the  
1153 strategy detailed in this section applied for assessing the impacts of disturbances due to  
1154 both human activities and climate change. However, as mentioned previously the impacts  
1155 due to climate change may be smoother and expand over a longer time period. Thus, the  
1156 monitoring period should be adapted accordingly.

1157 The first step towards a suitable monitoring strategy is to generate a detailed project  
1158 description based on the baseline study and modelling, in order to identify the main risks  
1159 for the environment and assess the potential impacts. From the environmental impact  
1160 assessment, a recommendation of mitigation measures and a plan for environmental  
1161 management and spatiotemporal monitoring should be established. The next step is to  
1162 plan the management and monitoring strategy based on the risk and impact assessment.  
1163 Surveys carried out during the baseline study should be repeated. It could include  
1164 autonomous underwater vehicles (AUVs), monitoring vessels, water column moorings  
1165 and lander deployments, as used for the baseline study (Klar et al., 2019). Multiple  
1166 surveys should be conducted for full areal coverage. However, each survey should be  
1167 conducted at a specific height above the seabed, along with permanent monitoring on and  
1168 of the seabed by fixed installations such as observation wells and deployed sensors, to  
1169 achieve optimal results. Additional targeted studies will have to be conducted, if active

1 1170 formation water seeps, gas seeps, geological features such as mud volcano and  
2 1171 pockmarks, etc., connected to the NGHD producing reservoir are observed at the seabed.  
3 1172 These sites must be revisited on a regular basis to determine emission rates of gases and  
4 1173 fluids. Such periodic visits are key to check for instance, if any seepage has strengthened  
5 1174 and/or seafloor geological structure formation is (re-)activated by the NGHD production  
6 1175 operation. If new seeps develop during the production operational phase, they must be  
7 1176 investigated and sampled in detail to determine the origin and chemical composition of  
8 1177 the seeping fluids and gases and their emission rates.

11 1178 Especially during the NGHD production it is also important to accurately monitor seabed  
12 1179 deformation, since deformation and subsidence processes around the center of activity  
13 1180 could already be an imminent hazard precursor. This type of monitoring relies on lander-  
14 1181 deployed high precision, high stability pressure sensors together with inclination  
15 1182 measurements at several positions within the production field. Acoustic Long Baseline  
16 1183 (LBL) methodology can be used to monitor relative positions in between the measuring  
17 1184 nodes at the seafloor (Klar et al., 2019).

18 1185

## 19 1186 **CONCLUSION AND PERSPECTIVES**

20 1187 Natural gas hydrates have been investigated for multiples purposes for decades, whether  
21 1188 to understand their role in the oceanic methane (carbon) cycle, as a geohazard, or as a  
22 1189 potential energy resource. Whatever the purpose of their study, the question of their  
23 1190 decomposition, -the main factors that trigger this process, its speed and duration, as well  
24 1191 as the methane flux released-, are highly relevant. In the present review, the  
25 1192 environmental impacts related to hydrate decomposition have been discussed and  
26 1193 monitoring strategies have been proposed to identify and better characterize those  
27 1194 impacts.

28 1195 Hydrate decomposition can be relatively fast, from a few months/ years to few decades,  
29 1196 if it is voluntarily caused by human activities. On the other hand, the changing climate of  
30 1197 our planet may also trigger the decomposition of vulnerable NGHDs located in the  
31 1198 permafrost and the shallow sediments on the ocean margins. The kinetics of such a  
32 1199 decomposition will likely be slower but will last over a longer time period. There are  
33 1200 natural biogeochemical processes that degrade methane within both the sediment and the  
34 1201 water column, preventing any large accumulation of it in the water masses and mitigating  
35 1202 its transfer to the atmosphere. However, the question of the efficiency of these processes  
36 1203 under a changing climate needs to be understood. How will the increase of sea bottom  
37 1204 temperature affect the microbial communities that perform the aerobic and anaerobic  
38 1205 oxidation of methane, and accordingly the amount of methane that will be released from  
39 1206 hydrates? What will be the consequences of such releases over decades and centuries?  
40 1207 These questions remain to be answered.

41 1208 Coastal regions are amongst the most populated areas on Earth. The decomposition of  
42 1209 hydrates, mainly due to climate change, may reduce seafloor stability and cause



1210 submarine landslides with associated tsunamis impacting coastal communities. The  
1211 potential occurrence of such catastrophic socio-economic events that threaten human life,  
1212 natural resources and key infrastructure in populated coastal regions highlight the need to  
1213 monitor the dynamics of NGHD. This review has shown that field observations and  
1214 measurements are limited in space and time. Field observations are crucial to achieving  
1215 an in-depth and comprehensive understanding of the operating environment, and to  
1216 developing an appropriate environmental monitoring and management plan. Currently,  
1217 what we observe on a given site is not representative for other sites and an intensification  
1218 of the measurements of key parameters, both spatially and temporally, is urgently needed.

1219

## 1220 **Acknowledgements**

1221 Financial support for the study was provided by the COST action ES1405, entitled Marine  
1222 gas hydrate – an indigenous source of natural gas for Europe (MIGRATE) and the  
1223 European project H2020 DOORS (Grant Agreement 101000518).

1224

1225

## 1226 References

- 1  
2  
3 1227 Alessandrini, G., Tinivella, U., Giustiniani, M., de la Cruz Vargas-Cordero, I., and Castellaro, S.,  
4 1228 2019, Potential instability of gas hydrates along the Chilean margin due to ocean  
5 1229 warming: *Geosciences*, v. 9, no. 5, p. 234.
- 6 1230 Andreassen, K., Hubbard, A., Winsborrow, M., Patton, H., Vadakkepuliambatta, S., Plaza-  
7 1231 Faverola, A., Gudlaugsson, E., Serov, P., Deryabin, A., and Mattingsdal, R., 2017, Massive  
8 1232 blow-out craters formed by hydrate-controlled methane expulsion from the Arctic  
9 1233 seafloor: *Science*, v. 356, no. 6341, p. 948-953.
- 10 1234 Archer, D., 2007, Methane hydrate stability and anthropogenic climate change: *Biogeosciences*,  
11 1235 v. 4, no. 4, p. 521-544.
- 12 1236 Arenson, L. U., Springman, S. M., and Segó, D. C., 2007, The rheology of frozen soils: *Applied*  
13 1237 *Rheology*, v. 17, no. 1, p. 12147-12141-12147-12114.
- 14 1238 Argentino, C., Waghorn, K. A., Bünz, S., and Panieri, G., 2021, Sulfate reduction and anaerobic  
15 1239 oxidation of methane in sediments of the South-Western Barents Sea: *Biogeosciences*  
16 1240 *Discussions*, p. 1-14.
- 17 1241 Atlas, R. M., and Hazen, T. C., 2011, Oil biodegradation and bioremediation: a tale of the two  
18 1242 worst spills in US history, ACS Publications.
- 19 1243 Baumberger, T., Leifer, I., Scherwath, M., and Joye, S., 2022, Editorial: Recent Advances in  
20 1244 Natural Methane Seep and Gas Hydrate Systems: *Frontiers in Earth Science*, v. 10.
- 21 1245 Bayrakci, G., Scalabrin, C., Dupre, S., Leblond, I., Tary, J. B., Lanteri, N., Augustin, J. M., Berger,  
22 1246 L., Cros, E., Ogor, A., Tsabaris, C., Lescanne, M., and Geli, L., 2014, Acoustic monitoring  
23 1247 of gas emissions from the seafloor. Part II: a case study from the Sea of Marmara: *Marine*  
24 1248 *Geophysical Research*, v. 35, no. 3, p. 211-229.
- 25 1249 Berchet, A., Bousquet, P., Pison, I., Locatelli, R., Chevallier, F., Paris, J.-D., Dlugokencky, E. J.,  
26 1250 Laurila, T., Hatakka, J., and Viisanen, Y., 2016, Atmospheric constraints on the methane  
27 1251 emissions from the East Siberian Shelf: *Atmospheric Chemistry and Physics*, v. 16, no. 6,  
28 1252 p. 4147-4157.
- 29 1253 Berndt, C., Feseker, T., Treude, T., Krastel, S., Liebetrau, V., Niemann, H., Bertics, V. J., Dumke,  
30 1254 I., Duennbier, K., Ferre, B., Graves, C., Gross, F., Hissmann, K., Huehnerbach, V., Krause,  
31 1255 S., Lieser, K., Schauer, J., and Steinle, L., 2014, Temporal Constraints on Hydrate-  
32 1256 Controlled Methane Seepage off Svalbard: *Science*, v. 343, no. 6168, p. 284-287.
- 33 1257 Biastoch, A., Treude, T., Rüpke, L. H., Riebesell, U., Roth, C., Burwicz, E. B., Park, W., Latif, M.,  
34 1258 Böning, C. W., and Madec, G., 2011, Rising Arctic Ocean temperatures cause gas hydrate  
35 1259 destabilization and ocean acidification: *Geophysical Research Letters*, v. 38, no. 8.
- 36 1260 Bigalke, N. K., Rehder, G., and Gust, G., 2009, Methane hydrate dissolution rates in  
37 1261 undersaturated seawater under controlled hydrodynamic forcing: *Marine Chemistry*, v.  
38 1262 115, no. 3-4, p. 226-234.
- 39 1263 Bižić, M., Klintzsch, T., Ionescu, D., Hindiyeh, M., Günthel, M., Muro-Pastor, A. M., Eckert, W.,  
40 1264 Urich, T., Keppler, F., and Grossart, H.-P., 2020, Aquatic and terrestrial cyanobacteria  
41 1265 produce methane: *Science advances*, v. 6, no. 3, p. eaax5343.
- 42 1266 Boetius, A., Ravensschlag, K., Schubert, C. J., Rickert, D., Widdel, F., Gieseke, A., Amann, R.,  
43 1267 Jorgensen, B. B., Witte, U., and Pfannkuche, O., 2000, A marine microbial consortium  
44 1268 apparently mediating anaerobic oxidation of methane: *Nature*, v. 407, no. 6804, p. 623-  
45 1269 626.
- 46 1270 Boetius, A., and Suess, E., 2004, Hydrate Ridge: a natural laboratory for the study of microbial  
47 1271 life fueled by methane from near-surface gas hydrates: *Chemical Geology*, v. 205, no. 3-  
48 1272 4, p. 291-310.
- 49 1273 Bogoyavlensky, V., Bogoyavlensky, I., Nikonov, R., and Kishankov, A., 2020, Complex of  
50 1274 geophysical studies of the Seyakha catastrophic gas blowout crater on the Yamal  
51 1275 Peninsula, Russian Arctic: *Geosciences*, v. 10, no. 6, p. 215.
- 52  
53  
54  
55  
56  
57  
58  
59  
60  
61  
62  
63  
64  
65

1276 Borowski, W. S., Paull, C. K., and Ussler, W., 1996, Marine pore-water sulfate profiles indicate in  
1277 situ methane flux from underlying gas hydrate: *Geology*, v. 24, no. 7, p. 655-658.

1278 Borowski, W. S., Paull, C. K., and Ussler, W., 1999, Global and local variations of interstitial sulfate  
1279 gradients in deep-water, continental margin sediments: Sensitivity to underlying  
1280 methane and gas hydrates: *Marine Geology*, v. 159, no. 1-4, p. 131-154.

1281 Boswell, R., Schoderbek, D., Collett, T. S., Ohtsuki, S., White, M., and Anderson, B. J., 2017, The  
1282 Inik Sikumi Field Experiment, Alaska North Slope: Design, Operations, and Implications  
1283 for CO<sub>2</sub>-CH<sub>4</sub> Exchange in Gas Hydrate Reservoirs: *Energy & Fuels*, v. 31, no. 1, p. 140-  
1284 153.

1285 Böttner, C., Haeckel, M., Schmidt, M., Berndt, C., Vielstädte, L., Kutsch, J. A., Karstens, J., and  
1286 Weiß, T., 2020, Greenhouse gas emissions from marine decommissioned hydrocarbon  
1287 wells: leakage detection, monitoring and mitigation strategies: *International Journal of*  
1288 *Greenhouse Gas Control*, v. 100, p. 103119.

1289 Bourry, C., Chazallon, B., Charlou, J. L., Donval, J. P., Ruffine, L., Henry, P., Geli, L., Cagatay, M.  
1290 N., Inan, S., and Moreau, M., 2009, Free gas and gas hydrates from the Sea of Marmara,  
1291 Turkey Chemical and structural characterization: *Chemical Geology*, v. 264, no. 1-4, p.  
1292 197-206.

1293 Braga, R., Iglesias, R. S., Romio, C., Praeg, D., Miller, D. J., Viana, A., and Ketzer, J. M., 2020,  
1294 Modelling methane hydrate stability changes and gas release due to seasonal  
1295 oscillations in bottom water temperatures on the Rio Grande cone, offshore southern  
1296 Brazil: *Marine and Petroleum Geology*, v. 112.

1297 Brown, H. E., Holbrook, W. S., Hornbach, M. J., and Nealon, J., 2006, Slide structure and role of  
1298 gas hydrate at the northern boundary of the Storegga Slide, offshore Norway: *Marine*  
1299 *Geology*, v. 229, no. 3-4, p. 179-186.

1300 Bugge, T., Belderson, R., and Kenyon, N., 1988, The storegga slide: *Philosophical Transactions of*  
1301 *the Royal Society of London. Series A, Mathematical and Physical Sciences*, v. 325, no.  
1302 1586, p. 357-388.

1303 Bünz, S., Mienert, J., Vanneste, M., and Andreassen, K., 2005, Gas hydrates at the Storegga Slide:  
1304 Constraints from an analysis of multicomponent, wide-angle seismic data *Gas Hydrates*  
1305 *at the Storegga Slide: Geophysics*, v. 70, no. 5, p. B19-B34.

1306 Burwicz, E., and Haeckel, M., 2020, Basin-scale estimates on petroleum components generation  
1307 in the Western Black Sea basin based on 3-D numerical modelling: *Marine and*  
1308 *Petroleum Geology*, v. 113.

1309 Burwicz, E. B., Rupke, L. H., and Wallmann, K., 2011, Estimation of the global amount of  
1310 submarine gas hydrates formed via microbial methane formation based on numerical  
1311 reaction-transport modeling and a novel parameterization of Holocene sedimentation:  
1312 *Geochimica et Cosmochimica Acta*, v. 75, no. 16, p. 4562-4576.

1313 Chazallon, B., Rodriguez, C. T., Ruffine, L., Carpentier, Y., Donval, J. P., Ker, S., and Riboulot, V.,  
1314 2020, Characterizing the variability of natural gas hydrate composition from a selected  
1315 site of the Western Black Sea, off Romania: *Marine and Petroleum Geology*, p. 104785.

1316 Chen, Y., Wu, S., Xie, Y., Yang, C., and Zhang, J., 2007, A novel mechanical gas-tight sampler for  
1317 hydrothermal fluids: *IEEE Journal of Oceanic Engineering*, v. 32, no. 3, p. 603-608.

1318 Chernykh, D., Yusupov, V., Salomatina, A., Kosmach, D., Shakhova, N., Gershelis, E., Konstantinov,  
1319 A., Grinko, A., Chuvilin, E., and Dudarev, O., 2020, Sonar estimation of methane bubble  
1320 flux from thawing subsea permafrost: a case study from the Laptev sea shelf:  
1321 *Geosciences*, v. 10, no. 10, p. 411.

1322 Collett, T. S., Boswell, R., Cochran, J. R., Kumar, P., Lall, M., Mazumdar, A., Ramana, M. V.,  
1323 Ramprasad, T., Riedel, M., Sain, K., Sathe, A. V., Vishwanath, K., and Party, N. E. S., 2014,  
1324 Geologic implications of gas hydrates in the offshore of India: Results of the National  
1325 Gas Hydrate Program Expedition 01: *Marine and Petroleum Geology*, v. 58, p. 3-28.

1326 Collett, T. S., Boswell, R., Lee, M. W., Anderson, B. J., Rose, K., and Lewis, K. A., 2012, Evaluation  
1327 of Long-Term Gas-Hydrate-Production Testing Locations on the Alaska North Slope: Spe  
1328 Reservoir Evaluation & Engineering, v. 15, no. 2, p. 243-264.

1329 Conrad, R., 2009, The global methane cycle: recent advances in understanding the microbial  
1330 processes involved: Environmental microbiology reports, v. 1, no. 5, p. 285-292.

1331 Conrad, R., 2020, Importance of hydrogenotrophic, acetoclastic and methylotrophic  
1332 methanogenesis for methane production in terrestrial, aquatic and other anoxic  
1333 environments: A mini review: Pedosphere, v. 30, no. 1, p. 25-39.

1334 Cragg, B., Parkes, R., Fry, J., Weightman, A., Rochelle, P., and Maxwell, J., 1996, Bacterial  
1335 populations and processes in sediments containing gas hydrates (ODP Leg 146: Cascadia  
1336 Margin): Earth and Planetary Science Letters, v. 139, no. 3-4, p. 497-507.

1337 Cragg, B. A., Parkes, R. J., Fry, J. C., Weightman, A. J., Rochelle, P. A., Maxwell, J. R., Kastner, M.,  
1338 Hovland, M., Whiticar, M. J., and Sample, J. C., The impact of fluid and gas venting on  
1339 bacterial populations and processes in sediments from the Cascadia Margin  
1340 accretionary system (sites 888-892) and the geochemical consequences, *in* Proceedings  
1341 Proceedings of the Ocean Drilling Program Scientific Results 1995, Volume 146, Ocean  
1342 Drilling Program, p. 399-411.

1343 Daigle, H., and Dugan, B., 2011a, Capillary controls on methane hydrate distribution and  
1344 fracturing in advective systems: Geochemistry Geophysics Geosystems, v. 12.

1345 -, 2011b, Origin and evolution of fracture-hosted methane hydrate deposits: Journal of  
1346 Geophysical Research-Solid Earth, v. 115.

1347 Dawson, A., Bondevik, S., and Teller, J., 2011, Relative timing of the Storegga submarine slide,  
1348 methane release, and climate change during the 8.2 ka cold event: The Holocene, v. 21,  
1349 no. 7, p. 1167-1171.

1350 de Garidel-Thoron, T., Beaufort, L., Bassinot, F., and Henry, P., 2004, Evidence for large methane  
1351 releases to the atmosphere from deep-sea gas-hydrate dissociation during the last  
1352 glacial episode: Proceedings of the National Academy of Sciences of the United States  
1353 of America, v. 101, no. 25, p. 9187-9192.

1354 de la Cruz Vargas-Cordero, I., Villar-Muñoz, L., Tinivella, U., Giustiniani, M., Bangs, N., Bento, J.  
1355 P., and Contreras-Reyes, E., 2021, Gas origin linked to paleo BSR: Scientific Reports, v.  
1356 11, no. 1, p. 1-13.

1357 de Prunelé, A., 2015, Dynamics of gas hydrate-bearing pockmarks : learnings from two cases  
1358 studies from the Gulf of Guinea: Ph D Thesis, v. Université Bretagne Occidentale, IUEM,  
1359 no. Ecole doctorale des sciences de la mer.

1360 de Prunelé, A., Ruffine, L., Riboulot, V., Peters, C. A., Croguennec, C., Guyader, V., Pape, T.,  
1361 Bollinger, C., Bayon, G., Caprais, J. C., Germain, Y., Donval, J. P., Marsset, T., Bohrmann,  
1362 G., Geli, L., Rabiou, A., Lescanne, M., Cauquil, E., and Sultan, N., 2017, Focused  
1363 hydrocarbon-migration in shallow sediments of a pockmark cluster in the Niger Delta  
1364 (Off Nigeria): Geochemistry Geophysics Geosystems, v. 18, no. 1, p. 93-112.

1365 Dickens, G. R., 2001, Modeling the global carbon cycle with a gas hydrate capacitor: significance  
1366 for the latest Paleocene thermal maximum: Geophysical monograph, v. 124, p. 19-38.

1367 Dickens, G. R., Castillo, M. M., and Walker, J. C., 1997, A blast of gas in the latest Paleocene:  
1368 Simulating first-order effects of massive dissociation of oceanic methane hydrate:  
1369 Geology, v. 25, no. 3, p. 259-262.

1370 Dickens, G. R., and Quinby-Hunt, M. S., 1997, Methane hydrate stability in pore water: a simple  
1371 theoretical approach for geophysical applications: Journal of geophysical research, v.  
1372 102, no. B1, p. 773-783.

1373 Edson, J. B., Hinton, A. A., Prada, K. E., Hare, J. E., and Fairall, C. W., 1998, Direct covariance flux  
1374 estimates from mobile platforms at sea: Journal of Atmospheric and Oceanic  
1375 Technology, v. 15, no. 2, p. 547-562.

- 1376 Egeberg, P. K., and Dickens, G. R., 1999, Thermodynamic and pore water halogen constraints on  
1 1377 gas hydrate distribution at ODP Site 997 (Blake Ridge): *Chemical Geology*, v. 153, no. 1-  
2 1378 4, p. 53-79.
- 3 1379 Egger, M., Riedinger, N., Mogollón, J. M., and Jørgensen, B. B., 2018, Global diffusive fluxes of  
4 1380 methane in marine sediments: *Nature Geoscience*, v. 11, no. 6, p. 421-425.
- 5 1381 Ehhalt, D., Prather, M., Dentener, F., Derwent, R., Dlugokencky, E., Holland, E., Isaksen, I.,  
6 1382 Katima, J., Kirchhoff, V., and Matson, P., 2001, Atmospheric chemistry and greenhouse  
7 1383 gases.
- 8 1384 Elger, J., Berndt, C., Rüpke, L., Krastel, S., Gross, F., and Geissler, W. H., 2018, Submarine slope  
9 1385 failures due to pipe structure formation: *Nature communications*, v. 9, no. 1, p. 1-6.
- 10 1386 Etiope, G., Ciotoli, G., Schwietzke, S., and Schoell, M., 2019, Gridded maps of geological methane  
11 1387 emissions and their isotopic signature: *Earth System Science Data*, v. 11, no. 1, p. 1-22.
- 12 1388 Farahani, M. V., Hassanpouryouzband, A., Yang, J., and Tohidi, B., 2021a, Development of a  
13 1389 coupled geophysical–geothermal scheme for quantification of hydrates in gas hydrate-  
14 1390 bearing permafrost sediments: *Physical Chemistry Chemical Physics*, v. 23, no. 42, p.  
15 1391 24249-24264.
- 16 1392 Farahani, M. V., Hassanpouryouzband, A., Yang, J., and Tohidi, B., 2021b, Insights into the  
17 1393 climate-driven evolution of gas hydrate-bearing permafrost sediments: implications for  
18 1394 prediction of environmental impacts and security of energy in cold regions: *RSC*  
19 1395 *advances*, v. 11, no. 24, p. 14334-14346.
- 20 1396 Ferre, B., Jansson, P. G., Moser, M., Serov, P., Portnov, A., Graves, C. A., Panieri, G., Grundger,  
21 1397 F., Berndt, C., Lehmann, M. F., and Niemann, H., 2020, Reduced methane seepage from  
22 1398 Arctic sediments during cold bottom-water conditions: *Nature Geoscience*, v. 13, no. 2,  
23 1399 p. 144-+.
- 24 1400 Fischer, D., Mogollon, J. M., Strasser, M., Pape, T., Bohrmann, G., Fekete, N., Spiess, V., and  
25 1401 Kasten, S., 2013, Subduction zone earthquake as potential trigger of submarine  
26 1402 hydrocarbon seepage: *Nature Geoscience*, v. 6, no. 8, p. 647-651.
- 27 1403 Fischer, D., Sahling, H., Nöthen, K., Bohrmann, G., Zabel, M., and Kasten, S., 2012, Interaction  
28 1404 between hydrocarbon seepage, chemosynthetic communities and bottom water redox  
29 1405 at cold seeps of the Makran accretionary prism: insights from habitat-specific pore  
30 1406 water sampling and modeling: *Biogeosciences*, v. 9, p. 2013-2031.
- 31 1407 Franek, P., Plaza-Faverola, A., Mienert, J., Buenz, S., Ferré, B., and Hubbard, A., 2017,  
32 1408 Microseismicity linked to gas migration and leakage on the Western Svalbard Shelf:  
33 1409 *Geochemistry, Geophysics, Geosystems*, v. 18, no. 12, p. 4623-4645.
- 34 1410 Fu, X., Waite, W. F., and Ruppel, C. D., 2021, Hydrate Formation on Marine Seep Bubbles and  
35 1411 the Implications for Water Column Methane Dissolution: *Journal of Geophysical*  
36 1412 *Research-Oceans*, v. 126, no. 9.
- 37 1413 Gao, Y., Wang, Y., Lee, H.-S., and Jin, P., 2022, Significance of anaerobic oxidation of methane  
38 1414 (AOM) in mitigating methane emission from major natural and anthropogenic sources:  
39 1415 a review of AOM rates in recent publications: *Environmental Science: Advances*.
- 40 1416 Garcia-Tigreros, F., Leonte, M., Ruppel, C. D., Ruiz-Angulo, A., Joung, D. J., Young, B., and Kessler,  
41 1417 J. D., 2021, Estimating the impact of seep methane oxidation on ocean pH and dissolved  
42 1418 inorganic radiocarbon along the US Mid-Atlantic Bight: *Journal of Geophysical Research:*  
43 1419 *Biogeosciences*, v. 126, no. 1, p. e2019JG005621.
- 44 1420 Geissler, W. H., Gebhardt, A. C., Gross, F., Wollenburg, J., Jensen, L., Schmidt-Aursch, M. C.,  
45 1421 Krastel, S., Elger, J., and Osti, G., 2016, Arctic megaslide at presumed rest: *Scientific*  
46 1422 *reports*, v. 6, no. 1, p. 1-8.
- 47 1423 Gentz, T., Damm, E., von Deimling, J. S., Mau, S., McGinnis, D. F., and Schluter, M., 2014, A water  
48 1424 column study of methane around gas flares located at the West Spitsbergen continental  
49 1425 margin: *Continental Shelf Research*, v. 72, p. 107-118.

1426 Greinert, J., Artemov, Y., Egorov, V., De Batist, M., and McGinnis, D., 2006, 1300-m-high rising  
1427 bubbles from mud volcanoes at 2080m in the Black Sea: *Hydroacoustic characteristics*  
1428 and temporal variability: *Earth and Planetary Science Letters*, v. 244, no. 1-2, p. 1-15.  
1429 Greinert, J., and Nützel, B., 2004, Hydroacoustic experiments to establish a method for the  
1430 determination of methane bubble fluxes at cold seeps: *Geo-Marine Letters*, v. 24, no. 2,  
1431 p. 75-85.  
1432 Gross, F., Mountjoy, J. J., Crutchley, G. J., Böttner, C., Koch, S., Bialas, J., Pecher, I., Woelz, S.,  
1433 Dannowski, A., and Micallef, A., 2018, Free gas distribution and basal shear zone  
1434 development in a subaqueous landslide—Insight from 3D seismic imaging of the Tuaheni  
1435 Landslide Complex, New Zealand: *Earth and Planetary Science Letters*, v. 502, p. 231-  
1436 243.  
1437 Grozic, J., 2010, Interplay between gas hydrates and submarine slope failure, *Submarine mass*  
1438 *movements and their consequences*, Springer, p. 11-30.  
1439 Guo, K., Fan, S. S., Wang, Y. H., Lang, X. M., Zhang, W. X., and Li, Y. P., 2020, Physical and chemical  
1440 characteristics analysis of hydrate samples from northern South China sea: *Journal of*  
1441 *Natural Gas Science and Engineering*, v. 81.  
1442 Gupta, S., Schmidt, C., Böttner, C., Rüpke, L., and Hartz, E. H., 2022, Spontaneously exsolved free  
1443 gas during major storms as an ephemeral gas source for pockmark formation:  
1444 *Geochemistry, Geophysics, Geosystems*, v. 23, no. 8, p. e2021GC010289.  
1445 Handwerger, A. L., Rempel, A. W., and Skarbak, R. M., 2017, Submarine landslides triggered by  
1446 destabilization of high-saturation hydrate anomalies: *Geochemistry, Geophysics,*  
1447 *Geosystems*, v. 18, no. 7, p. 2429-2445.  
1448 Hassanpouryouzband, A., Joonaki, E., Farahani, M. V., Takeya, S., Ruppel, C., Yang, J., English, N.  
1449 J., Schicks, J. M., Edlmann, K., Mehrabian, H., Aman, Z. M., and Tohidi, B., 2020, Gas  
1450 hydrates in sustainable chemistry: *Chemical Society Reviews*, v. 49, no. 15, p. 5225-5309.  
1451 Hassol, S., 2004, *Impacts of a warming Arctic-Arctic climate impact assessment*, Cambridge  
1452 University Press.  
1453 Hassol, S. J., and Corell, R. W., 2006, *Arctic climate impact assessment: Avoiding dangerous*  
1454 *climate change*, p. 205.  
1455 Hautala, S. L., Solomon, E. A., Johnson, H. P., Harris, R. N., and Miller, U. K., 2014, Dissociation of  
1456 Cascadia margin gas hydrates in response to contemporary ocean warming: *Geophysical*  
1457 *Research Letters*, v. 41, no. 23, p. 8486-8494.  
1458 He, X., Sun, L., Xie, Z., Huang, W., Long, N., Li, Z., and Xing, G., 2013, Sea ice in the Arctic Ocean:  
1459 Role of shielding and consumption of methane: *Atmospheric Environment*, v. 67, p. 8-  
1460 13.  
1461 Heeschen, K. U., Collier, R. W., de Angelis, M. A., Suess, E., Rehder, G., Linke, P., and  
1462 Klinkhammer, G. P., 2005, Methane sources, distributions, and fluxes from cold vent  
1463 sites at Hydrate Ridge, Cascadia Margin: *Global Biogeochemical Cycles*, v. 19, no. 2.  
1464 Hester, K. C., Peltzer, E. T., Walz, P. M., Dunk, R. M., Sloan, E. D., and Brewer, P. G., 2009, A  
1465 natural hydrate dissolution experiment on complex multi-component hydrates on the  
1466 sea floor: *Geochimica et Cosmochimica Acta*, v. 73, no. 22, p. 6747-6756.  
1467 Hinrichs, K.-U., and Boetius, A., 2002, The anaerobic oxidation of methane: new insights in  
1468 microbial ecology and biogeochemistry: *Ocean margin systems*, p. 457-477.  
1469 Hinrichs, K.-U., Hayes, J. M., Sylva, S. P., Brewer, P. G., and DeLong, E. F., 1999, Methane-  
1470 consuming archaeobacteria in marine sediments: *Nature*, v. 398, no. 6730, p. 802-805.  
1471 Hoehler, T., Losey, N. A., Gunsalus, R. P., and McInerney, M. J., 2018, Environmental constraints  
1472 that limit methanogenesis: *Univ. of Oklahoma, Norman, OK (United States)*.  
1473 Holler, T., Widdel, F., Knittel, K., Amann, R., Kellermann, M. Y., Hinrichs, K.-U., Teske, A., Boetius,  
1474 A., and Wegener, G., 2011, Thermophilic anaerobic oxidation of methane by marine  
1475 microbial consortia: *The ISME journal*, v. 5, no. 12, p. 1946-1956.  
1476 Hong, W.-L., Sauer, S., Panieri, G., Ambrose, W. G., Jr., James, R. H., Plaza-Faverola, A., and  
1477 Schneider, A., 2016, Removal of methane through hydrological, microbial, and

1478 geochemical processes in the shallow sediments of pockmarks along eastern Vestnesa  
1479 Ridge (Svalbard): *Limnology and Oceanography*, v. 61, p. S324-S343.

1480 Hornbach, M. J., Saffer, D. M., and Steven Holbrook, W., 2004, Critically pressured free-gas  
1481 reservoirs below gas-hydrate provinces: *Nature*, v. 427, no. 6970, p. 142-144.

1482 Horozal, S., Bahk, J.-J., Urgeles, R., Kim, G. Y., Cukur, D., Kim, S.-P., Lee, G. H., Lee, S. H., Ryu, B.-  
1483 J., and Kim, J.-H., 2017, Mapping gas hydrate and fluid flow indicators and modeling gas  
1484 hydrate stability zone (GHSZ) in the Ulleung Basin, East (Japan) Sea: Potential linkage  
1485 between the occurrence of mass failures and gas hydrate dissociation: *Marine and  
1486 Petroleum Geology*, v. 80, p. 171-191.

1487 Hovland, M., Gardner, J. V., and Judd, A. G., 2002, The significance of pockmarks to  
1488 understanding fluid flow processes and geohazards: *Geofluids*, v. 2, no. 2, p. 127-136.

1489 Hovland, M., and Gudmestad, O. T., 2001, Potential influence of gas hydrates on seabed  
1490 installations: *Geophysical monograph-american geophysical union*, v. 124, p. 307-315.

1491 Hovland, M., and Svensen, H., 2006, Submarine pingoes: Indicators of shallow gas hydrates in a  
1492 pockmark at Nyegga, Norwegian Sea: *Marine Geology*, v. 228, no. 1, p. 15-23.

1493 Hunter, S. J., Goldobin, D. S., Haywood, A. M., Ridgwell, A., and Rees, J. G., 2013, Sensitivity of  
1494 the global submarine hydrate inventory to scenarios of future climate change: *Earth and  
1495 Planetary Science Letters*, v. 367, p. 105-115.

1496 Inagaki, F., Hinrichs, K.-U., Kubo, Y., Bowles, M. W., Heuer, V. B., Hong, W.-L., Hoshino, T., Ijiri,  
1497 A., Imachi, H., and Ito, M., 2015, Exploring deep microbial life in coal-bearing sediment  
1498 down to ~ 2.5 km below the ocean floor: *Science*, v. 349, no. 6246, p. 420-424.

1499 IOGP, R.-. October 2017, Guidelines for the conduct of offshore drilling hazard site surveys:  
1500 International Association of Oil & Gas Producers.

1501 James, R. H., Bousquet, P., Bussmann, I., Haeckel, M., Kipfer, R., Leifer, I., Niemann, H.,  
1502 Ostrovsky, I., Piskozub, J., Rehder, G., Treude, T., Vielstaedte, L., and Greinert, J., 2016,  
1503 Effects of climate change on methane emissions from seafloor sediments in the Arctic  
1504 Ocean: A review: *Limnology and Oceanography*, v. 61, p. S283-S299.

1505 Jerram, K., Weber, T. C., and Beaudoin, J., 2015, Split-beam echo sounder observations of natural  
1506 methane seep variability in the northern Gulf of Mexico: *Geochemistry, Geophysics,  
1507 Geosystems*, v. 16, no. 3, p. 736-750.

1508 Johnson, H. P., Miller, U. K., Salmi, M. S., and Solomon, E. A., 2015, Analysis of bubble plume  
1509 distributions to evaluate methane hydrate decomposition on the continental slope:  
1510 *Geochemistry Geophysics Geosystems*, v. 16, no. 11, p. 3825-3839.

1511 Jørgensen, B. B., and Kasten, S., 2006, Sulfur cycling and methane oxidation, *Marine  
1512 geochemistry*, Springer, p. 271-309.

1513 Joung, D., Leonte, M., Valentine, D. L., Sparrow, K. J., Weber, T., and Kessler, J. D., 2020,  
1514 Radiocarbon in Marine Methane Reveals Patchy Impact of Seeps on Surface Waters:  
1515 *Geophysical Research Letters*, v. 47, no. 20.

1516 Joung, D., Ruppel, C., Southon, J., Weber, T. S., and Kessler, J. D., 2022, Negligible atmospheric  
1517 release of methane from decomposing hydrates in mid-latitude oceans: *Nature  
1518 Geoscience*, v. 15, no. 11, p. 885-891.

1519 Judd, A. G., 2004, Natural seabed gas seeps as sources of atmospheric methane: *Environmental  
1520 Geology*, v. 46, no. 8, p. 988-996.

1521 Kasten, S., Zabel, M., Heuer, V., and Hensen, C., 2003, Processes and signals of nonsteady-state  
1522 diagenesis in deep-sea sediments and their pore waters, *The South Atlantic in the late  
1523 quaternary*, Springer, p. 431-459.

1524 Kennett, J. P., Cannariato, K. G., Hendy, I. L., and Behl, R. J., 2003, Methane hydrates in  
1525 Quaternary climate change: The clathrate gun hypothesis, *American Geophysical Union*.

1526 Ker, S., Thomas, Y., Riboulot, V., Sultan, N., Bernard, C., Scalabrin, C., Ion, G., and Marsset, B.,  
1527 2019, Anomalously Deep BSR Related to a Transient State of the Gas Hydrate System in  
1528 the Western Black Sea: *Geochemistry Geophysics Geosystems*, v. 20, no. 1, p. 442-459.

1529 Ketzer, M., Praeg, D., Rodrigues, L. F., Augustin, A., Pivel, M. A. G., Rahmati-Abkenar, M., Miller,  
1 1530 D. J., Viana, A. R., and Cupertino, J. A., 2020, Gas hydrate dissociation linked to  
2 1531 contemporary ocean warming in the southern hemisphere: *Nature Communications*, v.  
3 1532 11, no. 1.

4 1533 Kirschke, S., Bousquet, P., Ciais, P., Saunoy, M., Canadell, J. G., Dlugokencky, E. J., Bergamaschi,  
5 1534 P., Bergmann, D., Blake, D. R., Bruhwiler, L., Cameron-Smith, P., Castaldi, S., Chevallier,  
6 1535 F., Feng, L., Fraser, A., Heimann, M., Hodson, E. L., Houweling, S., Josse, B., Fraser, P. J.,  
7 1536 Krummel, P. B., Lamarque, J.-F., Langenfelds, R. L., Le Quere, C., Naik, V., O'Doherty, S.,  
8 1537 Palmer, P. I., Pison, I., Plummer, D., Poulter, B., Prinn, R. G., Rigby, M., Ringeval, B.,  
9 1538 Santini, M., Schmidt, M., Shindell, D. T., Simpson, I. J., Spahni, R., Steele, L. P., Strode, S.  
10 1539 A., Sudo, K., Szopa, S., van der Werf, G. R., Voulgarakis, A., van Weele, M., Weiss, R. F.,  
11 1540 Williams, J. E., and Zeng, G., 2013, Three decades of global methane sources and sinks:  
12 1541 *Nature Geoscience*, v. 6, no. 10, p. 813-823.

13 1542 Klar, A., Deerberg, G., Janicki, G., Schicks, J., Riedel, M., Fietzek, P., Mosch, T., Tinivella, U., De La  
14 1543 Fuente Ruiz, M., and Gatt, P., 2019, Marine gas hydrate technology: State of the art and  
15 1544 future possibilities for Europe.

16 1545 Klintzsch, T., Langer, G., Nehrke, G., Wieland, A., Lenhart, K., and Keppler, F., 2019, Methane  
17 1546 production by three widespread marine phytoplankton species: release rates, precursor  
18 1547 compounds, and potential relevance for the environment: *Biogeosciences*, v. 16, no. 20,  
19 1548 p. 4129-4144.

20 1549 Knoblauch, C., Beer, C., Liebner, S., Grigoriev, M. N., and Pfeiffer, E.-M., 2018, Methane  
21 1550 production as key to the greenhouse gas budget of thawing permafrost: *Nature Climate  
22 1551 Change*, v. 8, no. 4, p. 309-312.

23 1552 Konno, Y., Fujii, T., Sato, A., Akamine, K., Naiki, M., Masuda, Y., Yamamoto, K., and Nagao, J.,  
24 1553 2017, Key findings of the world's first offshore methane hydrate production test off the  
25 1554 coast of Japan: Toward future commercial production: *Energy & Fuels*, v. 31, no. 3, p.  
26 1555 2607-2616.

27 1556 Kort, E., Wofsy, S., Daube, B., Diao, M., Elkins, J., Gao, R., Hintsa, E., Hurst, D., Jimenez, R., and  
28 1557 Moore, F., 2012, Atmospheric observations of Arctic Ocean methane emissions up to 82  
29 1558 north: *Nature Geoscience*, v. 5, no. 5, p. 318-321.

30 1559 Kossel, E., Deusner, C., Bigalke, N., and Haeckel, M., 2018, The Dependence of Water  
31 1560 Permeability in Quartz Sand on Gas Hydrate Saturation in the Pore Space: *Journal of  
32 1561 Geophysical Research-Solid Earth*, v. 123, no. 2, p. 1235-1251.

33 1562 Kretschmer, K., Biastoch, A., Riepke, L., and Burwicz, E., 2015, Modeling the fate of methane  
34 1563 hydrates under global warming: *Global biogeochemical cycles*, v. 29, no. 5, p. 610-625.

35 1564 Kurth, J. M., Müller, M.-C., Welte, C. U., and Wagner, T., 2021, Structural insights into the  
36 1565 methane-generating enzyme from a methoxydotrophic methanogen reveal a restrained  
37 1566 gallery of post-translational modifications: *Microorganisms*, v. 9, no. 4, p. 837.

38 1567 Kvenvolden, K., 1995, A review of the geochemistry of methane in natural gas hydrate: *Organic  
39 1568 Geochemistry*, v. 23, no. 11-12, p. 997-1008.

40 1569 Kvenvolden, K. A., and Field, M. E., 1981, Thermogenic hydrocarbons in unconsolidated  
41 1570 sediment of Eel River Basin, offshore northern California: *AAPG Bulletin*, v. 65, no. 9, p.  
42 1571 1642-1646.

43 1572 Kvenvolden, K. A., Lorenson, T. D., and Reeburgh, W. S., 2001, Attention turns to naturally  
44 1573 occurring methane seepage: *Eos, Transactions American Geophysical Union*, v. 82, no.  
45 1574 40, p. 457-457.

46 1575 L'Haridon, S., Chalopin, M., Colombo, D., and Toffin, L., 2014, *Methanococcoides vulcani* sp.  
47 1576 nov., a marine methylotrophic methanogen that uses betaine, choline and N,  
48 1577 N-dimethylethanolamine for methanogenesis, isolated from a mud volcano, and emended  
49 1578 description of the genus *Methanococcoides*: *International journal of systematic and  
50 1579 evolutionary microbiology*, v. 64, no. Pt\_6, p. 1978-1983.



1580 La Cono, V., Smedile, F., Bortoluzzi, G., Arcadi, E., Maimone, G., Messina, E., Borghini, M., Oliveri,  
1 1581 E., Mazzola, S., and L'Haridon, S., 2011, Unveiling microbial life in new deep-sea  
2 1582 hypersaline Lake Thetis. Part I: Prokaryotes and environmental settings: *Environmental*  
3 1583 *Microbiology*, v. 13, no. 8, p. 2250-2268.

4 1584 Lambert, G., and Schmidt, S., 1993, Reevaluation of the oceanic flux of methane: Uncertainties  
5 1585 and long term variations: *Chemosphere*, v. 26, no. 1-4, p. 579-589.

6 1586 Lapham, L., Wilson, R., Riedel, M., Paull, C. K., and Holmes, M. E., 2013, Temporal variability of  
7 1587 in situ methane concentrations in gas hydrate-bearing sediments near Bullseye Vent,  
8 1588 Northern Cascadia Margin: *Geochemistry Geophysics Geosystems*, v. 14, no. 7, p. 2445-  
9 1589 2459.

10 1590 Lapham, L. L., Chanton, J. P., Chapman, R., and Martens, C. S., 2010, Methane under-saturated  
11 1591 fluids in deep-sea sediments: Implications for gas hydrate stability and rates of  
12 1592 dissolution: *Earth and Planetary Science Letters*, v. 298, no. 3-4, p. 275-285.

13 1593 Lapham, L. L., Wilson, R. M., MacDonald, I. R., and Chanton, J. P., 2014, Gas hydrate dissolution  
14 1594 rates quantified with laboratory and seafloor experiments: *Geochimica et*  
15 1595 *Cosmochimica Acta*, v. 125, p. 492-503.

16 1596 Laso-Pérez, R., Hahn, C., van Vliet, D. M., Tegetmeyer, H. E., Schubotz, F., Smit, N. T., Pape, T.,  
17 1597 Sahling, H., Bohrmann, G., and Boetius, A., 2019, Anaerobic degradation of non-  
18 1598 methane alkanes by “*Candidatus Methanoliparia*” in hydrocarbon seeps of the Gulf of  
19 1599 Mexico: *MBio*, v. 10, no. 4, p. e01814-01819.

20 1600 Lazar, C. S., Parkes, R. J., Cragg, B. A., L'Haridon, S., and Toffin, L., 2011, Methanogenic diversity  
21 1601 and activity in hypersaline sediments of the centre of the Napoli mud volcano, Eastern  
22 1602 Mediterranean Sea: *Environmental Microbiology*, v. 13, no. 8, p. 2078-2091.

23 1603 Le, T. X., Rodts, S., Hautemayou, D., Aïmedieu, P., Bornert, M., Chabot, B., and Tang, A. M., 2020,  
24 1604 Kinetics of methane hydrate formation and dissociation in sand sediment:  
25 1605 *Geomechanics for Energy and the Environment*, v. 23, p. 100103.

26 1606 Leblond, I., Scalabrin, C., and Berger, L., 2014, Acoustic monitoring of gas emissions from the  
27 1607 seafloor. Part I: quantifying the volumetric flow of bubbles: *Marine Geophysical*  
28 1608 *Research*, v. 35, no. 3, p. 191-210.

29 1609 Lee, H. J., 2009, Timing of occurrence of large submarine landslides on the Atlantic Ocean  
30 1610 margin: *Marine Geology*, v. 264, no. 1-2, p. 53-64.

31 1611 Lee, J., Santamarina, J. C., and Ruppel, C., 2010, Volume change associated with formation and  
32 1612 dissociation of hydrate in sediment: *Geochemistry, Geophysics, Geosystems*, v. 11, no.  
33 1613 3.

34 1614 Lee, T. R., Phrampus, B. J., Skarke, A., and Wood, W. T., 2022, Global Estimates of Biogenic  
35 1615 Methane Production in Marine Sediments Using Machine Learning and Deterministic  
36 1616 Modeling: *Global Biogeochemical Cycles*, v. 36, no. 7.

37 1617 Leifer, I., Solomon, E., von Deimling, J. S., Rehder, G., Coffin, R., and Linke, P., 2015, The fate of  
38 1618 bubbles in a large, intense bubble megaplume for stratified and unstratified water:  
39 1619 Numerical simulations of 22/4b expedition field data: *Marine and Petroleum Geology*,  
40 1620 v. 68, p. 806-823.

41 1621 Leslie, S. C., and Mann, P., 2016, Giant submarine landslides on the Colombian margin and  
42 1622 tsunami risk in the Caribbean Sea: *Earth and Planetary Science Letters*, v. 449, p. 382-  
43 1623 394.

44 1624 Levin, L. A., 2018, Manifestation, drivers, and emergence of open ocean deoxygenation: *Annual*  
45 1625 *review of marine science*, v. 10, p. 229-260.

46 1626 Li, J.-f., Ye, J.-l., Qin, X.-w., Qiu, H.-j., Wu, N.-y., Lu, H.-l., Xie, W.-w., Lu, J.-a., Peng, F., and Xu, Z.-  
47 1627 q., 2018, The first offshore natural gas hydrate production test in South China Sea: *China*  
48 1628 *Geology*, v. 1, no. 1, p. 5-16.

49 1629 Li, Y., Liu, W., Zhu, Y., Chen, Y., Song, Y., and Li, Q., 2016, Mechanical behaviors of permafrost-  
50 1630 associated methane hydrate-bearing sediments under different mining methods:  
51 1631 *Applied energy*, v. 162, p. 1627-1632.

1632 Li, Y., Luo, T., Sun, X., Liu, W., Li, Q., Li, Y., and Song, Y., 2019, Strength Behaviors of Remolded  
1633 Hydrate-Bearing Marine Sediments in Different Drilling Depths of the South China Sea:  
1634 *Energies*, v. 12, no. 2, p. 253.

1635 Linke, P., Suess, E., Torres, M., Martens, V., Rugh, W., Ziebis, W., and Kulm, L., 1994, In situ  
1636 measurement of fluid flow from cold seeps at active continental margins: *Deep Sea*  
1637 *Research Part I: Oceanographic Research Papers*, v. 41, no. 4, p. 721-739.

1638 Liu, L., Ryu, B., Sun, Z., Wu, N., Cao, H., Geng, W., Zhang, X., Jia, Y., Xu, C., Guo, L., and Wang, L.,  
1639 2019, Monitoring and research on environmental impacts related to marine natural gas  
1640 hydrates: Review and future perspective: *Journal of Natural Gas Science and*  
1641 *Engineering*, v. 65, p. 82-107.

1642 Liu, W., Zhao, J., Luo, Y., Song, Y., Li, Y., Yang, M., Zhang, Y., Liu, Y., and Wang, D., 2013,  
1643 Experimental measurements of mechanical properties of carbon dioxide hydrate-  
1644 bearing sediments: *Marine and petroleum geology*, v. 46, p. 201-209.

1645 Long, A. J., Barlow, N. L., Dawson, S., Hill, J., Innes, J. B., Kelham, C., Milne, F. D., and Dawson, A.,  
1646 2016, Lateglacial and Holocene relative sea-level changes and first evidence for the  
1647 Storegga tsunami in Sutherland, Scotland: *Journal of Quaternary Science*, v. 31, no. 3, p.  
1648 239-255.

1649 Loreto, M. F., Tinivella, U., Accaino, F., and Giustiniani, M., 2011, Offshore Antarctic Peninsula  
1650 Gas Hydrate Reservoir Characterization by Geophysical Data Analysis: *Energies*, v. 4, no.  
1651 1, p. 39-56.

1652 Luff, R., and Wallmann, K., 2003, Fluid flow, methane fluxes, carbonate precipitation and  
1653 biogeochemical turnover in gas hydrate-bearing sediments at Hydrate Ridge, Cascadia  
1654 Margin: Numerical modeling and mass balances: *Geochimica et Cosmochimica Acta*, v.  
1655 67, no. 18, p. 3403-3421.

1656 Luo, T., Li, Y., Sun, X., Shen, S., and Wu, P., 2018, Effect of sediment particle size on the  
1657 mechanical properties of CH<sub>4</sub> hydrate-bearing sediments: *Journal of Petroleum Science*  
1658 *and Engineering*, v. 171, p. 302-314.

1659 Lyu, Z., Shao, N., Akinyemi, T., and Whitman, W. B., 2018, Methanogenesis: *Current Biology*, v.  
1660 28, no. 13, p. R727-R732.

1661 MacDonald, I., Guinasso Jr, N., Sassen, R., Brooks, J., Lee, L., and Scott, K., 1994, Gas hydrate that  
1662 breaches the sea floor on the continental slope of the Gulf of Mexico: *Geology*, v. 22,  
1663 no. 8, p. 699-702.

1664 Malagar, B. R. C., Lijith, K. P., and Singh, D. N., 2019, Formation & dissociation of methane gas  
1665 hydrates in sediments: A critical review: *Journal of Natural Gas Science and Engineering*,  
1666 v. 65, p. 168-184.

1667 Maltby, J., Steinle, L., Löscher, C. R., Bange, H. W., Fischer, M. A., Schmidt, M., and Treude, T.,  
1668 2018, Microbial methanogenesis in the sulfate-reducing zone of sediments in the  
1669 Eckernförde Bay, SW Baltic Sea: *Biogeosciences*, v. 15, no. 1, p. 137-157.

1670 Mao, S.-H., Zhang, H.-H., Zhuang, G.-C., Li, X.-J., Liu, Q., Zhou, Z., Wang, W.-L., Li, C.-Y., Lu, K.-Y.,  
1671 and Liu, X.-T., 2022, Aerobic oxidation of methane significantly reduces global diffusive  
1672 methane emissions from shallow marine waters: *Nature Communications*, v. 13, no. 1,  
1673 p. 7309.

1674 Marcelle-De Silva, J., and Dawe, R., 2011, Towards Commercial Gas Production from Hydrate  
1675 Deposits: *Energies*, v. 4, no. 2, p. 215-238.

1676 Marchenko, S., Gorbunov, A., and Romanovsky, V., 2007, Permafrost warming in the Tien Shan  
1677 mountains, central Asia: *Global and Planetary Change*, v. 56, no. 3-4, p. 311-327.

1678 Marcon, Y., Ondreas, H., Sahling, H., Bohrmann, G., and Olu, K., 2014, Fluid flow regimes and  
1679 growth of a giant pockmark: *Geology*, v. 42, no. 1, p. 63-66.

1680 Marcon, Y., Romer, M., Scherwath, M., Riedel, M., Dolven, K. O., and Heesemann, M., 2022,  
1681 Variability of Marine Methane Bubble Emissions on the Clayoquot Slope, Offshore  
1682 Vancouver Island, Between 2017 and 2021: *Frontiers in Earth Science*, v. 10.

1683 Marin-Moreno, H., Minshull, T. A., Westbrook, G. K., and Sinha, B., 2015, Estimates of future  
1684 warming-induced methane emissions from hydrate offshore west Svalbard for a range  
1685 of climate models: *Geochemistry Geophysics Geosystems*, v. 16, no. 5, p. 1307-1323.  
1686 Marin-Moreno, H., Minshull, T. A., Westbrook, G. K., Sinha, B., and Sarkar, S., 2013, The response  
1687 of methane hydrate beneath the seabed offshore Svalbard to ocean warming during the  
1688 next three centuries: *Geophysical Research Letters*, v. 40, no. 19, p. 5159-5163.  
1689 Marlow, J. J., Hoer, D., Jungbluth, S. P., Reynard, L. M., Gartman, A., Chavez, M. S., El-Naggar, M.  
1690 Y., Tuross, N., Orphan, V. J., and Girguis, P. R., 2021, Carbonate-hosted microbial  
1691 communities are prolific and pervasive methane oxidizers at geologically diverse marine  
1692 methane seep sites: *Proceedings of the National Academy of Sciences*, v. 118, no. 25, p.  
1693 e2006857118.  
1694 Marlow, J. J., Steele, J. A., Ziebis, W., Thurber, A. R., Levin, L. A., and Orphan, V. J., 2014,  
1695 Carbonate-hosted methanotrophy represents an unrecognized methane sink in the  
1696 deep sea: *Nature communications*, v. 5, no. 1, p. 1-12.  
1697 Maslin, M., Owen, M., Betts, R., Day, S., Dunkley Jones, T., and Ridgwell, A., 2010, Gas hydrates:  
1698 past and future geohazard?: *Philosophical Transactions of the Royal Society a-  
1699 Mathematical Physical and Engineering Sciences*, v. 368, no. 1919, p. 2369-2393.  
1700 Maslin, M. A., and Thomas, E., 2003, Balancing the deglacial global carbon budget: the hydrate  
1701 factor: *Quaternary Science Reviews*, v. 22, no. 15-17, p. 1729-1736.  
1702 Max, M., 2003, *Natural gas hydrate: in oceanic and permafrost environments*, Kluwer Academic  
1703 Pub.  
1704 Max, M., and Lowrie, A., 1996, Oceanic methane hydrates: A frontier gas resource: *Journal of  
1705 Petroleum Geology*, v. 19, no. 1, p. 41-56.  
1706 Max, M. D., and Johnson, A. H., 2019, Commercial potential of natural gas hydrate, *Exploration  
1707 and Production of Oceanic Natural Gas Hydrate*, Springer, p. 419-468.  
1708 McConnell, D. R., Zhang, Z., and Boswell, R., 2012, Review of progress in evaluating gas hydrate  
1709 drilling hazards: *Marine and Petroleum Geology*, v. 34, no. 1, p. 209-223.  
1710 McGinnis, D. F., Greinert, J., Artemov, Y., Beaubien, S. E., and Wuest, A., 2006, Fate of rising  
1711 methane bubbles in stratified waters: How much methane reaches the atmosphere?:  
1712 *Journal of Geophysical Research-Oceans*, v. 111, no. C9.  
1713 McInerney, F. A., and Wing, S. L., 2011, The Paleocene-Eocene Thermal Maximum: a  
1714 perturbation of carbon cycle, climate, and biosphere with implications for the future:  
1715 *Annual Review of Earth and Planetary Sciences*, v. 39, p. 489-516.  
1716 McIver, R. D., 1982, Role of naturally occurring gas hydrates in sediment transport: *AAPG  
1717 bulletin*, v. 66, no. 6, p. 789-792.  
1718 Merle, S. G., Embley, R. W., Johnson, H. P., Lau, T.-K., Phrampus, B. J., Raineault, N. A., and Gee,  
1719 L. J., 2021, Distribution of methane plumes on Cascadia Margin and implications for the  
1720 landward limit of methane hydrate stability: *Frontiers in Earth Science*, v. 9, p. 531714.  
1721 Metcalf, W. W., Griffin, B. M., Cicchillo, R. M., Gao, J., Janga, S. C., Cooke, H. A., Circello, B. T.,  
1722 Evans, B. S., Martens-Habbena, W., and Stahl, D. A., 2012, Synthesis of  
1723 methylphosphonic acid by marine microbes: a source for methane in the aerobic ocean:  
1724 *Science*, v. 337, no. 6098, p. 1104-1107.  
1725 Meurer, W. P., Blum, J., and Shipman, G., 2021, Volumetric Mapping of Methane Concentrations  
1726 at the Bush Hill Hydrocarbon Seep, Gulf of Mexico: *Frontiers in Earth Science*, v. 9, p.  
1727 604930.  
1728 Michel, A. P., Preston, V. L., Fauria, K. E., and Nicholson, D. P., 2021, Observations of shallow  
1729 methane bubble emissions from cascadia margin: *Frontiers in Earth Science*, v. 9, p.  
1730 613234.  
1731 Mienert, J., Berndt, C., Tréhu, A. M., Camerlenghi, A., and Liu, C.-S., 2022, *World Atlas of  
1732 Submarine Gas Hydrates in Continental Margins*, Springer Nature.

1733 Mienert, J., Vanneste, M., Bunz, S., Andreassen, K., Hafliðason, H., and Sejrup, H. P., 2005, Ocean  
1734 warming and gas hydrate stability on the mid-Norwegian margin at the Storegga Slide:  
1735 Marine and Petroleum Geology, v. 22, no. 1-2, p. 233-244.

1736 Miesner, F., Overduin, P., Grosse, G., Strauss, J., Langer, M., Westermann, S., Schneider von  
1737 Deimling, T., Brovkin, V., and Arndt, S., 2023, Subsea permafrost organic carbon stocks  
1738 are large and of dominantly low reactivity: Scientific Reports, v. 13, no. 1, p. 9425.

1739 Milkov, A. V., 2004, Global estimates of hydrate-bound gas in marine sediments: how much is  
1740 really out there?: Earth-Science Reviews, v. 66, no. 3-4, p. 183-197.

1741 -, 2005, Molecular and stable isotope compositions of natural gas hydrates: A revised global  
1742 dataset and basic interpretations in the context of geological settings: Organic  
1743 Geochemistry, v. 36, no. 5, p. 681-702.

1744 Milkov, A. V., and Etiope, G., 2018, Revised genetic diagrams for natural gases based on a global  
1745 dataset of > 20,000 samples: Organic Geochemistry, v. 125, p. 109-120.

1746 Moridis, G., and Collett, T., 2003, Strategies for gas production from hydrate accumulations  
1747 under various geologic conditions.

1748 Moridis, G. J., Collett, T. S., Boswell, R., Kurihara, M., Reagan, M. T., Koh, C., and Sloan, E. D.,  
1749 2009, Toward Production From Gas Hydrates: Current Status, Assessment of Resources,  
1750 and Simulation-Based Evaluation of Technology and Potential: Spe Reservoir Evaluation  
1751 & Engineering, v. 12, no. 5, p. 745-771.

1752 Mountjoy, J. J., Pecher, I., Henrys, S., Crutchley, G., Barnes, P. M., and Plaza-Faverola, A., 2014,  
1753 Shallow methane hydrate system controls ongoing, downslope sediment transport in a  
1754 low-velocity active submarine landslide complex, Hikurangi Margin, New Zealand:  
1755 Geochemistry, Geophysics, Geosystems, v. 15, no. 11, p. 4137-4156.

1756 Myhre, C. L., Ferre, B., Platt, S. M., Silyakova, A., Hermansen, O., Allen, G., Pizzo, I., Schmidbauer,  
1757 N., Stohl, A., Pitt, J., Jansson, P., Greinert, J., Percival, C., Fjaeraa, A. M., O'Shea, S. J.,  
1758 Gallagher, M., Le Breton, M., Bower, K. N., Bauguitte, S. J. B., Dalsoren, S.,  
1759 Vadakkepuliambatta, S., Fisher, R. E., Nisbet, E. G., Lowry, D., Myhre, G., Pyle, J. A.,  
1760 Cain, M., and Mienert, J., 2016, Extensive release of methane from Arctic seabed west  
1761 of Svalbard during summer 2014 does not influence the atmosphere: Geophysical  
1762 Research Letters, v. 43, no. 9, p. 4624-4631.

1763 Naudts, L., Khlystov, O., Granin, N., Chensky, A., Poort, J., and De Batist, M., 2012, Stratigraphic  
1764 and structural control on the distribution of gas hydrates and active gas seeps on the  
1765 Posolsky Bank, Lake Baikal: Geo-Marine Letters, v. 32, no. 5-6, p. 395-406.

1766 Nauhaus, K., Albrecht, M., Elvert, M., Boetius, A., and Widdel, F., 2007, In vitro cell growth of  
1767 marine archaeal-bacterial consortia during anaerobic oxidation of methane with sulfate:  
1768 Environmental microbiology, v. 9, no. 1, p. 187-196.

1769 Newberry, C. J., Webster, G., Cragg, B. A., Parkes, R. J., Weightman, A. J., and Fry, J. C., 2004,  
1770 Diversity of prokaryotes and methanogenesis in deep subsurface sediments from the  
1771 Nankai Trough, Ocean Drilling Program Leg 190: Environmental Microbiology, v. 6, no.  
1772 3, p. 274-287.

1773 Nguyen-Sy, T., Tang, A.-M., To, Q.-D., and Vu, M.-N., 2019, A model to predict the elastic  
1774 properties of gas hydrate-bearing sediments: Journal of Applied Geophysics, v. 169, p.  
1775 154-164.

1776 Niemann, H., Lösekann, T., De Beer, D., Elvert, M., Nadalig, T., Knittel, K., Amann, R., Sauter, E.  
1777 J., Schlüter, M., and Klages, M., 2006, Novel microbial communities of the Haakon  
1778 Mosby mud volcano and their role as a methane sink: Nature, v. 443, no. 7113, p. 854-  
1779 858.

1780 Nisbet, E. G., Dlugokencky, E. J., and Bousquet, P., 2014, Methane on the Rise-Again: Science, v.  
1781 343, no. 6170, p. 493-495.

1782 Nisbet, E. G., Dlugokencky, E. J., Manning, M. R., Lowry, D., Fisher, R. E., France, J. L., Michel, S.  
1783 E., Miller, J. B., White, J. W. C., Vaughn, B., Bousquet, P., Pyle, J. A., Warwick, N. J., Cain,  
1784 M., Brownlow, R., Zazzeri, G., Lanoiselle, M., Manning, A. C., Gloor, E., Worthy, D. E. J.,

- 1785 Brunke, E. G., Labuschagne, C., Wolff, E. W., and Ganesan, A. L., 2016, Rising  
1786 atmospheric methane: 2007-2014 growth and isotopic shift: *Global biogeochemical*  
1787 *cycles*, v. 30, no. 9, p. 1356-1370.
- 1788 Norris, R. D., and Röhl, U., 1999, Carbon cycling and chronology of climate warming during the  
1789 Palaeocene/Eocene transition: *Nature*, v. 401, no. 6755, p. 775-778.
- 1790 Olu, K., Caprais, J. C., Galeron, J., Causse, R., von Cosel, R., Budzinski, H., Le Menach, K., Le Roux,  
1791 C., Levache, D., Khrpounoff, A., and Sibuet, M., 2009, Influence of seep emission on the  
1792 non-symbiont-bearing fauna and vagrant species at an active giant pockmark in the Gulf  
1793 of Guinea (Congo-Angola margin): *Deep-Sea Research Part II-Topical Studies in*  
1794 *Oceanography*, v. 56, no. 23, p. 2380-2393.
- 1795 Pape, T., Bahr, A., Klapp, S. A., Abegg, F., and Bohrmann, G., 2011a, High-intensity gas seepage  
1796 causes rafting of shallow gas hydrates in the southeastern Black Sea: *Earth and Planetary*  
1797 *Science Letters*, v. 307, no. 1-2, p. 35-46.
- 1798 Pape, T., Feseker, T., Kasten, S., Fischer, D., and Bohrmann, G., 2011b, Distribution and  
1799 abundance of gas hydrates in near-surface deposits of the Hakon Mosby Mud Volcano,  
1800 SW Barents Sea: *Geochemistry Geophysics Geosystems*, v. 12.
- 1801 Pape, T., Ruffine, L., Hong, W. L., Sultan, N., Riboulot, V., Peters, C. A., Kölling, M., Zabel, M.,  
1802 Garziglia, S., and Bohrmann, G., 2020, Shallow gas hydrate accumulations at a Nigerian  
1803 deepwater pockmark—Quantities and dynamics: *Journal of Geophysical Research: Solid*  
1804 *Earth*, v. 125, no. 9, p. e2019JB018283.
- 1805 Parkes, R. J., Cragg, B., Roussel, E., Webster, G., Weightman, A., and Sass, H., 2014, A review of  
1806 prokaryotic populations and processes in sub-seafloor sediments, including biosphere:  
1807 geosphere interactions: *Marine Geology*, v. 352, p. 409-425.
- 1808 Parkes, R. J., Cragg, B. A., Banning, N., Brock, F., Webster, G., Fry, J. C., Hornibrook, E., Pancost,  
1809 R. D., Kelly, S., Knab, N., Jorgensen, B. B., Rinna, J., and Weightman, A. J., 2007,  
1810 Biogeochemistry and biodiversity of methane cycling in subsurface marine sediments  
1811 (Skagerrak, Denmark): *Environmental Microbiology*, v. 9, no. 5, p. 1146-1161.
- 1812 Paull, C., and Dillon, W., 2001, *Natural gas hydrates: occurrence, distribution, and detection*,  
1813 American Geophysical Union, Washington, DC.
- 1814 Paull, C. K., Ussler, W., Dallimore, S. R., Blasco, S. M., Lorenson, T. D., Melling, H., Medioli, B. E.,  
1815 Nixon, F. M., and McLaughlin, F. A., 2007, Origin of pingo-like features on the Beaufort  
1816 Sea shelf and their possible relationship to decomposing methane gas hydrates:  
1817 *Geophysical Research Letters*, v. 34, no. 1.
- 1818 Petersen, J. M., and Dubilier, N., 2009, Methanotrophic symbioses in marine invertebrates:  
1819 *Environmental Microbiology Reports*, v. 1, no. 5, p. 319-335.
- 1820 Phrampus, B. J., and Hornbach, M. J., 2012, Recent changes to the Gulf Stream causing  
1821 widespread gas hydrate destabilization: *Nature*, v. 490, no. 7421, p. 527-+.
- 1822 Phrampus, B. J., Hornbach, M. J., Ruppel, C. D., and Hart, P. E., 2014, Widespread gas hydrate  
1823 instability on the upper U.S. Beaufort margin: *Journal of Geophysical Research-Solid*  
1824 *Earth*, v. 119, no. 12, p. 8594-8609.
- 1825 Pinero, E., Marquardt, M., Hensen, C., Haeckel, M., and Wallmann, K., 2013, Estimation of the  
1826 global inventory of methane hydrates in marine sediments using transfer functions:  
1827 *Biogeosciences*, v. 10, no. 2, p. 959-975.
- 1828 Platt, S. M., Eckhardt, S., Ferre, B., Fisher, R. E., Hermansen, O., Jansson, P., Lowry, D., Nisbet, E.  
1829 G., Pisso, I., Schmidbauer, N., Silyakova, A., Stohl, A., Svendby, T. M.,  
1830 Vadakkepuliambatta, S., Mienert, J., and Myhre, C. L., 2018, Methane at Svalbard and  
1831 over the European Arctic Ocean: *Atmospheric Chemistry and Physics*, v. 18, no. 23, p.  
1832 17207-17224.
- 1833 Pohlman, J. W., Ruppel, C., Hutchinson, D. R., Downer, R., and Coffin, R. B., 2008, Assessing  
1834 sulfate reduction and methane cycling in a high salinity pore water system in the  
1835 northern Gulf of Mexico: *Marine and Petroleum Geology*, v. 25, no. 9, p. 942-951.

- 1836 Polyakov, I., Akasofu, S. I., Bhatt, U., Colony, R., Ikeda, M., Makshtas, A., Swingley, C., Walsh, D.,  
1837 and Walsh, J., 2002, Trends and variations in Arctic climate system, Wiley Online Library.
- 1838 Pop Ristova, P., Wenzhöfer, F., Ramette, A., Zabel, M., Fischer, D., Kasten, S., and Boetius, A.,  
1839 2012, Bacterial diversity and biogeochemistry of different chemosynthetic habitats of  
1840 the REGAB cold seep (West African margin, 3160 m water depth): *Biogeosciences*, v. 9,  
1841 no. 12, p. 5031-5048.
- 1842 Portnov, A., Vadakkepuliambatta, S., Mienert, J., and Hubbard, A., 2016, Ice-sheet-driven  
1843 methane storage and release in the Arctic: *Nature communications*, v. 7, no. 1, p. 1-7.
- 1844 Priest, J. A., and Grozic, J. L., 2016, Stability of fine-grained sediments subject to gas hydrate  
1845 dissociation in the Arctic continental margin, *Submarine Mass Movements and their  
1846 Consequences*, Springer, p. 427-436.
- 1847 Reeburgh, W. S., 2007, Oceanic methane biogeochemistry: *Chemical Reviews*, v. 107, no. 2, p.  
1848 486-513.
- 1849 Rehder, G., Kirby, S. H., Durham, W. B., Stern, L. A., Peltzer, E. T., Pinkston, J., and Brewer, P. G.,  
1850 2004, Dissolution rates of pure methane hydrate and carbon-dioxide hydrate in  
1851 undersaturated seawater at 1000-m depth: *Geochimica et Cosmochimica Acta*, v. 68,  
1852 no. 2, p. 285-292.
- 1853 Riboulot, V., Ker, S., Sultan, N., Thomas, Y., Marsset, B., Scalabrin, C., Ruffine, L., Boulart, C., and  
1854 Ion, G., 2018, Freshwater lake to salt-water sea causing widespread hydrate dissociation  
1855 in the Black Sea: *Nature Communications*, v. 9.
- 1856 Riboulot, V., Sultan, N., Imbert, P., and Ker, S., 2016, Initiation of gas-hydrate pockmark in deep-  
1857 water Nigeria: Geo-mechanical analysis and modelling: *Earth and Planetary Science  
1858 Letters*, v. 434, p. 252-263.
- 1859 Riedel, M., Collett, T., Malone, M., and Scientists, E., Expedition 311 synthesis: scientific findings,  
1860 *in Proceedings Proc. IODP| Volume2010, Volume 311*, p. 2.
- 1861 Riedel, M., Wallmann, K., Berndt, C., Pape, T., Freudenthal, T., Bergenthal, M., Bunz, S., and  
1862 Bohrmann, G., 2018, In Situ Temperature Measurements at the Svalbard Continental  
1863 Margin: Implications for Gas Hydrate Dynamics: *Geochemistry Geophysics Geosystems*,  
1864 v. 19, no. 4, p. 1165-1177.
- 1865 Rogener, M. K., Bracco, A., Hunter, K. S., Saxton, M. A., and Joye, S. B., 2018, Long-term impact  
1866 of the Deepwater Horizon oil well blowout on methane oxidation dynamics in the  
1867 northern Gulf of Mexico: *Elementa: Science of the Anthropocene*, v. 6.
- 1868 Römer, M., Blumenberg, M., Heeschen, K., Schloemer, S., Müller, H., Müller, S., Hilgenfeldt, C.,  
1869 Barckhausen, U., and Schwalenberg, K., 2021, Seafloor methane seepage related to salt  
1870 diapirism in the northwestern part of the German North Sea: *Frontiers in Earth Science*,  
1871 v. 9, p. 556329.
- 1872 Römer, M., Riedel, M., Scherwath, M., Heesemann, M., and Spence, G. D., 2016, Tidally  
1873 controlled gas bubble emissions: A comprehensive study using long-term monitoring  
1874 data from the NEPTUNE cabled observatory offshore Vancouver Island: *Geochemistry,  
1875 Geophysics, Geosystems*, v. 17, no. 9, p. 3797-3814.
- 1876 Rosentreter, J. A., Borges, A. V., Deemer, B. R., Holgerson, M. A., Liu, S., Song, C., Melack, J.,  
1877 Raymond, P. A., Duarte, C. M., and Allen, G. H., 2021, Half of global methane emissions  
1878 come from highly variable aquatic ecosystem sources: *Nature Geoscience*, v. 14, no. 4,  
1879 p. 225-230.
- 1880 Ruff, S. E., Felden, J., Gruber-Vodicka, H. R., Marcon, Y., Knittel, K., Ramette, A., and Boetius, A.,  
1881 2019, In situ development of a methanotrophic microbiome in deep-sea sediments: *The  
1882 ISME journal*, v. 13, no. 1, p. 197-213.
- 1883 Ruffine, L., Donval, J. P., Croguennec, C., Bignon, L., Birot, D., Battani, A., Bayon, G., Caprais, J.  
1884 C., Lanteri, N., Levache, D., and Dupre, S., 2018a, Gas Seepage along the Edge of the  
1885 Aquitaine Shelf (France): Origin and Local Fluxes: *Geofluids*.
- 1886 Ruffine, L., Ondreas, H., Blanc-Valleron, M.-M., Teichert, B. M. A., Scalabrin, C., Rinnert, E., Birot,  
1887 D., Croguennec, C., Ponzevera, E., Pierre, C., Donval, J.-P., Alix, A.-S., Germain, Y., Bignon,

1888 L., Etoubleau, J., Caprais, J.-C., Knoery, J., Lesongeur, F., Thomas, B., Roubi, A., Legoix, L.  
1 1889 N., Burnard, P., Chevalier, N., Lu, H., Dupré, S., Fontanier, C., Dissard, D., Olgun, N., Yang,  
2 1890 H., Strauss, H., Özaksoy, V., Perchoc, J., Podeur, C., Tarditi, C., Özbeki, E., Guyader, V.,  
3 1891 Marty, B., Madre, D., Pitel-Roudaut, M., Grall, C., Embriaco, D., Polonia, A., Gasperini, L.,  
4 1892 Çağatay, M. N., Henry, P., and Géli, L., 2018b, Multidisciplinary investigation on cold  
5 1893 seeps with vigorous gas emissions in the Sea of Marmara (MarsiteCruise): Strategy for  
6 1894 site detection and sampling and first scientific outcome: Deep Sea Research Part II:  
7 1895 Topical Studies in Oceanography.  
8 1896 Ruppel, C., 2011, Methane hydrates and contemporary climate change: Nature Education  
9 1897 Knowledge, v. 3, no. 10, p. 29.  
10 1898 Ruppel, C., 2015, Permafrost-associated gas hydrate: Is it really approximately 1% of the global  
11 1899 system?: Journal of Chemical & Engineering Data, v. 60, no. 2, p. 429-436.  
12 1900 Ruppel, C., Boswell, R., and Jones, E., 2008, Scientific results from Gulf of Mexico gas hydrates  
13 1901 Joint Industry Project Leg 1 drilling: introduction and overview: Marine and Petroleum  
14 1902 Geology, v. 25, no. 9, p. 819-829.  
15 1903 Ruppel, C. D., and Kessler, J. D., 2017, The interaction of climate change and methane hydrates:  
16 1904 Reviews of Geophysics, v. 55, no. 1, p. 126-168.  
17 1905 Ruppel, C. D., and Waite, W. F., 2020, Timescales and Processes of Methane Hydrate Formation  
18 1906 and Breakdown, With Application to Geologic Systems: Journal of Geophysical Research:  
19 1907 Solid Earth, v. 125, no. 8, p. e2018JB016459.  
20 1908 Ryerson, T. B., Aikin, K. C., Angevine, W. M., Atlas, E. L., Blake, D. R., Brock, C. A., Fehsenfeld, F.  
21 1909 C., Gao, R. S., de Gouw, J. A., Fahey, D. W., Holloway, J. S., Lack, D. A., Lueb, R. A.,  
22 1910 Meinardi, S., Middlebrook, A. M., Murphy, D. M., Neuman, J. A., Nowak, J. B., Parrish, D.  
23 1911 D., Peischl, J., Perring, A. E., Pollack, I. B., Ravishankara, A. R., Roberts, J. M., Schwarz, J.  
24 1912 P., Spackman, J. R., Stark, H., Warneke, C., and Watts, L. A., 2011, Atmospheric emissions  
25 1913 from the Deepwater Horizon spill constrain air-water partitioning, hydrocarbon fate,  
26 1914 and leak rate: Geophysical Research Letters, v. 38.  
27 1915 Sahling, H., Rickert, D., Lee, R. W., Linke, P., and Suess, E., 2002, Macrofaunal community  
28 1916 structure and sulfide flux at gas hydrate deposits from the Cascadia convergent margin,  
29 1917 NE Pacific: Marine Ecology Progress Series, v. 231, p. 121-138.  
30 1918 Sassen, R., Joye, S., Sweet, S., DeFreitas, D., Milkov, A., and MacDonald, I., 1999, Thermogenic  
31 1919 gas hydrates and hydrocarbon gases in complex chemosynthetic communities, Gulf of  
32 1920 Mexico continental slope: Organic Geochemistry, v. 30, no. 7, p. 485-497.  
33 1921 Sassen, R., Roberts, H. H., Aharon, P., Larkin, J., Chinn, E. W., and Carney, R., 1993,  
34 1922 Chemosynthetic bacterial mats at cold hydrocarbon seeps, Gulf of Mexico continental  
35 1923 slope: Organic Geochemistry, v. 20, no. 1, p. 77-89.  
36 1924 Sauniois, M., Bousquet, P., Poulter, B., Peregon, A., Ciais, P., Canadell, J. G., Dlugokencky, E. J.,  
37 1925 Etiope, G., Bastviken, D., Houweling, S., Janssens-Maenhout, G., Tubiello, F. N., Castaldi,  
38 1926 S., Jackson, R. B., Alexe, M., Arora, V. K., Beerling, D. J., Bergamaschi, P., Blake, D. R.,  
39 1927 Brailsford, G., Brovkin, V., Bruhwiler, L., Crevoisier, C., Crill, P., Covey, K., Curry, C.,  
40 1928 Frankenberg, C., Gedney, N., Hoeglund-Isaksson, L., Ishizawa, M., Ito, A., Joos, F., Kim,  
41 1929 H.-S., Kleinen, T., Krummel, P., Lamarque, J.-F., Langenfelds, R., Locatelli, R., Machida,  
42 1930 T., Maksyutov, S., McDonald, K. C., Marshall, J., Melton, J. R., Morino, I., Naik, V.,  
43 1931 O'Doherty, S., Parmentier, F.-J. W., Patra, P. K., Peng, C., Peng, S., Peters, G. P., Pison, I.,  
44 1932 Prigent, C., Prinn, R., Ramonet, M., Riley, W. J., Saito, M., Santini, M., Schroeder, R.,  
45 1933 Simpson, I. J., Spahni, R., Steele, P., Takizawa, A., Thornton, B. F., Tian, H., Tohjima, Y.,  
46 1934 Viovy, N., Voulgarakis, A., van Weele, M., van der Werf, G. R., Weiss, R., Wiedinmyer, C.,  
47 1935 Wilton, D. J., Wiltshire, A., Worthy, D., Wunch, D., Xu, X., Yoshida, Y., Zhang, B., Zhang,  
48 1936 Z., and Zhu, Q., 2016, The global methane budget 2000-2012: Earth System Science  
49 1937 Data, v. 8, no. 2, p. 697-751.  
50 1938 Sauniois, M., Bousquet, P., Poulter, B., Peregon, A., Ciais, P., Canadell, J. G., Dlugokencky, E. J.,  
51 1939 Etiope, G., Bastviken, D., Houweling, S., Janssens-Maenhout, G., Tubiello, F. N., Castaldi,

1940 S., Jackson, R. B., Alexe, M., Arora, V. K., Beerling, D. J., Bergamaschi, P., Blake, D. R.,  
1 1941 Brailsford, G., Bruhwiler, L., Crevoisier, C., Crill, P., Covey, K., Frankenberg, C., Gedney,  
2 1942 N., Hoglund-Isaksson, L., Ishizawa, M., Ito, A., Joos, F., Kim, H. S., Kleinen, T., Krummel,  
3 1943 P., Lamarque, J. F., Langenfelds, R., Locatelli, R., Machida, T., Maksyutov, S., Melton, J.  
4 1944 R., Morino, I., Naik, V., O'Doherty, S., Parmentier, F. J., Patra, P. K., Peng, C. H., Peng, S.  
5 1945 S., Peters, G. P., Pison, I., Prinn, R., Ramonet, M., Riley, W. J., Saito, M., Santini, M.,  
6 1946 Schroeder, R., Simpson, I. J., Spahni, R., Takizawa, A., Thornton, B. F., Tian, H. Q.,  
7 1947 Tohjima, Y., Viovy, N., Voulgarakis, A., Weiss, R., Wilton, D. J., Wiltshire, A., Worthy, D.,  
8 1948 Wunch, D., Xu, X. Y., Yoshida, Y., Zhang, B. W., Zhang, Z., and Zhu, Q. A., 2017, Variability  
9 1949 and quasi-decadal changes in the methane budget over the period 2000-2012:  
10 1950 Atmospheric Chemistry and Physics, v. 17, no. 18, p. 11135-11161.  
11 1951 Saunio, M., Stavert, A. R., Poulter, B., Bousquet, P., Canadell, J. G., Jackson, R. B., Raymond, P.  
12 1952 A., Dlugokencky, E. J., Houweling, S., Patra, P. K., Ciais, P., Arora, V. K., Bastviken, D.,  
13 1953 Bergamaschi, P., Blake, D. R., Brailsford, G., Bruhwiler, L., Carlson, K. M., Carrol, M.,  
14 1954 Castaldi, S., Chandra, N., Crevoisier, C., Crill, P. M., Covey, K., Curry, C. L., Etiope, G.,  
15 1955 Frankenberg, C., Gedney, N., Hegglin, M. I., Hoglund-Isaksson, L., Hugelius, G., Ishizawa,  
16 1956 M., Ito, A., Janssens-Maenhout, G., Jensen, K. M., Joos, F., Kleinen, T., Krummel, P. B.,  
17 1957 Langenfelds, R. L., Laruelle, G. G., Liu, L. C., Machida, T., Maksyutov, S., McDonald, K. C.,  
18 1958 McNorton, J., Miller, P. A., Melton, J. R., Morino, I., Muller, J., Murguia-Flores, F., Naik,  
19 1959 V., Niwa, Y., Noce, S., Doherty, S. O., Parker, R. J., Peng, C. H., Peng, S. S., Peters, G. P.,  
20 1960 Prigent, C., Prinn, R., Ramonet, M., Regnier, P., Riley, W. J., Rosentreter, J. A., Segers, A.,  
21 1961 Simpson, I. J., Shi, H., Smith, S. J., Steele, L. P., Thornton, B. F., Tian, H. Q., Tohjima, Y.,  
22 1962 Tubiello, F. N., Tsuruta, A., Viovy, N., Voulgarakis, A., Weber, T. S., van Weele, M., van  
23 1963 der Werf, G. R., Weiss, R. F., Worthy, D., Wunch, D., Yin, Y., Yoshida, Y., Zhang, W. X.,  
24 1964 Zhang, Z., Zhao, Y. H., Zheng, B., Zhu, Q., Zhu, Q. A., and Zhuang, Q. L., 2020, The Global  
25 1965 Methane Budget 2000-2017: Earth System Science Data, v. 12, no. 3, p. 1561-1623.  
26 1966 Schicks, J. M., Spangenberg, E., Giese, R., Steinhauer, B., Klump, J., and Luzi, M., 2011, New  
27 1967 Approaches for the Production of Hydrocarbons from Hydrate Bearing Sediments:  
28 1968 Energies, v. 4, no. 1, p. 151-172.  
29 1969 Schmale, O., Beaubien, S. E., Rehder, G., Greinert, J., and Lombardi, S., 2010a, Gas seepage in  
30 1970 the Dnepr paleo-delta area (NW-Black Sea) and its regional impact on the water column  
31 1971 methane cycle: Journal of Marine Systems, v. 80, no. 1-2, p. 90-100.  
32 1972 Schmale, O., Greinert, J., and Rehder, G., 2005, Methane emission from high-intensity marine  
33 1973 gas seeps in the Black Sea into the atmosphere: Geophysical Research Letters, v. 32, no.  
34 1974 7.  
35 1975 Schmale, O., von Deimling, J. S., Gulzow, W., Nausch, G., Waniek, J. J., and Rehder, G., 2010b,  
36 1976 Distribution of methane in the water column of the Baltic Sea: Geophysical Research  
37 1977 Letters, v. 37.  
38 1978 Schmidt, C., Gupta, S., Rupke, L., Burwicz-Galerie, E., and Hartz, E. H., 2022, Sedimentation-  
39 1979 driven cyclic rebuilding of gas hydrates: Marine and Petroleum Geology, v. 140.  
40 1980 Schneider von Deimling, T., Grosse, G., Strauss, J., Schirrmeister, L., Morgenstern, A., Schaphoff,  
41 1981 S., Meinshausen, M., and Boike, J., 2015, Observation-based modelling of permafrost  
42 1982 carbon fluxes with accounting for deep carbon deposits and thermokarst activity:  
43 1983 Biogeosciences, v. 12, no. 11, p. 3469-3488.  
44 1984 Serié, C., Huuse, M., and Schødt, N. H., 2012, Gas hydrate pingoes: Deep seafloor evidence of  
45 1985 focused fluid flow on continental margins: Geology, v. 40, no. 3, p. 207-210.  
46 1986 Shakhova, N., Semiletov, I., Leifer, I., Sergienko, V., Salyuk, A., Kosmach, D., Chernykh, D., Stubbs,  
47 1987 C., Nicolsky, D., Tumskoy, V., and Gustafsson, O., 2014, Ebullition and storm-induced  
48 1988 methane release from the East Siberian Arctic Shelf: Nature Geoscience, v. 7, no. 1, p.  
49 1989 64-70.



1990 Shakhova, N., Semiletov, I., Salyuk, A., Yusupov, V., Kosmach, D., and Gustafsson, O., 2010,  
1 1991 Extensive Methane Venting to the Atmosphere from Sediments of the East Siberian  
2 1992 Arctic Shelf: *Science*, v. 327, no. 5970, p. 1246-1250.  
3 1993 Simonetti, A., Knapp, J. H., Sleeper, K., Lutken, C. B., Macelloni, L., and Knapp, C. C., 2013, Spatial  
4 1994 distribution of gas hydrates from high-resolution seismic and core data, Woolsey  
5 1995 Mound, Northern Gulf of Mexico: *Marine and Petroleum Geology*, v. 44, p. 21-33.  
6 1996 Skarke, A., Ruppel, C., Kodis, M., Brothers, D., and Lobecker, E., 2014, Widespread methane  
7 1997 leakage from the sea floor on the northern US Atlantic margin: *Nature Geoscience*, v. 7,  
8 1998 no. 9, p. 657-661.  
9 1999 Solomon, E. A., Kastner, M., Jannasch, H., Robertson, G., and Weinstein, Y., 2008, Dynamic fluid  
10 2000 flow and chemical fluxes associated with a seafloor gas hydrate deposit on the northern  
11 2001 Gulf of Mexico slope: *Earth and Planetary Science Letters*, v. 270, no. 1-2, p. 95-105.  
12 2002 Solomon, E. A., Kastner, M., MacDonald, I. R., and Leifer, I., 2009, Considerable methane fluxes  
13 2003 to the atmosphere from hydrocarbon seeps in the Gulf of Mexico: *Nature Geoscience*,  
14 2004 v. 2, no. 8, p. 561-565.  
15 2005 Solomon, E. A., Spivack, A. J., Kastner, M., Torres, M. E., and Robertson, G., 2014, Gas hydrate  
16 2006 distribution and carbon sequestration through coupled microbial methanogenesis and  
17 2007 silicate weathering in the Krishna-Godavari Basin, offshore India: *Marine and Petroleum  
18 2008 Geology*, v. 58, p. 233-253.  
19 2009 Song, H., Du, Y., Algeo, T. J., Tong, J., Owens, J. D., Song, H., Tian, L., Qiu, H., Zhu, Y., and Lyons,  
20 2010 T. W., 2019, Cooling-driven oceanic anoxia across the Smithian/Spathian boundary (mid-  
21 2011 Early Triassic): *Earth-Science Reviews*, v. 195, p. 133-146.  
22 2012 Steeb, P., Linke, P., and Treude, T., 2014, A sediment flow-through system to study the impact  
23 2013 of shifting fluid and methane flow regimes on the efficiency of the benthic methane  
24 2014 filter: *Limnology and Oceanography: Methods*, v. 12, no. 1, p. 25-45.  
25 2015 Steinle, L., Graves, C. A., Treude, T., Ferré, B., Biastoch, A., Bussmann, I., Berndt, C., Krastel, S.,  
26 2016 James, R. H., and Behrens, E., 2015, Water column methanotrophy controlled by a rapid  
27 2017 oceanographic switch: *Nature Geoscience*, v. 8, no. 5, p. 378-382.  
28 2018 Stern, L. A., and Lorenson, T. D., 2014, Grain-scale imaging and compositional characterization  
29 2019 of cryo-preserved India NGHP 01 gas-hydrate-bearing cores: *Marine and Petroleum  
30 2020 Geology*, v. 58, p. 206-222.  
31 2021 Stern, L. A., Lorenson, T. D., and Pinkston, J. C., 2011, Gas hydrate characterization and grain-  
32 2022 scale imaging of recovered cores from the Mount Elbert Gas Hydrate Stratigraphic Test  
33 2023 Well, Alaska North Slope: *Marine and Petroleum Geology*, v. 28, no. 2, p. 394-403.  
34 2024 Suess, E., 2014, Marine cold seeps and their manifestations: geological control, biogeochemical  
35 2025 criteria and environmental conditions: *International Journal of Earth Sciences*, v. 103,  
36 2026 no. 7, p. 1889-1916.  
37 2027 Suess, E., Torres, M., Bohrmann, G., Collier, R., Greinert, J., Linke, P., Rehder, G., Trehu, A.,  
38 2028 Wallmann, K., and Winckler, G., 1999, Gas hydrate destabilization: enhanced  
39 2029 dewatering, benthic material turnover and large methane plumes at the Cascadia  
40 2030 convergent margin: *Earth and Planetary Science Letters*, v. 170, no. 1-2, p. 1-15.  
41 2031 Sultan, N., Bohrmann, G., Ruffine, L., Pape, T., Riboulot, V., Colliat, J. L., De Prunele, A.,  
42 2032 Dennielou, B., Garziglia, S., Himmler, T., Marsset, T., Peters, C. A., Rabiou, A., and Wei, J.,  
43 2033 2014, Pockmark formation and evolution in deep water Nigeria: Rapid hydrate growth  
44 2034 versus slow hydrate dissolution: *Journal of Geophysical Research-Solid Earth*, v. 119, no.  
45 2035 4, p. 2679-2694.  
46 2036 Sultan, N., Cochonat, P., Foucher, J., and Mienert, J., 2004, Effect of gas hydrates melting on  
47 2037 seafloor slope instability: *Marine Geology*, v. 213, no. 1-4, p. 379-401.  
48 2038 Sultan, N., Garziglia, S., and Ruffine, L., 2016, New insights into the transport processes  
49 2039 controlling the sulfate-methane-transition-zone near methane vents: *Scientific Reports*,  
50 2040 v. 6.

- 2041 Sultan, N., Marsset, B., Ker, S., Marsset, T., Voisset, M., Vernant, A. M., Bayon, G., Cauquil, E.,  
1 2042 Adamy, J., Colliat, J. L., and Drapeau, D., 2010, Hydrate dissolution as a potential  
2 2043 mechanism for pockmark formation in the Niger delta: *Journal of Geophysical Research-*  
3 2044 *Solid Earth*, v. 115.
- 4 2045 Sultan, N., Plaza-Faverola, A., Vadakkepuliambatta, S., Buenz, S., and Knies, J., 2020, Impact of  
5 2046 tides and sea-level on deep-sea Arctic methane emissions: *Nature communications*, v.  
6 2047 11, no. 1, p. 5087.
- 7 2048 Sultan, N., Voisset, M., Marsset, T., Vernant, A. M., Cauquil, E., Colliat, J. L., and Curinier, V.,  
8 2049 2007, Detection of free gas and gas hydrate based on 3D seismic data and cone  
9 2050 penetration testing: An example from the Nigerian Continental Slope: *Marine Geology*,  
10 2051 v. 240, no. 1-4, p. 235-255.
- 11 2052 Sweetman, A. K., Thurber, A. R., Smith, C. R., Levin, L. A., Mora, C., Wei, C.-L., Gooday, A. J., Jones,  
12 2053 D. O., Rex, M., and Yasuhara, M., 2017, Major impacts of climate change on deep-sea  
13 2054 benthic ecosystems: *Elementa: Science of the Anthropocene*, v. 5.
- 14 2055 Taleb, F., Lemaire, M., Garziglia, S., Marsset, T., and Sultan, N., 2020, Seafloor depressions on  
15 2056 the Nigerian margin: Seabed morphology and sub-seabed hydrate distribution: *Marine*  
16 2057 *and Petroleum Geology*, v. 114.
- 17 2058 Talling, P. J., Clare, M., Urlaub, M., Pope, E., Hunt, J. E., and Watt, S. F., 2014, Large submarine  
18 2059 landslides on continental slopes: geohazards, methane release, and climate change:  
19 2060 *Oceanography*, v. 27, no. 2, p. 32-45.
- 20 2061 Teske, A., Hinrichs, K.-U., Edgcomb, V., de Vera Gomez, A., Kysela, D., Sylva, S. P., Sogin, M. L.,  
21 2062 and Jannasch, H. W., 2002, Microbial diversity of hydrothermal sediments in the  
22 2063 Guaymas Basin: evidence for anaerobic methanotrophic communities: *Applied and*  
23 2064 *Environmental Microbiology*, v. 68, no. 4, p. 1994-2007.
- 24 2065 Thatcher, K. E., Westbrook, G. K., Sarkar, S., and Minshull, T. A., 2013, Methane release from  
25 2066 warming-induced hydrate dissociation in the West Svalbard continental margin: Timing,  
26 2067 rates, and geological controls: *Journal of Geophysical Research-Solid Earth*, v. 118, no.  
27 2068 1, p. 22-38.
- 28 2069 Thornton, B. F., Geibel, M. C., Crill, P. M., Humborg, C., and Mörth, C. M., 2016, Methane fluxes  
29 2070 from the sea to the atmosphere across the Siberian shelf seas: *Geophysical Research*  
30 2071 *Letters*, v. 43, no. 11, p. 5869-5877.
- 31 2072 Thornton, B. F., Prytherch, J., Andersson, K., Brook, I. M., Salisbury, D., Tjernstrom, M., and Crill,  
32 2073 P. M., 2020, Shipborne eddy covariance observations of methane fluxes constrain Arctic  
33 2074 sea emissions: *Science Advances*, v. 6, no. 5.
- 34 2075 Tinivella, U., and Giustiniani, M., 2013, Variations in BSR depth due to gas hydrate stability versus  
35 2076 pore pressure: *Global and Planetary Change*, v. 100, p. 119-128.
- 36 2077 -, 2016, Gas hydrate stability zone in shallow Arctic Ocean in presence of sub-sea permafrost:  
37 2078 *Rendiconti Lincei-Scienze Fisiche E Naturali*, v. 27, p. 163-171.
- 38 2079 Tinivella, U., Giustiniani, M., and Marin-Moreno, H., 2019, A Quick-Look Method for Initial  
39 2080 Evaluation of Gas Hydrate Stability below Subaqueous Permafrost: *Geosciences*, v. 9,  
40 2081 no. 8.
- 41 2082 Torres, M. E., McManus, J., Hammond, D. E., de Angelis, M. A., Heeschen, K. U., Colbert, S. L.,  
42 2083 Tryon, M. D., Brown, K. M., and Suess, E., 2002, Fluid and chemical fluxes in and out of  
43 2084 sediments hosting methane hydrate deposits on Hydrate Ridge, OR, I: Hydrological  
44 2085 provinces: *Earth and Planetary Science Letters*, v. 201, no. 3-4, p. 525-540.
- 45 2086 Treude, T., Krause, S., Steinle, L., Burwicz, E., Hamdan, L. J., Niemann, H., Feseker, T., Liebetrau,  
46 2087 V., Krastel, S., and Berndt, C., 2020, Biogeochemical Consequences of Nonvertical  
47 2088 Methane Transport in Sediment Offshore Northwestern Svalbard: *Journal of*  
48 2089 *Geophysical Research-Biogeosciences*, v. 125, no. 3.
- 49 2090 Tsyтовich, N. A., 1975, *Mechanics of frozen ground*, Scripta Book Co.

2091 Urgeles, R., and Camerlenghi, A., 2013, Submarine landslides of the Mediterranean Sea: Trigger  
2092 mechanisms, dynamics, and frequency-magnitude distribution: *Journal of Geophysical*  
2093 *Research: Earth Surface*, v. 118, no. 4, p. 2600-2618.

2094 Vanwonterghem, I., Evans, P. N., Parks, D. H., Jensen, P. D., Woodcroft, B. J., Hugenholtz, P., and  
2095 Tyson, G. W., 2016, Methylophilic methanogenesis discovered in the archaeal phylum  
2096 *Verstraetearchaeota*: *Nature microbiology*, v. 1, no. 12, p. 1-9.

2097 Vargas-Cordero, I., Tinivella, U., Villar-Munoz, L., Bento, J. P., Carcamo, C., Lopez-Acevedo, D.,  
2098 Fernandoy, F., Rivero, A., and Juan, M. S., 2020a, Gas hydrate versus seabed morphology  
2099 offshore Lebu (Chilean margin): *Scientific Reports*, v. 10, no. 1.

2100 Vargas-Cordero, I., Tinivella, U., Villar-Muñoz, L., Bento, J. P., Cárcamo, C., López-Acevedo, D.,  
2101 Fernandoy, F., Rivero, A., and Juan, M. S., 2020b, Gas hydrate versus seabed morphology  
2102 offshore Lebu (Chilean margin): *Scientific Reports*, v. 10, no. 1, p. 1-13.

2103 Vigneron, A., Cruaud, P., Pignet, P., Caprais, J.-C., Cambon-Bonavita, M.-A., Godfroy, A., and  
2104 Toffin, L., 2013, Archaeal and anaerobic methane oxidizer communities in the Sonora  
2105 Margin cold seeps, Guaymas Basin (Gulf of California): *Isme Journal*, v. 7, no. 8, p. 1595-  
2106 1608.

2107 Villar-Muñoz, L., Kinoshita, M., Bento, J. P., Vargas-Cordero, I., Contreras-Reyes, E., Tinivella, U.,  
2108 Giustiniani, M., Abe, N., Anma, R., and Orihashi, Y., 2021, A cold seep triggered by a hot  
2109 ridge subduction: *Scientific reports*, v. 11, no. 1, p. 1-14.

2110 von Deimling, J. S., Rehder, G., Greinert, J., McGinnis, D. F., Boetius, A., and Linke, P., 2011,  
2111 Quantification of seep-related methane gas emissions at Tommeliten, North Sea:  
2112 *Continental Shelf Research*, v. 31, no. 7-8, p. 867-878.

2113 Waage, M., Serov, P., Andreassen, K., Waghorn, K. A., and Buenz, S., 2020, Geological controls  
2114 of giant crater development on the Arctic seafloor: *Scientific Reports*, v. 10, no. 1.

2115 Waite, W. F., Santamarina, J. C., Cortes, D. D., Dugan, B., Espinoza, D. N., Germaine, J., Jang, J.,  
2116 Jung, J. W., Kneafsey, T. J., Shin, H., Soga, K., Winters, W. J., and Yun, T. S., 2009, Physical  
2117 properties of hydrate-bearing sediments: *Reviews of Geophysics*, v. 47.

2118 Wallenius, A. J., Dalcin Martins, P., Slomp, C. P., and Jetten, M. S., 2021, Anthropogenic and  
2119 environmental constraints on the microbial methane cycle in coastal sediments:  
2120 *Frontiers in Microbiology*, v. 12, p. 631621.

2121 Wallmann, K., Pinero, E., Burwicz, E., Haeckel, M., Hensen, C., Dale, A., and Ruppel, L., 2012, The  
2122 Global Inventory of Methane Hydrate in Marine Sediments: A Theoretical Approach:  
2123 *Energies*, v. 5, no. 7, p. 2449-2498.

2124 Wallmann, K., Riedel, M., Hong, W. L., Patton, H., Hubbard, A., Pape, T., Hsu, C. W., Schmidt, C.,  
2125 Johnson, J. E., Torres, M. E., Andreassen, K., Berndt, C., and Bohrmann, G., 2018, Gas  
2126 hydrate dissociation off Svalbard induced by isostatic rebound rather than global  
2127 warming: *Nature Communications*, v. 9.

2128 Wang, D. G., Li, Y., Liu, C. L., Zhan, L. S., Lu, H. L., Li, C. F., Sun, J. Y., Meng, Q. G., and Liu, L. L.,  
2129 2020, Study of hydrate occupancy, morphology and microstructure evolution with  
2130 hydrate dissociation in sediment matrices using X-ray micro-CT: *Marine and Petroleum*  
2131 *Geology*, v. 113.

2132 Wang, Y., Wegener, G., Williams, T. A., Xie, R., Hou, J., Tian, C., Zhang, Y., Wang, F., and Xiao, X.,  
2133 2021, A methylophilic origin of methanogenesis and early divergence of anaerobic  
2134 multicarbon alkane metabolism: *Science advances*, v. 7, no. 27, p. eabj1453.

2135 Wanninkhof, R., 1992, Relationship between wind speed and gas exchange over the ocean:  
2136 *Journal of Geophysical Research: Oceans*, v. 97, no. C5, p. 7373-7382.

2137 Wanninkhof, R., Asher, W. E., Ho, D. T., Sweeney, C., and McGillis, W. R., 2009, Advances in  
2138 quantifying air-sea gas exchange and environmental forcing.

2139 Weber, T., Wiseman, N. A., and Kock, A., 2019, Global ocean methane emissions dominated by  
2140 shallow coastal waters: *Nature Communications*, v. 10.

2141 Weinstein, A., Navarrete, L., Ruppel, C., Weber, T. C., Leonte, M., Kellermann, M. Y., Arrington,  
2142 E. C., Valentine, D. L., Scranton, M. I., and Kessler, J. D., 2016, Determining the flux of

2143 methane into Hudson Canyon at the edge of methane clathrate hydrate stability:  
2144 Geochemistry Geophysics Geosystems, v. 17, no. 10, p. 3882-3892.

2145 Wellsbury, P., Goodman, K., Cragg, B. A., and Parkes, R. J., The geomicrobiology of deep marine  
2146 sediments from Blake Ridge containing methane hydrate (Sites 994, 995 and 997), *in*  
2147 Proceedings Proceedings of the Ocean drilling program, Scientific results, 2000, Volume  
2148 164, Ocean Drilling Program College Station, TX, p. 379-391.

2149 Westbrook, G. K., Thatcher, K. E., Rohling, E. J., Piotrowski, A. M., Palike, H., Osborne, A. H.,  
2150 Nisbet, E. G., Minshull, T. A., Lanoiselle, M., James, R. H., Huhnerbach, V., Green, D.,  
2151 Fisher, R. E., Crocker, A. J., Chabert, A., Bolton, C., Beszczynska-Moller, A., Berndt, C.,  
2152 and Aquilina, A., 2009, Escape of methane gas from the seabed along the West  
2153 Spitsbergen continental margin: Geophysical Research Letters, v. 36.

2154 Whiticar, M. J., 1994, Correlation of natural gases with their sources: AAPG Memoir, Magoon, L.  
2155 B.; Dow, W. G. (Eds), The petroleum System: from Sources to Trap, v. vol.60, p. pp 261-  
2156 283.

2157 -, 1999, Carbon and hydrogen isotope systematics of bacterial formation and oxidation of  
2158 methane: Chemical Geology, v. 161, no. 1-3, p. 291-314.

2159 Wilson, R. M., Lapham, L. L., Riedel, M., Holmes, M. E., and Chanton, J. P., 2015, Observing  
2160 methane hydrate dissolution rates under sediment cover: Marine Chemistry, v. 172, p.  
2161 12-22.

2162 Wu, S.-J., Yang, C.-J., and Chen, C.-T. A., 2013, A Handheld Sampler for Collecting Organic  
2163 Samples from Shallow Hydrothermal Vents: Journal of Atmospheric and Oceanic  
2164 Technology, v. 30, no. 8, p. 1951-1958.

2165 Wu, S.-j., Yang, C.-j., Huang, H.-c., and Chen, Y., 2014, Development of an electric control gas-  
2166 tight sampler for seafloor hydrothermal fluids: Journal of Zhejiang University-Science A,  
2167 v. 15, no. 2, p. 120-129.

2168 Xu, S. A., Sun, Z. L., Geng, W., Cao, H., Zhang, X. L., Zhai, B., and Wu, Z. J., 2022, Advance in  
2169 Numerical Simulation Research of Marine Methane Processes: Frontiers in Earth  
2170 Science, v. 10.

2171 Xu, W., and Germanovich, L. N., 2006, Excess pore pressure resulting from methane hydrate  
2172 dissociation in marine sediments: A theoretical approach: Journal of Geophysical  
2173 Research: Solid Earth, v. 111, no. B1.

2174 Yan, C., Ren, X., Cheng, Y., Song, B., Li, Y., and Tian, W., 2020, Geomechanical issues in the  
2175 exploitation of natural gas hydrate: Gondwana Research, v. 81, p. 403-422.

2176 Yang, J., Hassanpouryouzband, A., Tohidi, B., Chuvilin, E., Bukhanov, B., Istomin, V., and  
2177 Cheremisin, A., 2019, Gas hydrates in permafrost: Distinctive effect of gas hydrates and  
2178 ice on the geomechanical properties of simulated hydrate-bearing permafrost  
2179 sediments: Journal of Geophysical Research: Solid Earth, v. 124, no. 3, p. 2551-2563.

2180 Yang, S., Choi, J. C., Vanneste, M., and Kvalstad, T., 2018, Effects of gas hydrates dissociation on  
2181 clays and submarine slope stability: Bulletin of Engineering Geology and the  
2182 Environment, v. 77, no. 3, p. 941-952.

2183 Yun, T. S., Santamarina, J. C., and Ruppel, C., 2007, Mechanical properties of sand, silt, and clay  
2184 containing tetrahydrofuran hydrate: Journal of geophysical research: solid earth, v. 112,  
2185 no. B4.

2186 Yvon-Lewis, S. A., Hu, L., and Kessler, J., 2011, Methane flux to the atmosphere from the  
2187 Deepwater Horizon oil disaster: Geophysical Research Letters, v. 38.

2188 Zander, T., Haeckel, M., Berndt, C., Chi, W. C., Klauke, I., Bialas, J., Klaeschen, D., Koch, S., and  
2189 Atgm, O., 2017, On the origin of multiple BSRs in the Danube deep-sea fan, Black Sea:  
2190 Earth and Planetary Science Letters, v. 462, p. 15-25.

2191 Zander, T., Haeckel, M., Klauke, I., Bialas, J., Klaeschen, D., Papenberg, C., Pape, T., Berndt, C.,  
2192 and Bohrmann, G., 2020, New insights into geology and geochemistry of the Kerch seep  
2193 area in the Black Sea: Marine and Petroleum Geology, v. 113, p. 104162.

2194 Zhang, Y. X., 2003, Methane escape from gas hydrate systems in marine environment, and  
2195 methane-driven oceanic eruptions: *Geophysical Research Letters*, v. 30, no. 7.  
1  
2  
3 2196  
4  
5  
6  
7  
8  
9  
10  
11  
12  
13  
14  
15  
16  
17  
18  
19  
20  
21  
22  
23  
24  
25  
26  
27  
28  
29  
30  
31  
32  
33  
34  
35  
36  
37  
38  
39  
40  
41  
42  
43  
44  
45  
46  
47  
48  
49  
50  
51  
52  
53  
54  
55  
56  
57  
58  
59  
60  
61  
62  
63  
64  
65